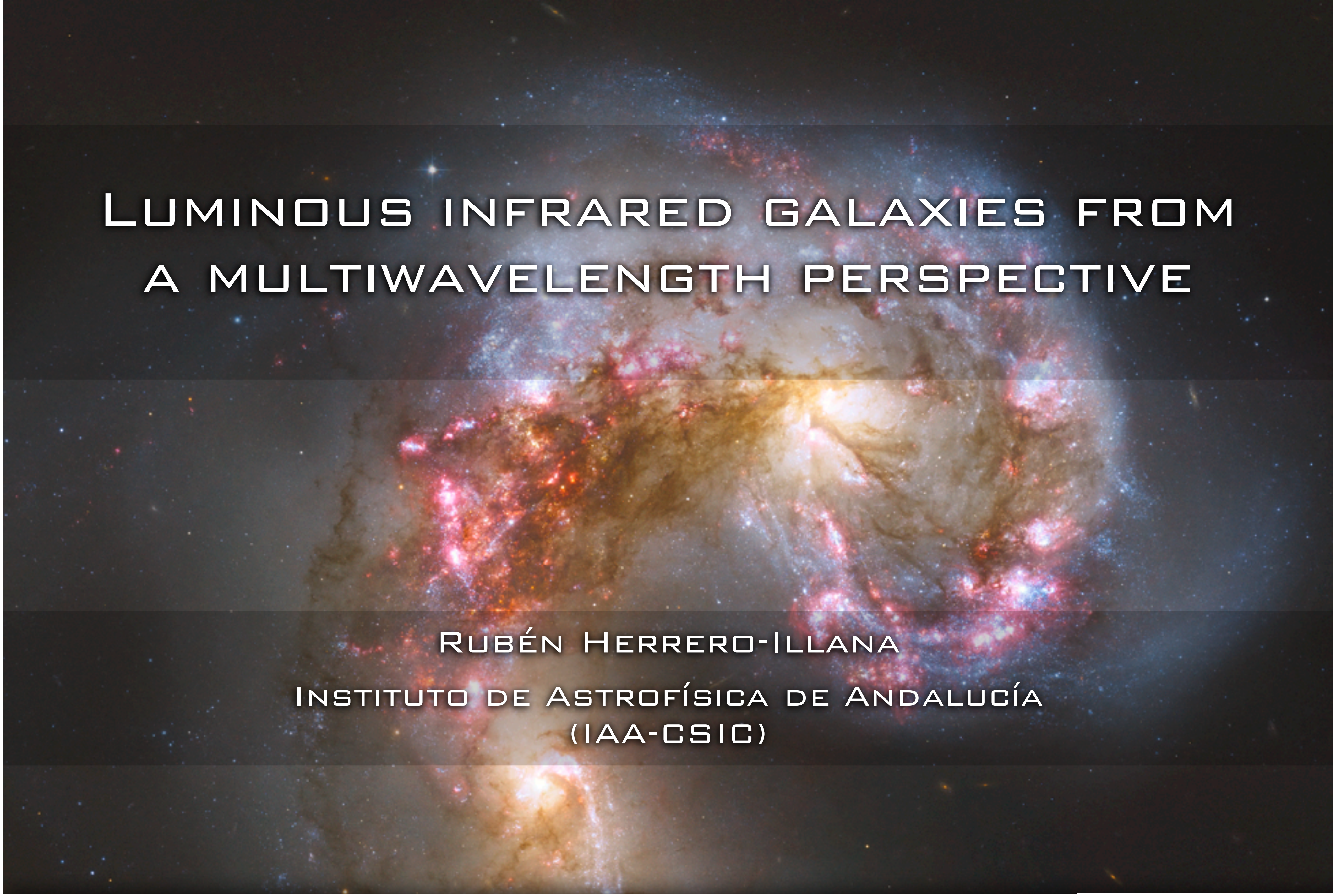

Luminous infrared galaxies from a multiwavelength perspective

Rubén Herrero-Illana

Instituto de Astrofísica de Andalucía (IAA-CSIC)

05/02/2015

[ESAC Science Seminar]

Consejo Superior de Investigaciones Científicas

Outline

1. Introduction
2. Observations
3. Results
    3.1. Molecular gas in (U)LIRGs
    3.2. NGC1614 as a case study
    3.3. Multiwavelength study of LIRGs
    3.4. Massive star formation in Arp299
    3.5. The radial distribution of supernovae
4. Conclusions

LIRGs & ULIRGs

- Morphological diversity
- Mostly mergers above $\sim 3 \times 10^{11} L_\odot$
- SFR up to 500 $M_\odot$/yr
- Very high CCSN rate

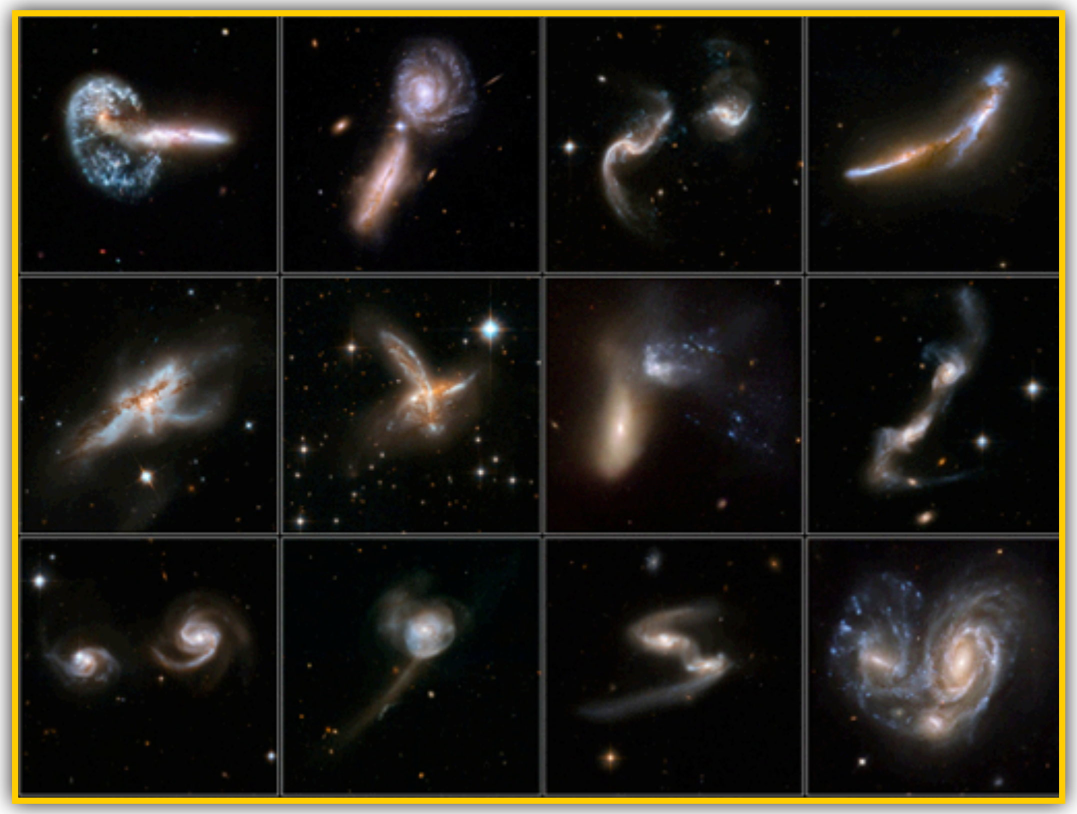

Credit: NASA, ESA, Aaron Evans

LIRGs	ULIRGs
$10^{11} L_\odot \leq L_{\mathrm{IR}} \leq 10^{12} L_\odot$	$L_{\mathrm{IR}} \geq 10^{12} L_\odot$

(U)LIRGs - Motivation

Fundamental at high-z

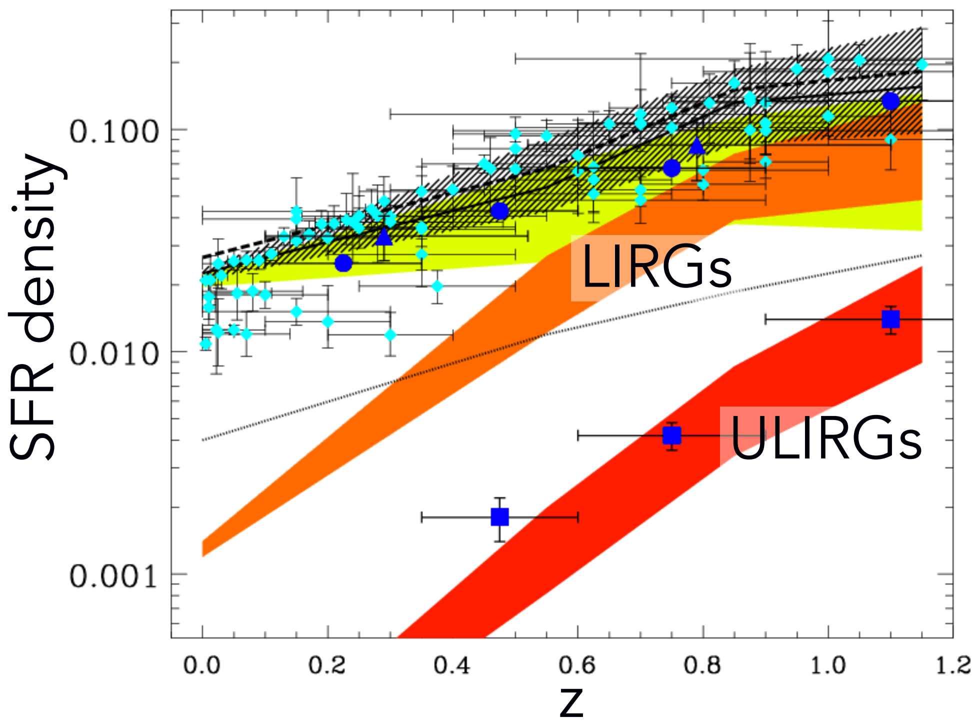

Magnelli *et al.*, 2009, A&A

(U)LIRGs - Motivation

Fundamental at high-z

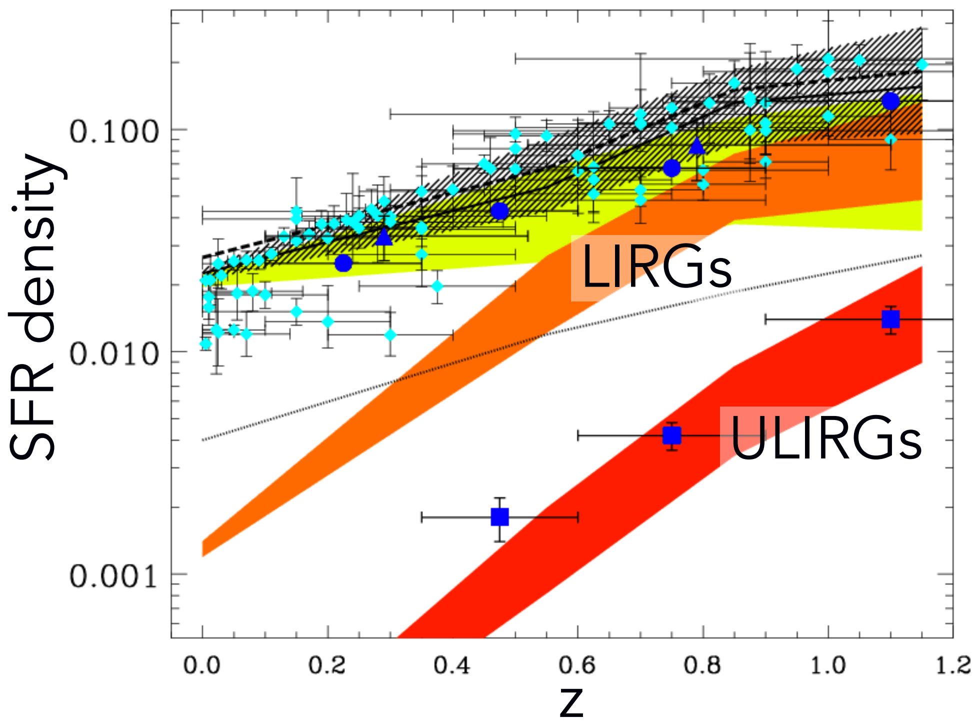

Magnelli *et al.*, 2009, A&A

Dust heating

powered by

Star formation ⟷ AGN

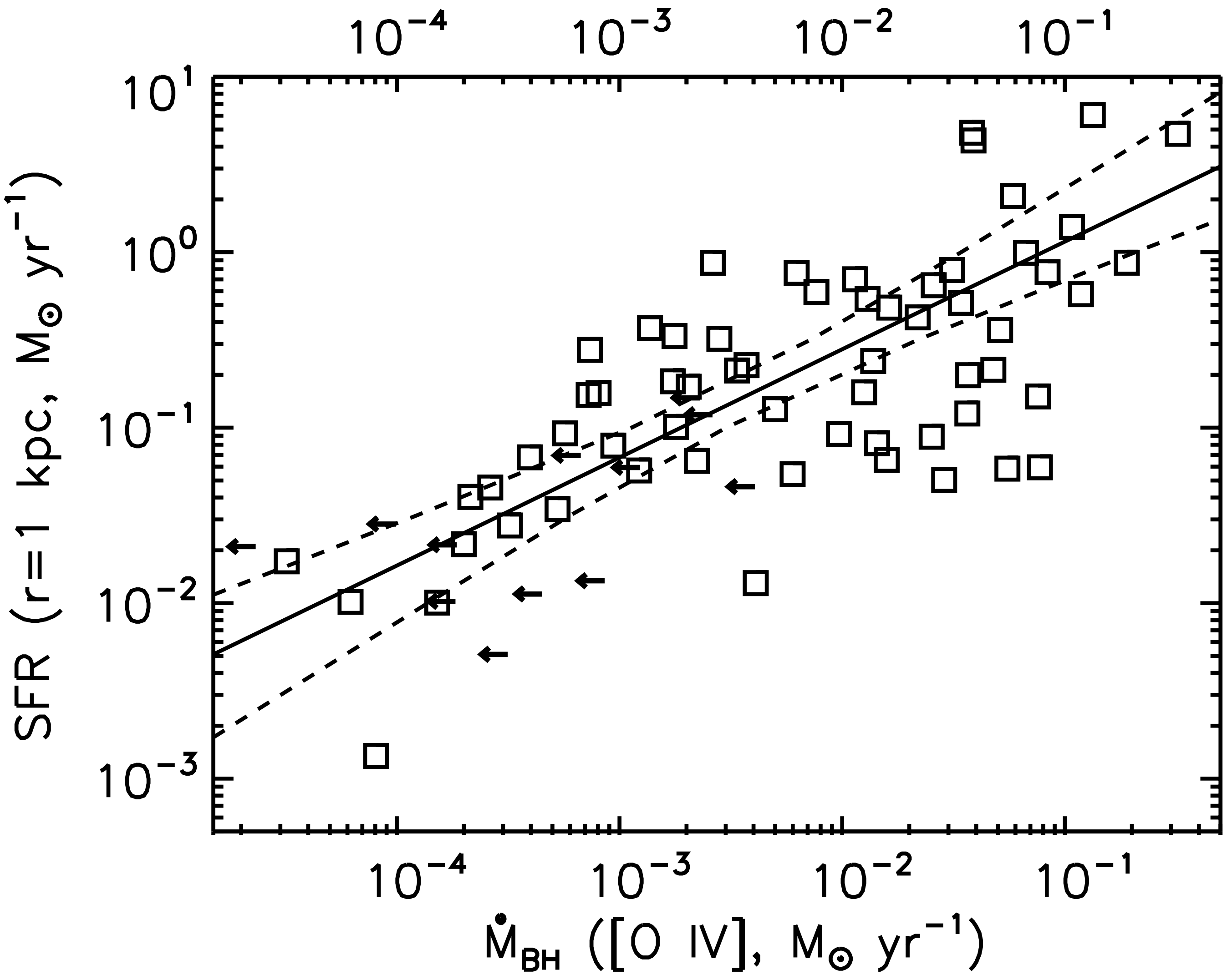

Adapted from Diamond-Stanic & Rieke, 2012, ApJ

Star formation ⟷ AGN

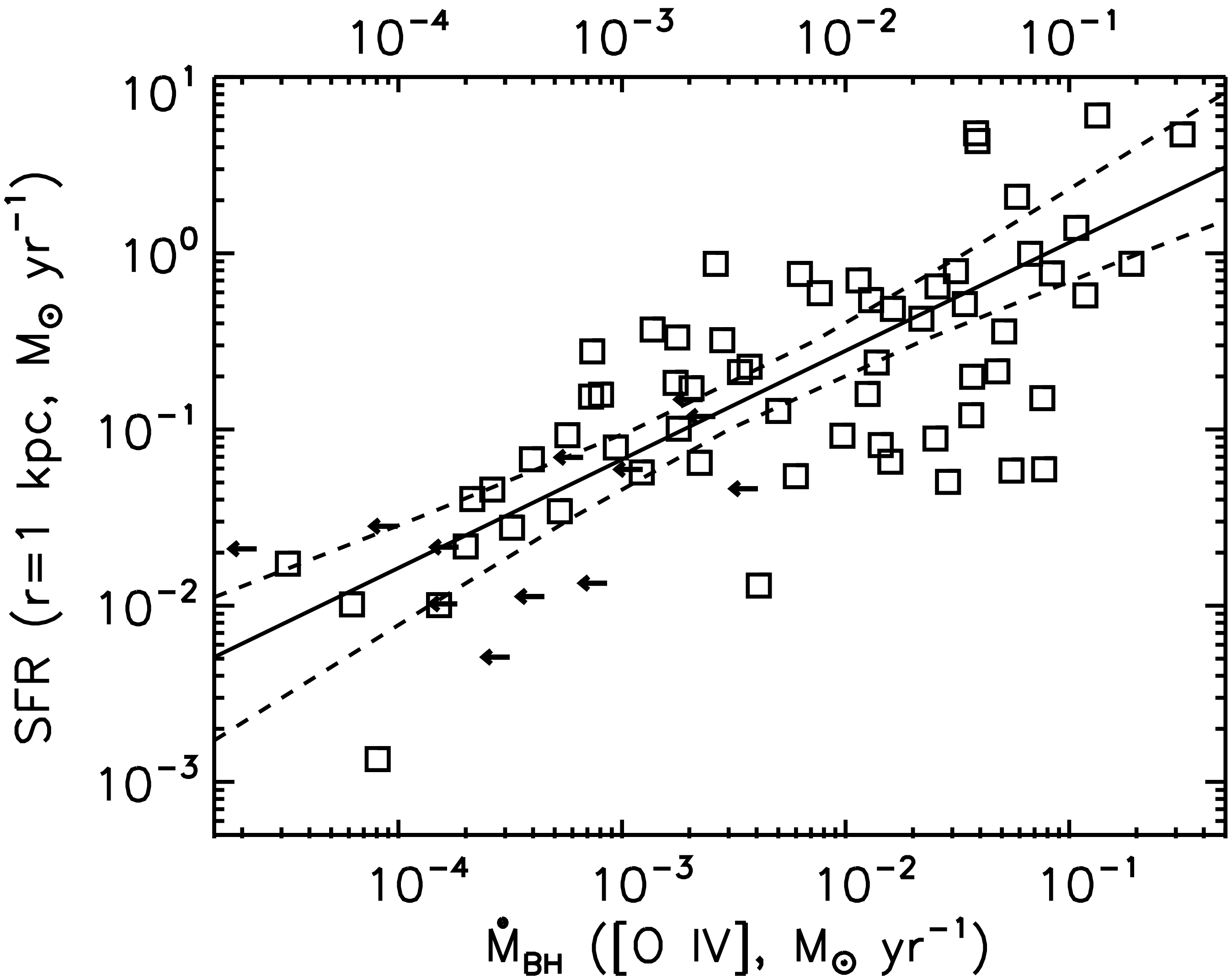

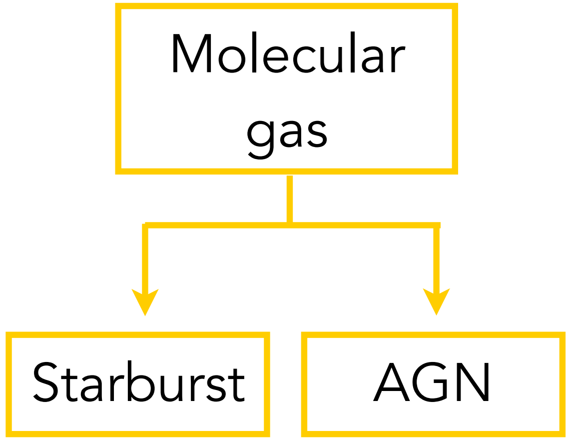

Adapted from Diamond-Stanic & Rieke, 2012, ApJ

The evolutionary pathway

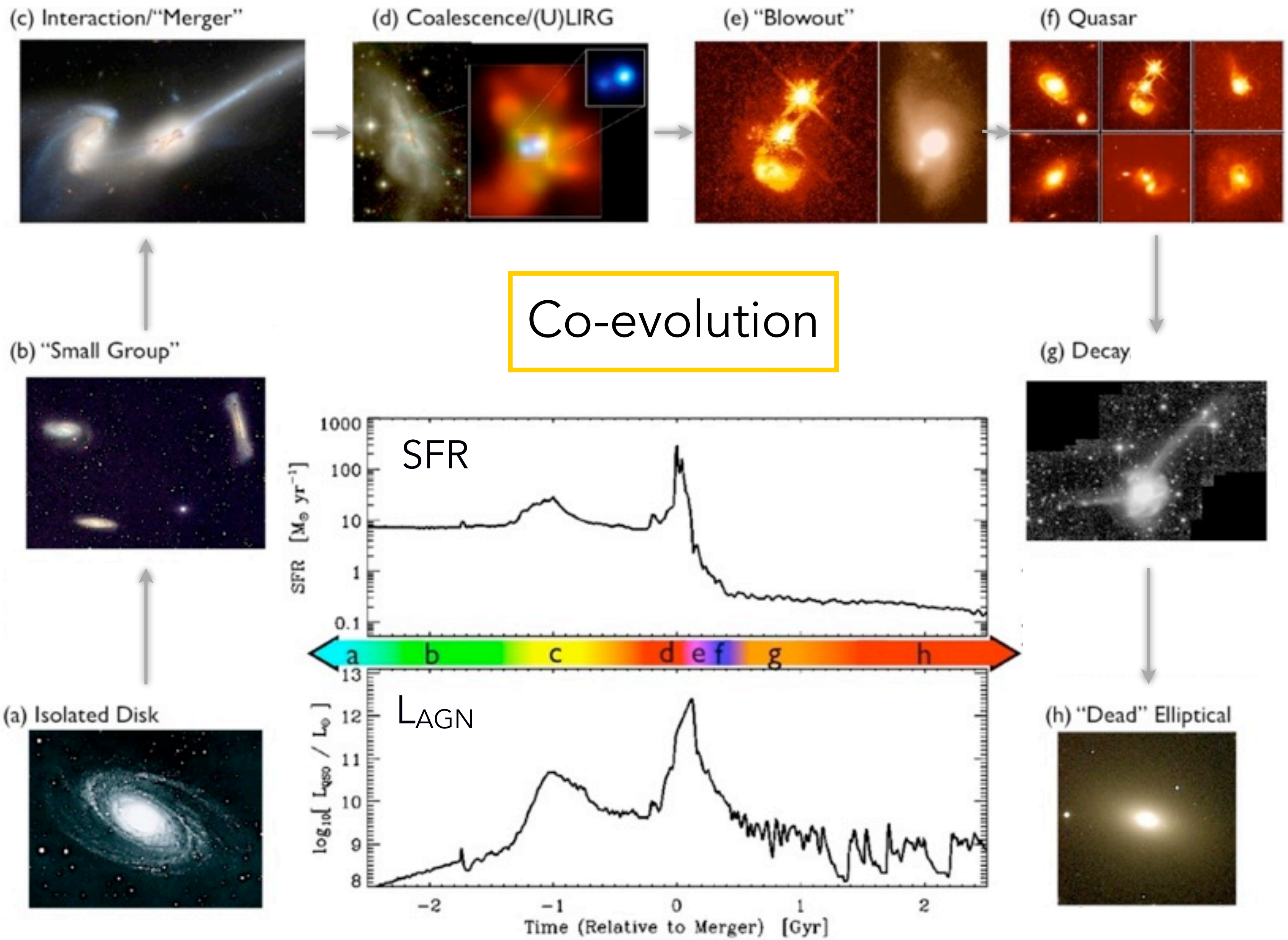

Adapted from Hopkins *et al.*, 2008, ApJS

Observations

Infrared mm Radio

Infrared

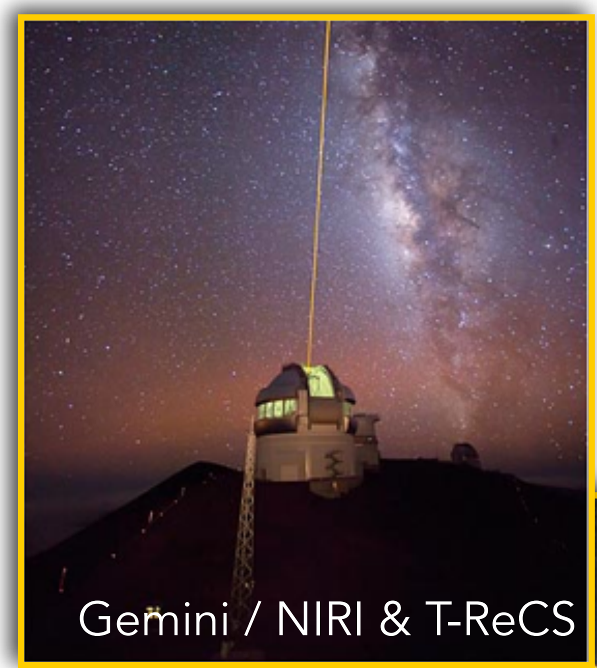

- Reduced extinction
- Mid-IR: 8.4 μm (θ~0.38″)
- Near-IR: 1.9 μm (θ~0.15″)

  2.2 μm (θ~0.07″)

Adaptive optics

Radio: single-dish

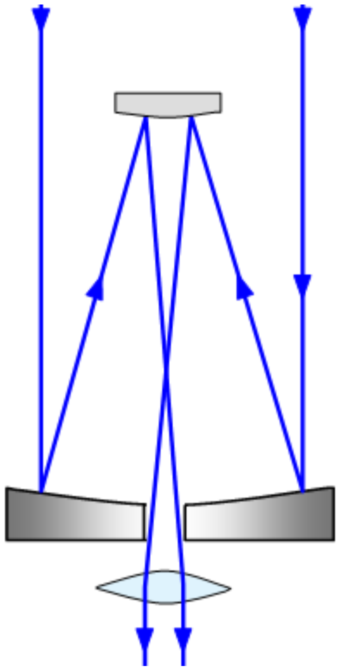

$$\theta \sim \frac{\lambda}{D}$$

Radio interferometry

$$\theta \sim \frac{\lambda}{D}$$

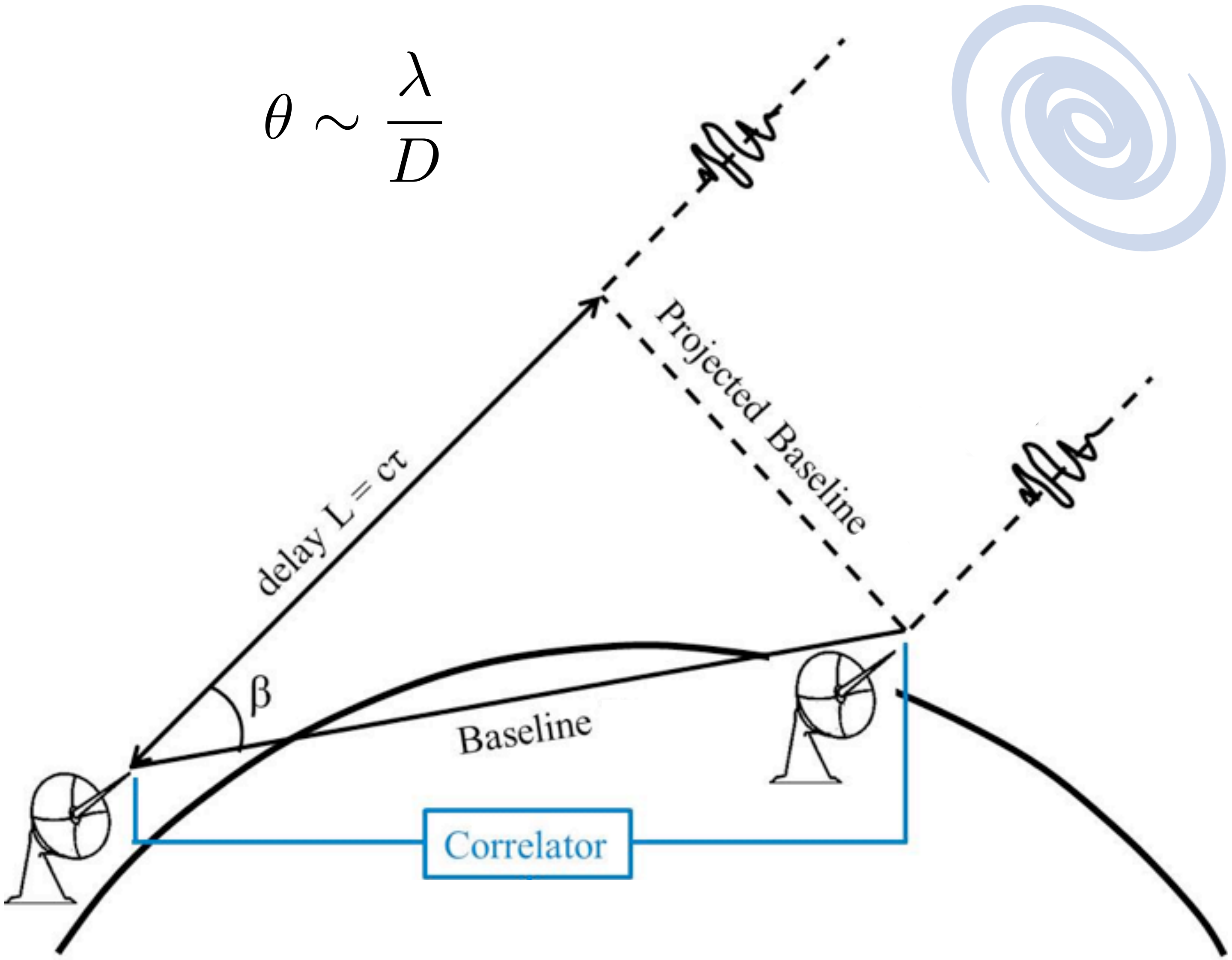

Radio interferometry

$$\theta \sim \frac{\lambda}{D}$$

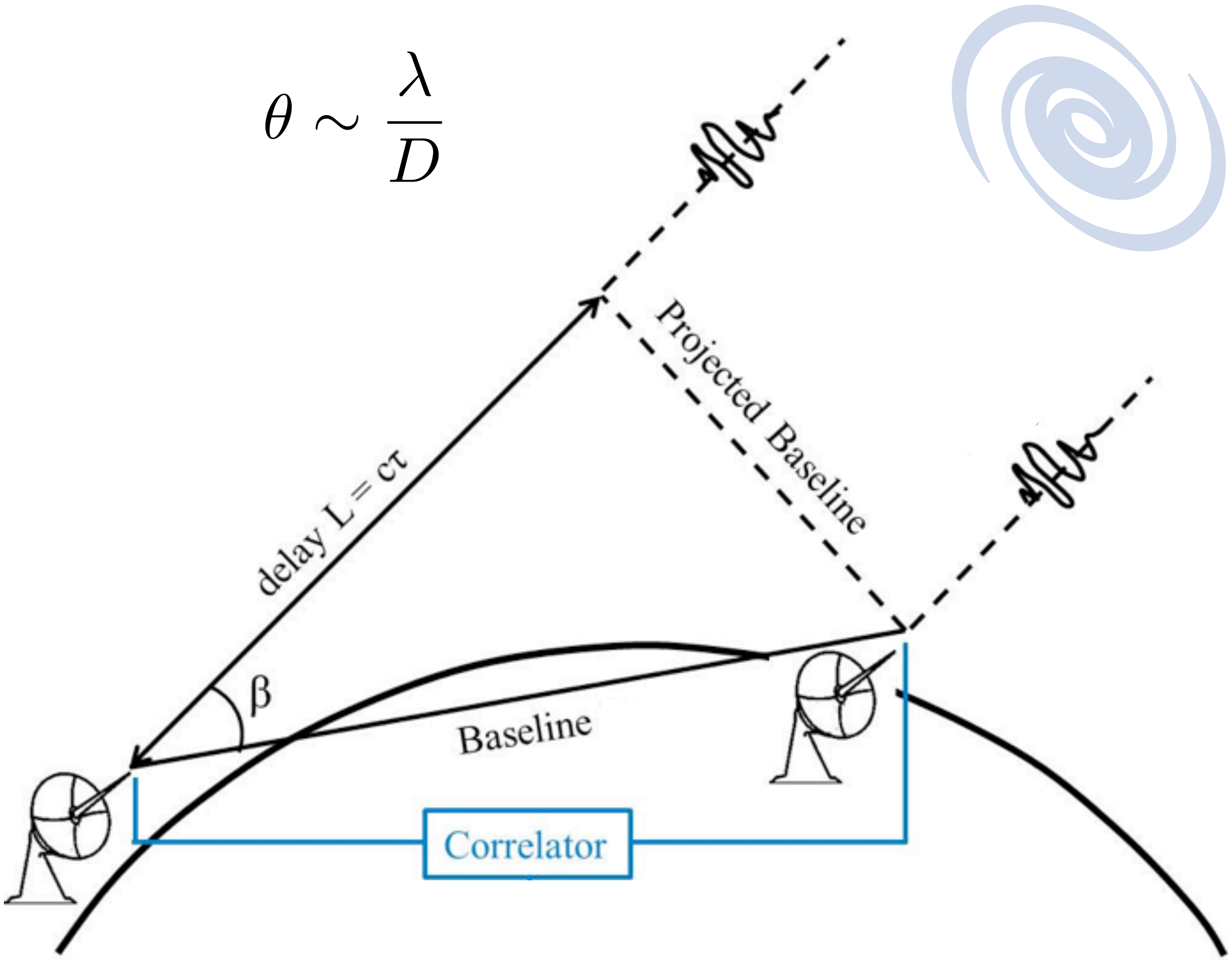

$$V(u,v) = \iint I(l,m) e^{2\pi i(ul+vm)} dl dm$$

Radio interferometry

~~$\theta \sim \frac{\lambda}{D}$~~

$$\theta \sim \frac{\lambda}{B}$$

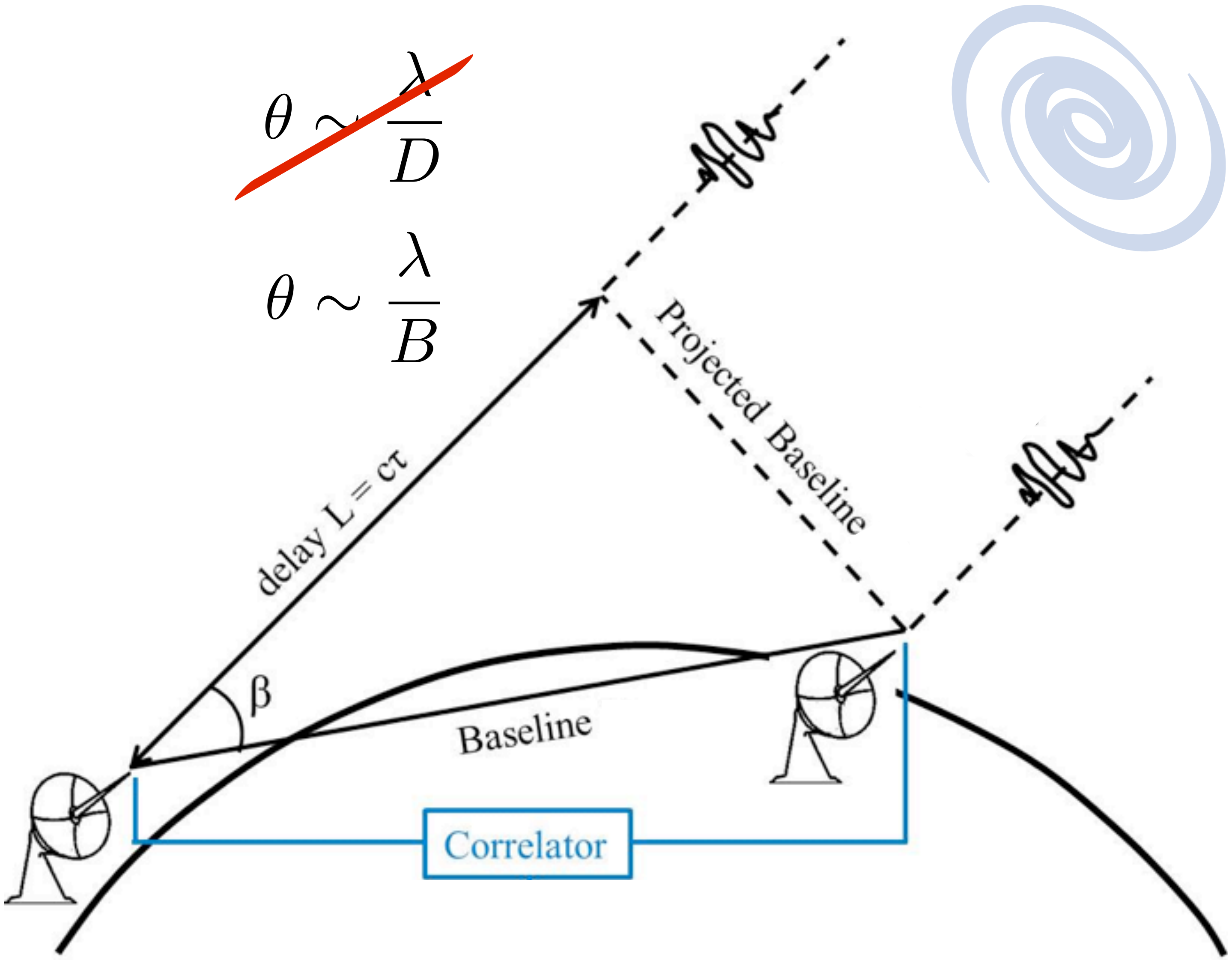

$$V(u,v) = \iint I(l,m) e^{2\pi i (ul+vm)} dl dm$$

Observations: Radio & mm

Single-dish

θ~20″

mm spectral study of molecular gas

Interferometers

θ~0.40″

θ~0.06″

θ~0.005″

Radio continuum in SB galaxies

M82 Radio SED

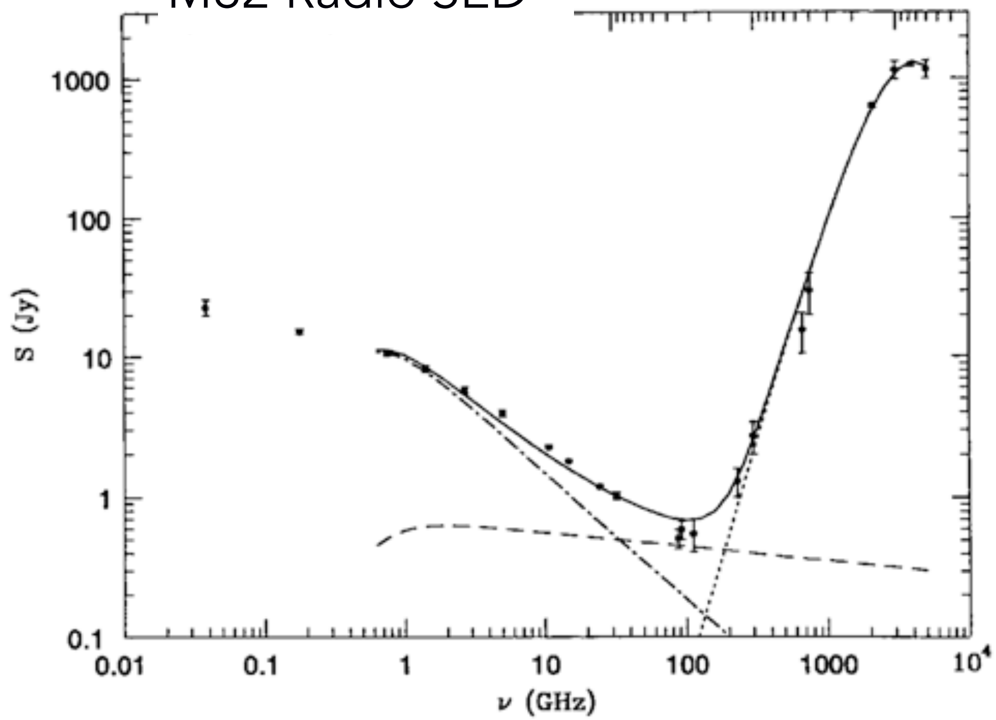

Condon, 1992, ARA&A

Radio continuum in SB galaxies

e⁻ accelerated in SNR

M82 Radio SED

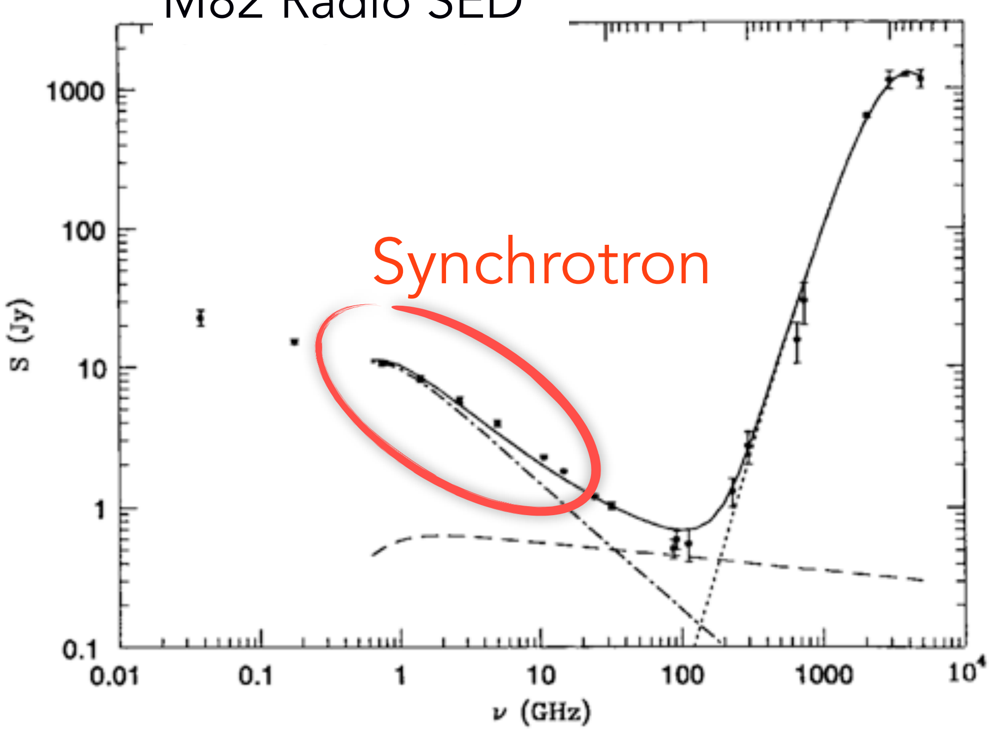

Condon, 1992, ARA&A

Radio continuum in SB galaxies

e⁻ accelerated in SNR

HII regions ionized by massive stars

M82 Radio SED

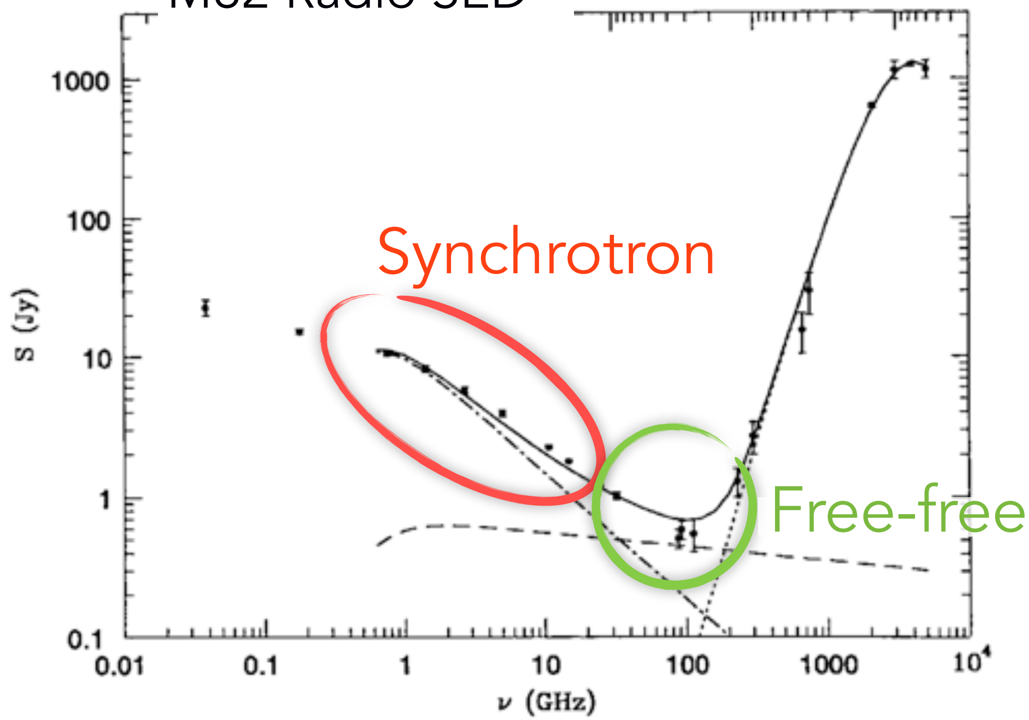

Condon, 1992, ARA&A

Radio continuum in SB galaxies

e⁻ accelerated in SNR

HII regions ionized by massive stars

Re-emission

M82 Radio SED

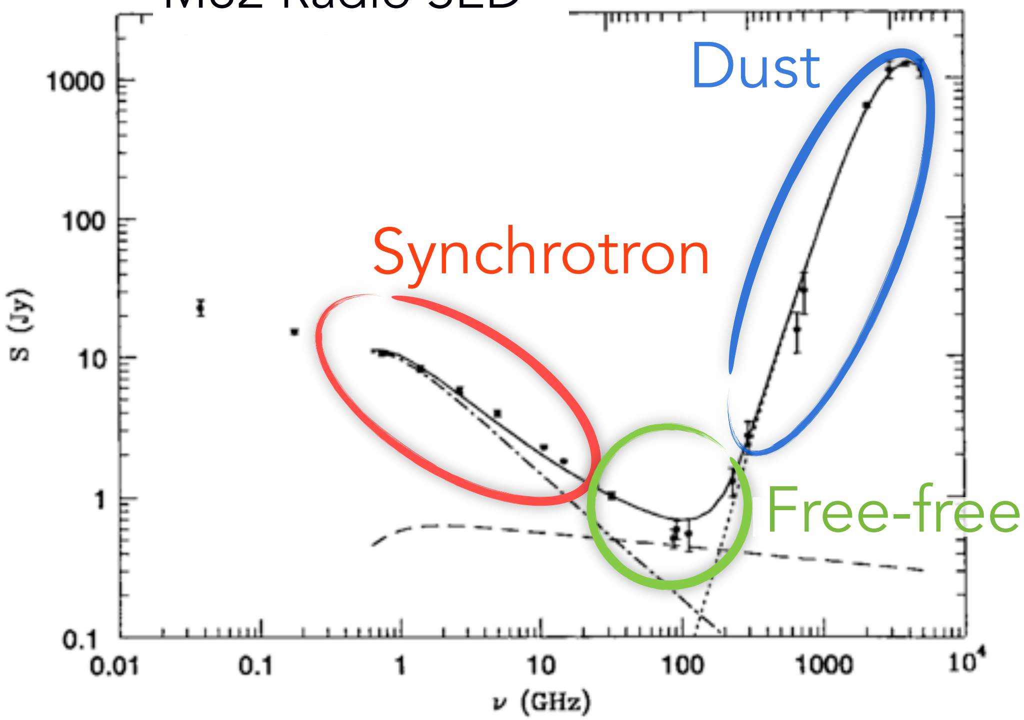

Condon, 1992, ARA&A

Outline

Molecular gas in (U)LIRGs

General framework

GOALS Great Observatory All-sky LIRG Survey

Molecular gas in (U)LIRGs

General framework

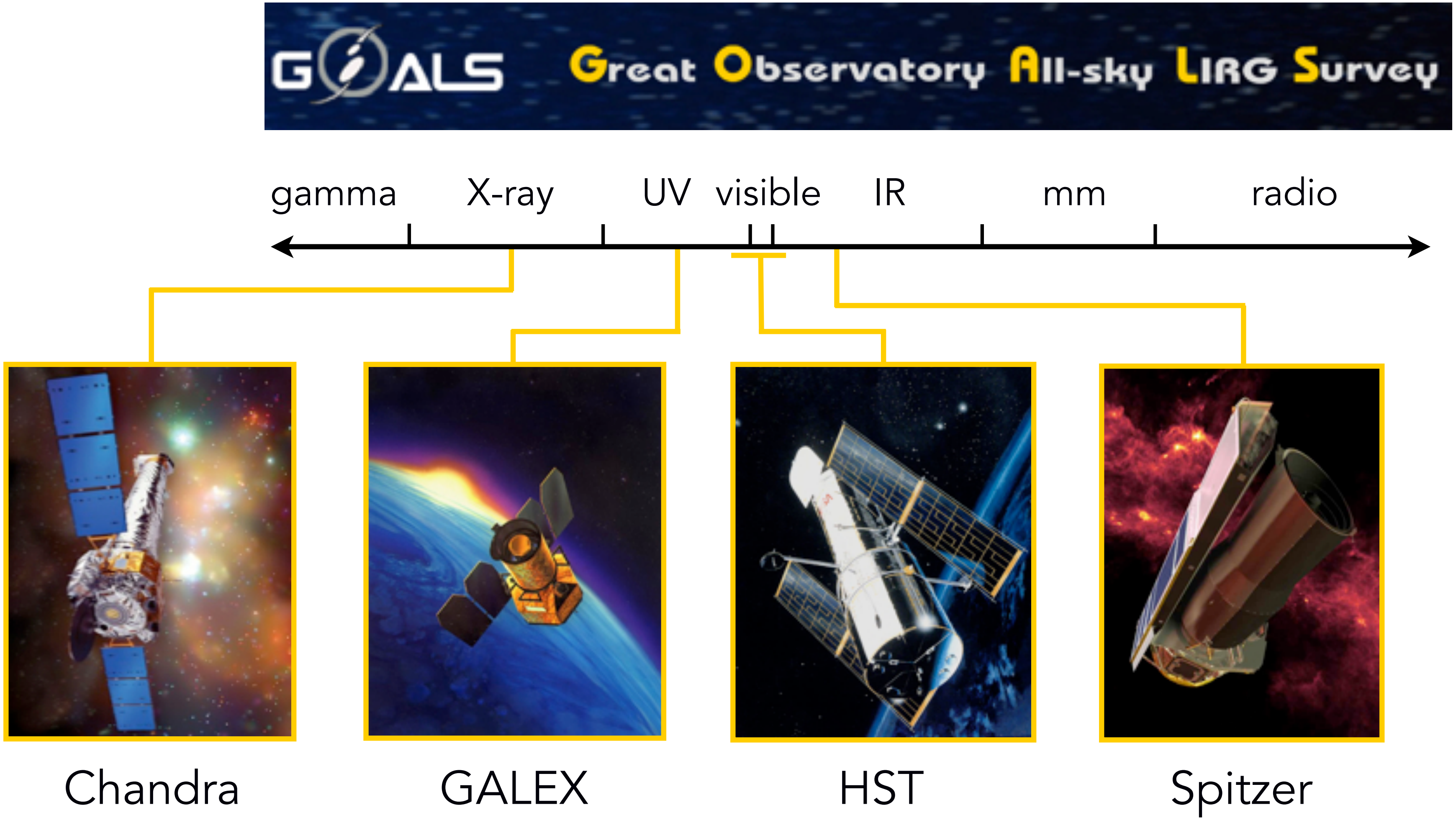

Molecular gas in (U)LIRGs

General framework

GOALS Great Observatory All-sky LIRG Survey

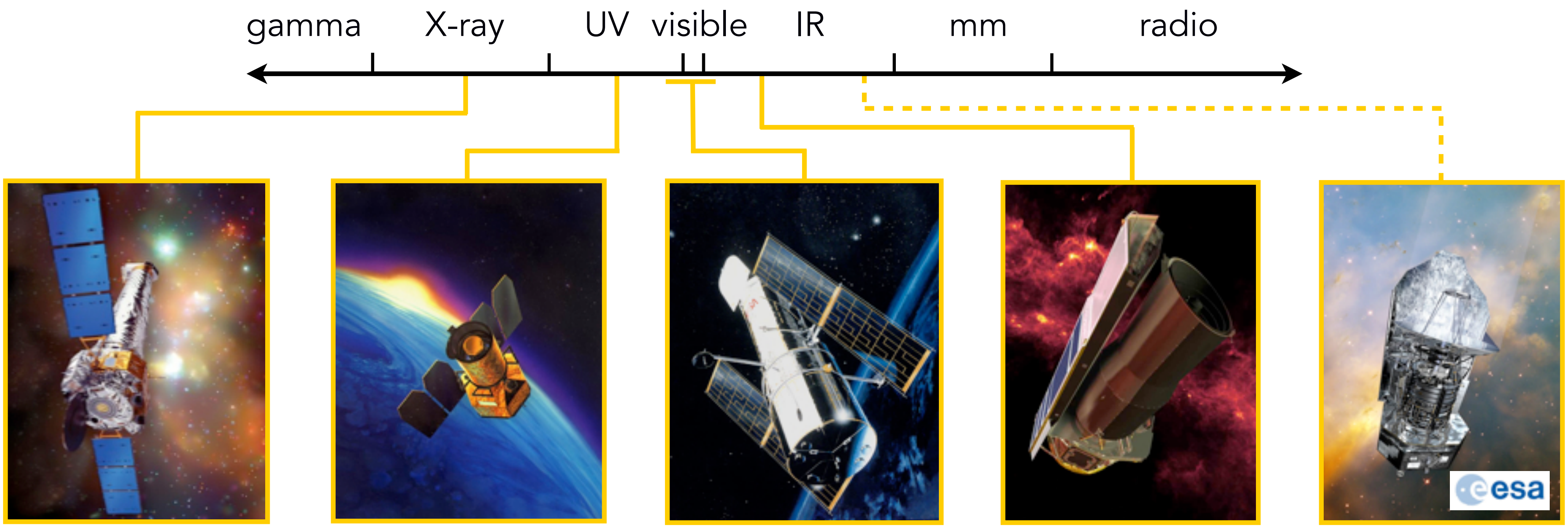

Chandra GALEX HST Spitzer *Herschel*

Molecular gas in (U)LIRGs

General framework

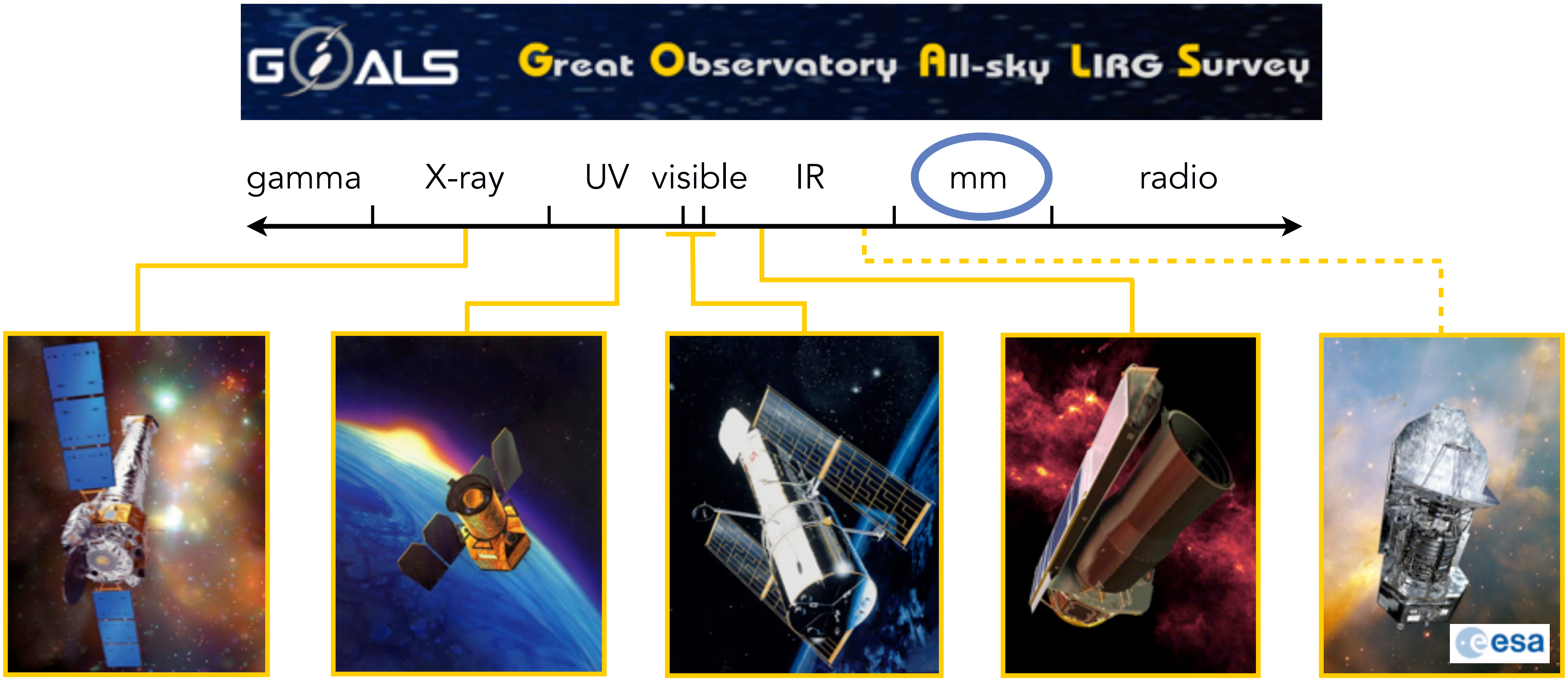

Chandra GALEX HST Spitzer *Herschel*

+ Ground based observations

Molecular gas in (U)LIRGs

- Stars formed in molecular clouds
- $H_2 \longrightarrow$ Tracers

NASA, ESA, J. Hester (ASU)

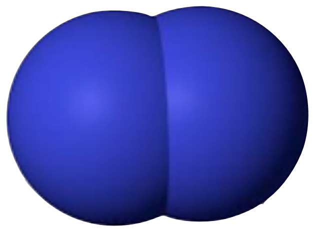

H_2

CO

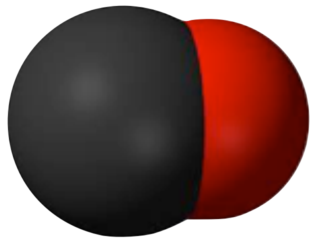

Molecular gas in (U)LIRGs

- Stars formed in molecular clouds
- H_2 ⟶ Tracers
- IRAM 30m observations:
  - 56 (U)LIRGs
  - GOALS Great Observatory All-sky LIRG Survey
  - Transitions around 80 - 115 GHz:
    - ^{12}CO ^{13}CO HCN HCO^+

NASA, ESA, J. Hester (ASU)

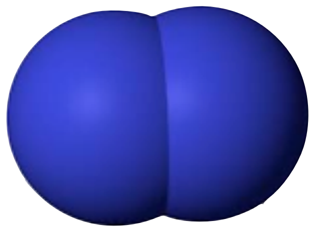

H_2

CO

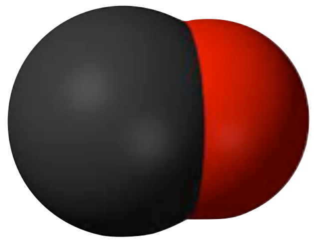

Molecular gas in (U)LIRGs

- Stars formed in molecular clouds
- H_2 ⟶ Tracers
- IRAM 30m observations:
  - 56 (U)LIRGs
  - GOALS Great Observatory All-sky LIRG Survey
  - Transitions around 80 - 115 GHz:
    - ^{12}CO ^{13}CO HCN HCO^+

NASA, ESA, J. Hester (ASU)

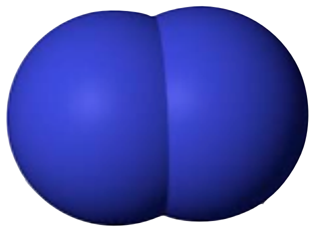

H_2

CO

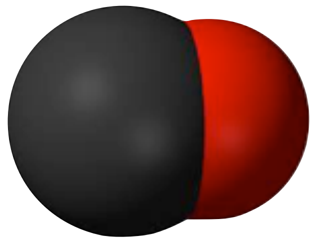

Data reduction

Basic reduction → Channel integration → Line luminosities → Molecular gas masses

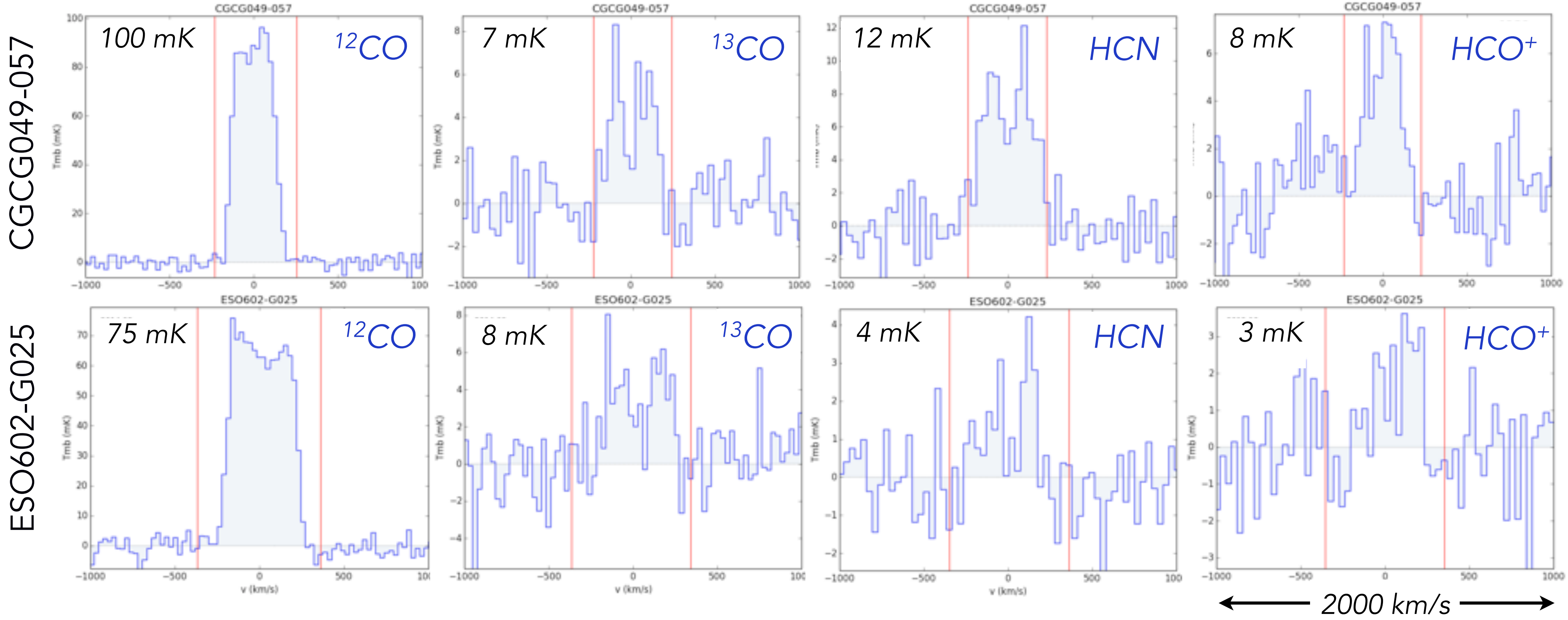

Star formation efficiency

$$\mathrm{SFE} = \frac{L_{\rm IR}}{M_{\rm H_2}}\left[\frac{L_\odot}{M_\odot}\right] \propto \frac{L_{\rm IR}}{L'_{\rm CO}}$$

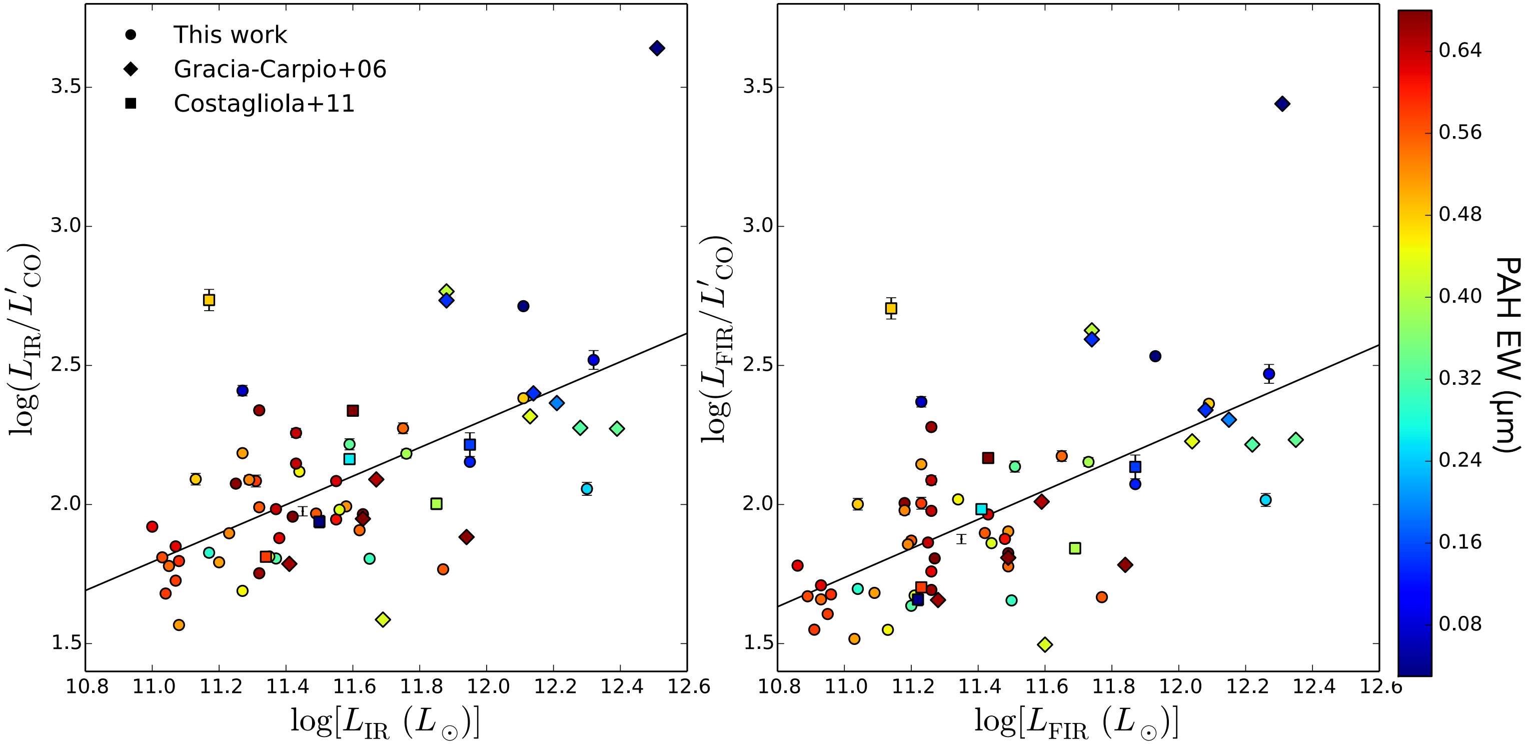

$$\log\left(L_{\rm IR}/L'_{\rm CO}\right) = 0.51\log(L_{\rm IR}) - 3.86$$

$$\log\left(L_{\rm FIR}/L'_{\rm CO}\right) = 0.52\log(L_{\rm FIR}) - 4.02$$

L_{IR} and L_{FIR} yield similar fits

Star formation efficiency

$$\mathrm{SFE} = \frac{L_{\mathrm{IR}}}{M_{\mathrm{H_2}}}\left[\frac{L_\odot}{M_\odot}\right] \propto \frac{L_{\mathrm{IR}}}{L'_{\mathrm{CO}}}$$

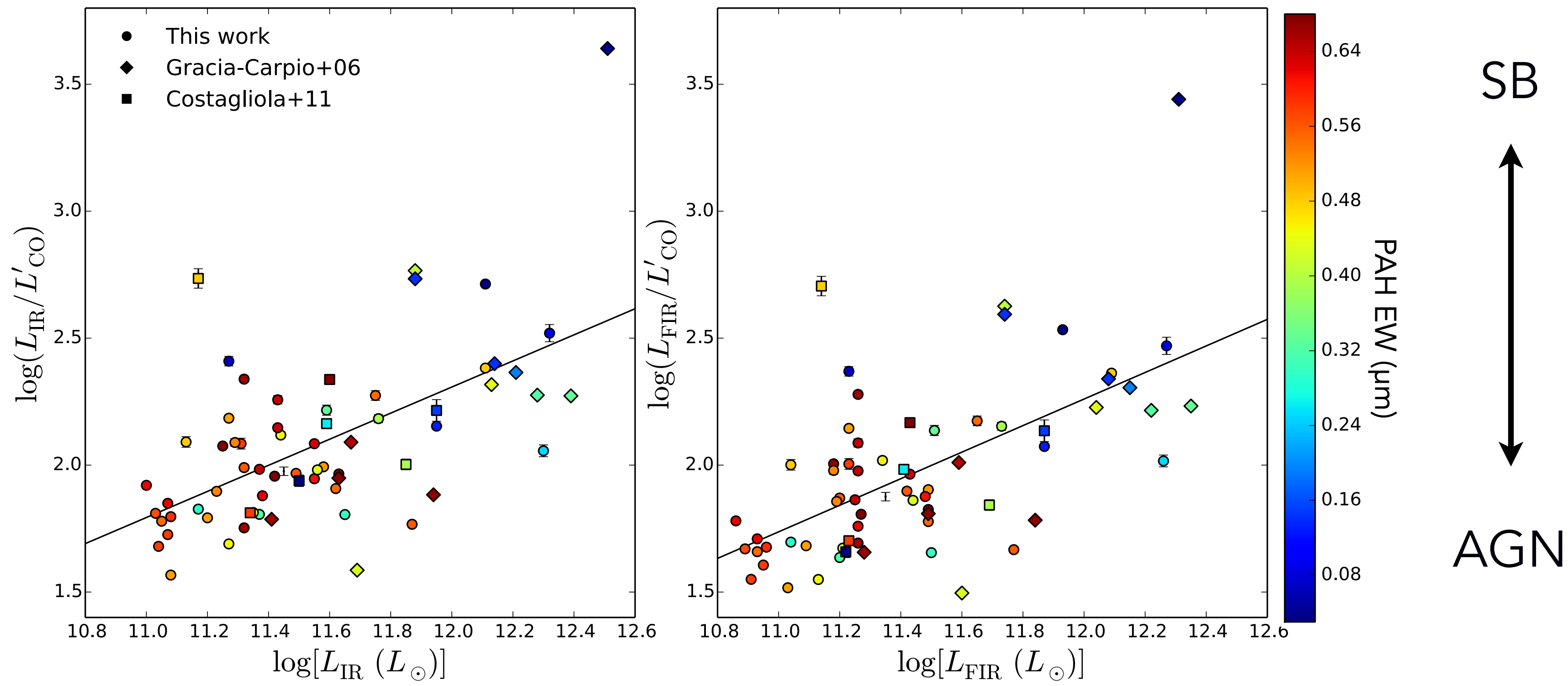

$$\log\left(L_{\mathrm{IR}}/L'_{\mathrm{CO}}\right) = 0.51\log(L_{\mathrm{IR}}) - 3.86 \qquad \log\left(L_{\mathrm{FIR}}/L'_{\mathrm{CO}}\right) = 0.52\log(L_{\mathrm{FIR}}) - 4.02$$

L_{IR} and L_{FIR} yield similar fits

Star formation efficiency

$$\mathrm{SFE} = \frac{L_{\mathrm{IR}}}{M_{\mathrm{H_2}}}\left[\frac{L_\odot}{M_\odot}\right] \propto \frac{L_{\mathrm{IR}}}{L'_{\mathrm{CO}}}$$

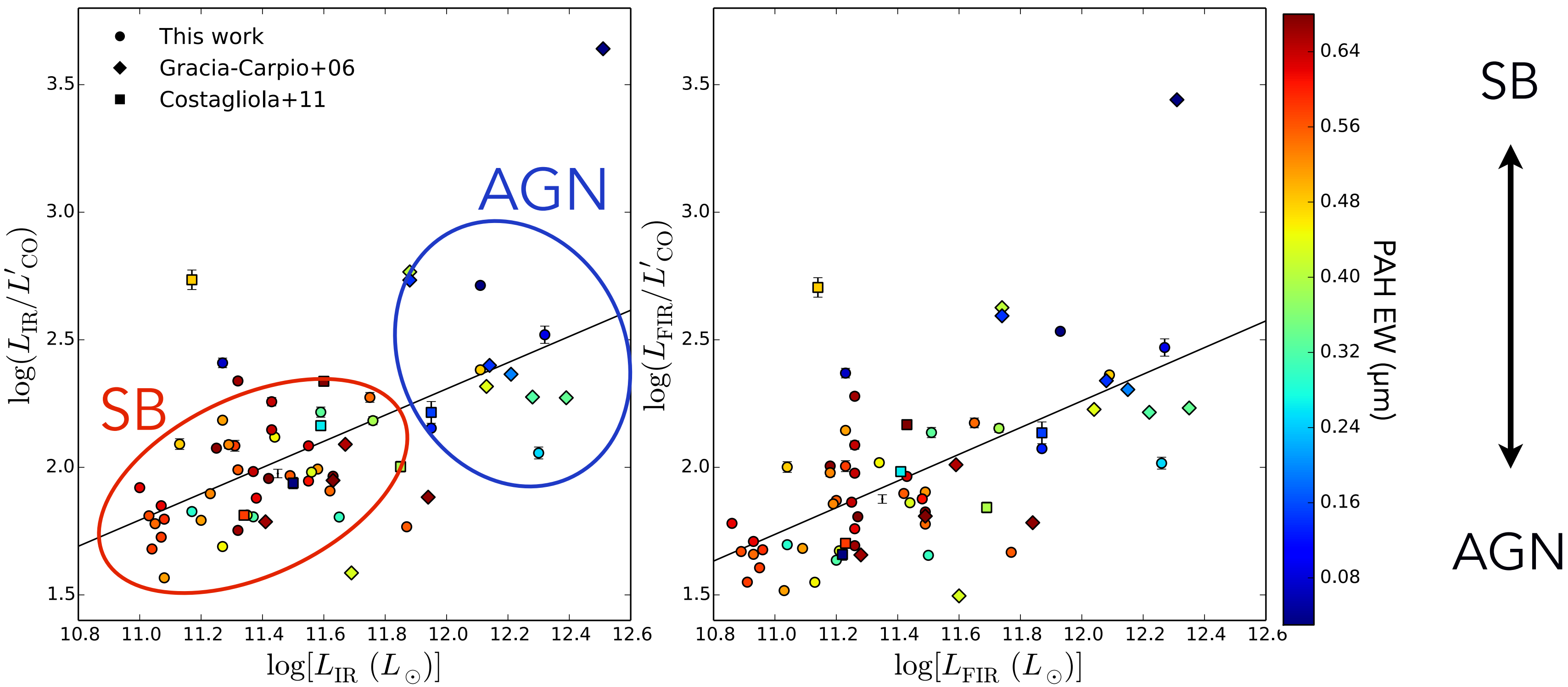

$\log(L_{\mathrm{IR}}/L'_{\mathrm{CO}}) = 0.51\log(L_{\mathrm{IR}}) - 3.86$ $\log(L_{\mathrm{FIR}}/L'_{\mathrm{CO}}) = 0.52\log(L_{\mathrm{FIR}}) - 4.02$

L_{IR} and L_{FIR} yield similar fits

AGN contributing significantly to dust heating

Dust properties (I)

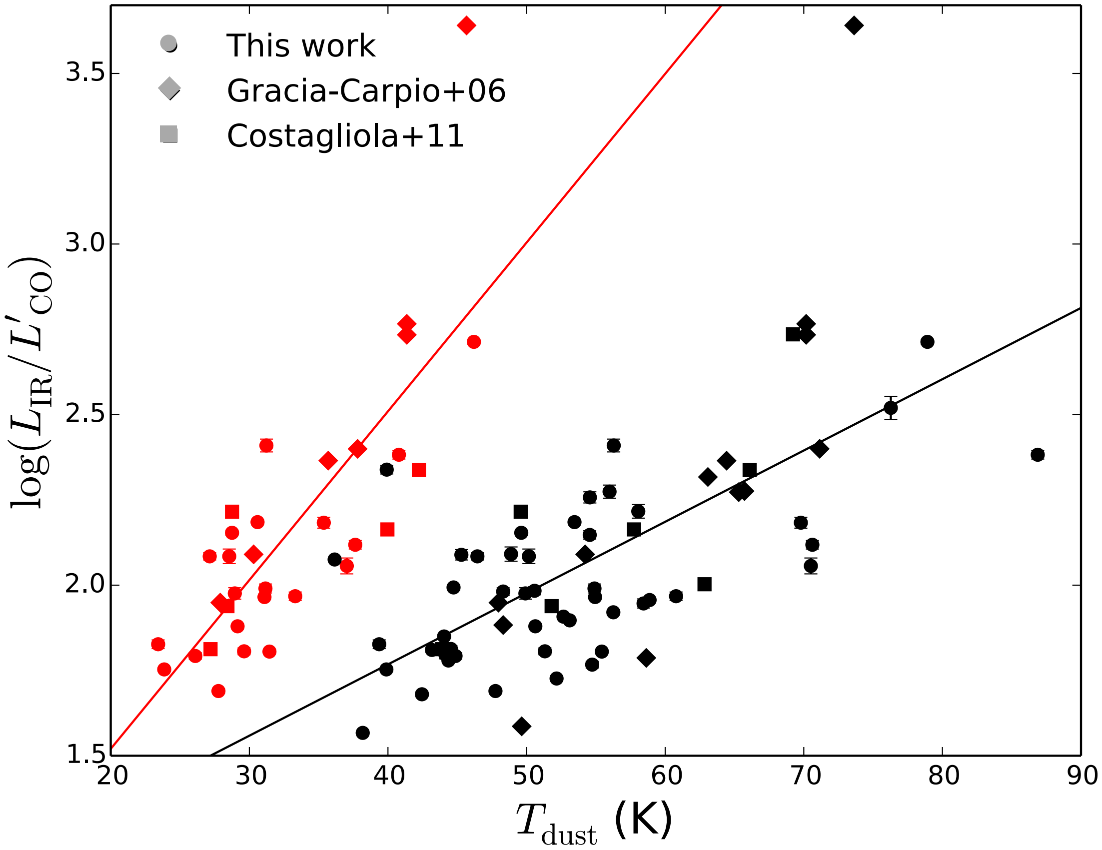

Classical approach

IRAS: 60µm, 100µm

Far-IR SED fitting

IRAS, IRAC, MIPS, SCUBA
[8µm - 850µm]

Dust properties (II)

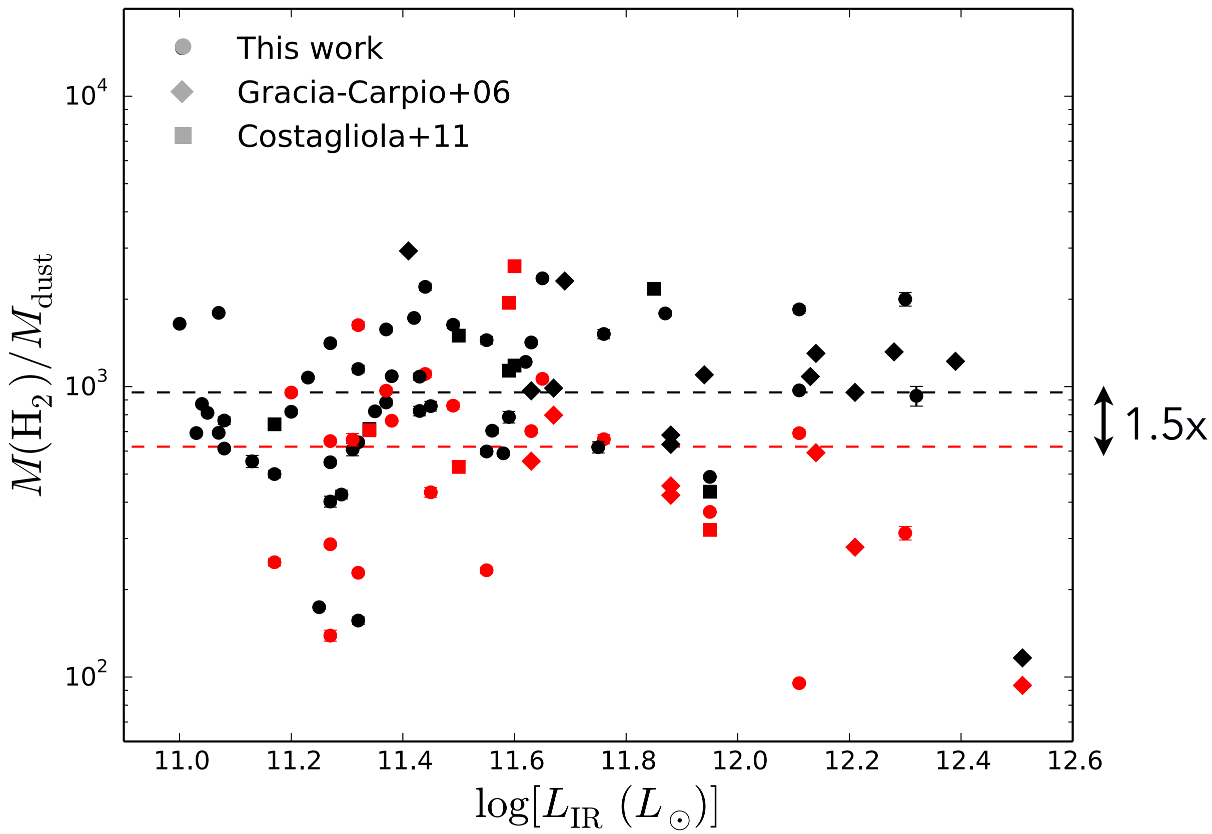

Classical approach

IRAS: 60µm, 100µm

Far-IR SED fitting

IRAS, IRAC, MIPS, SCUBA
[8µm - 850µm]

$$M(H_2)/M_{\rm dust} = 956$$

$$M(H_2)/M_{\rm dust} = 621$$

$$\alpha_{\rm CO} = \frac{M(H_2)}{L'_{\rm CO}} = 4\,M_\odot({\rm K\ km\ s^{-1}\ pc^2})^{-1}$$

Gas-to-dust mass ratio often used to estimate gas mass from high-z galaxies.

Spectral profiles

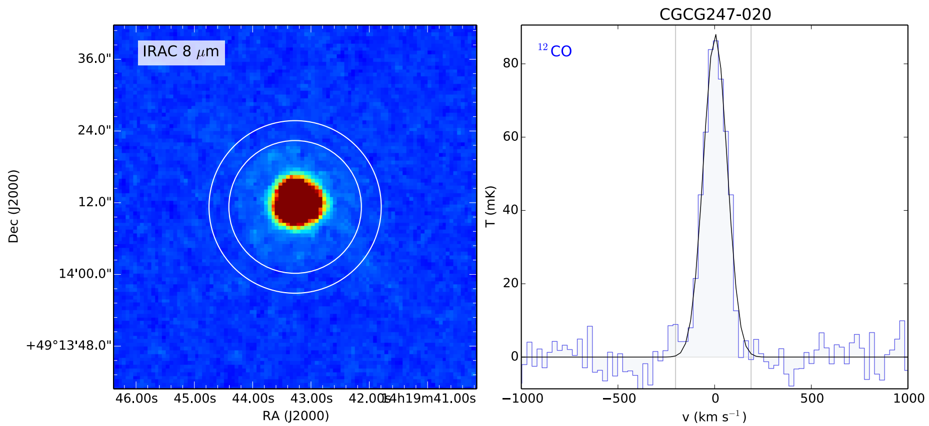

Single peak

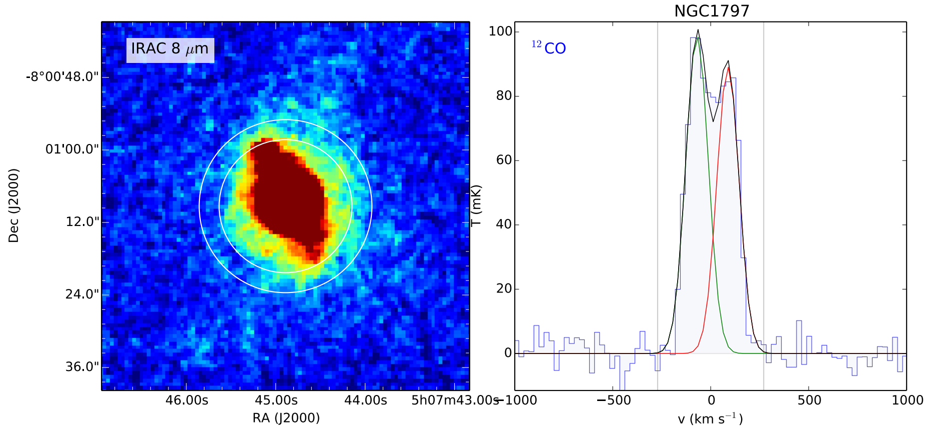

Symmetric double horn

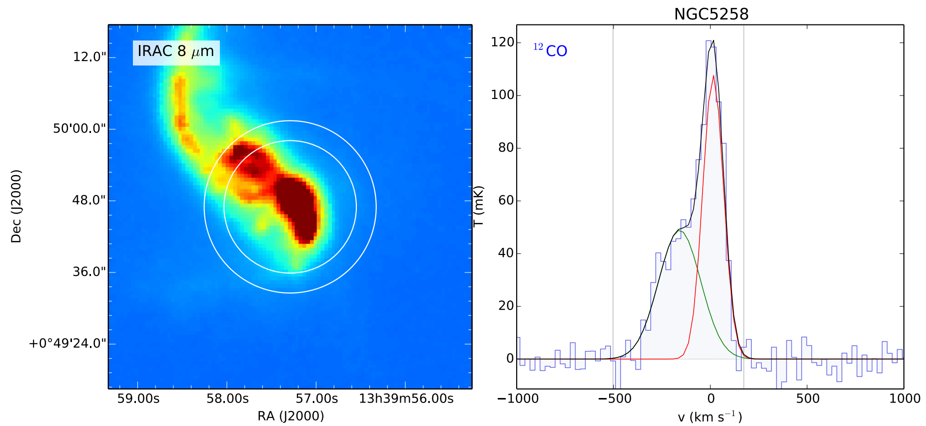

Asymmetric double horn

Spectral profiles

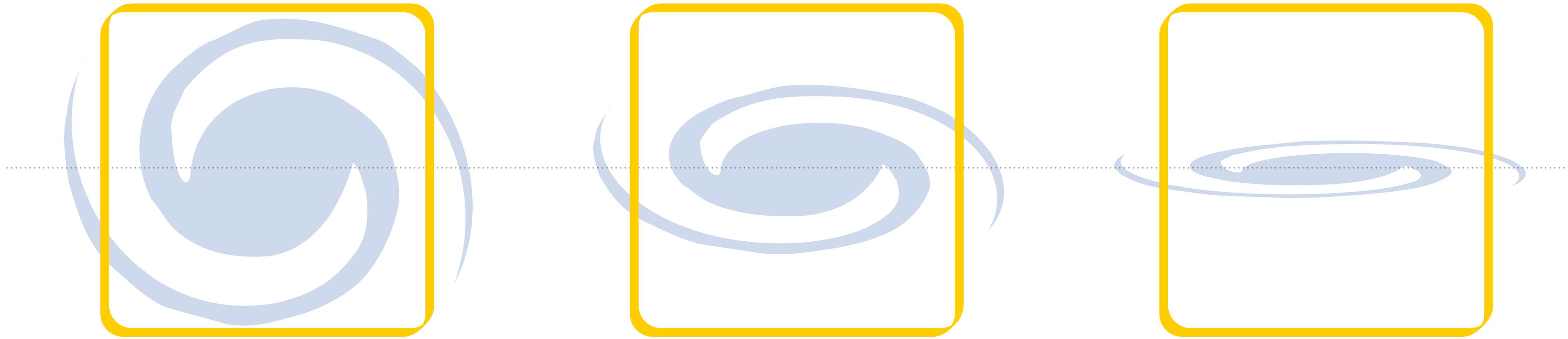

Face-on

Edge-on

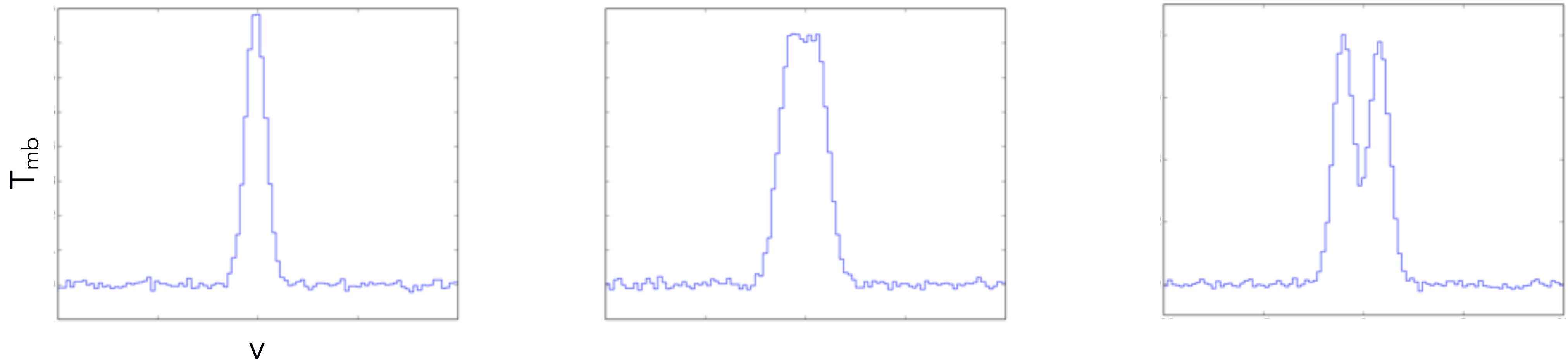

Spectral profiles

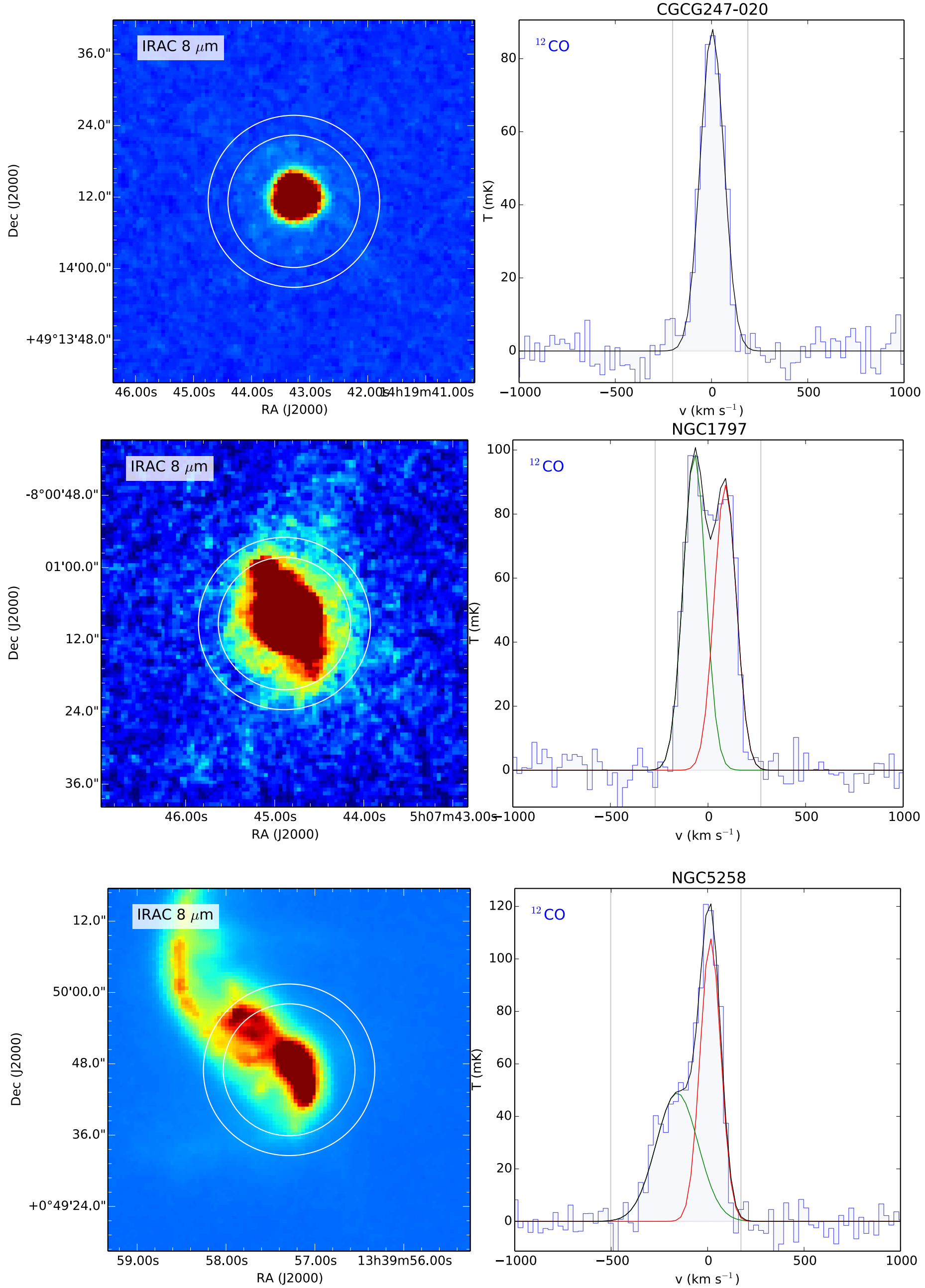

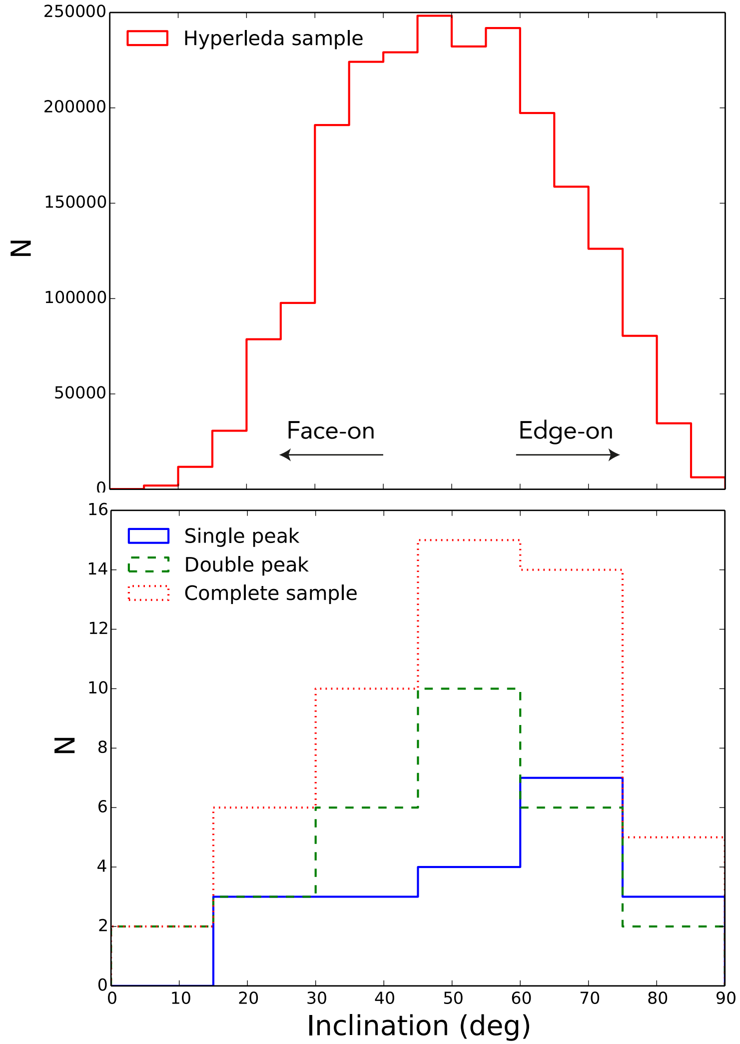

Spectral profiles

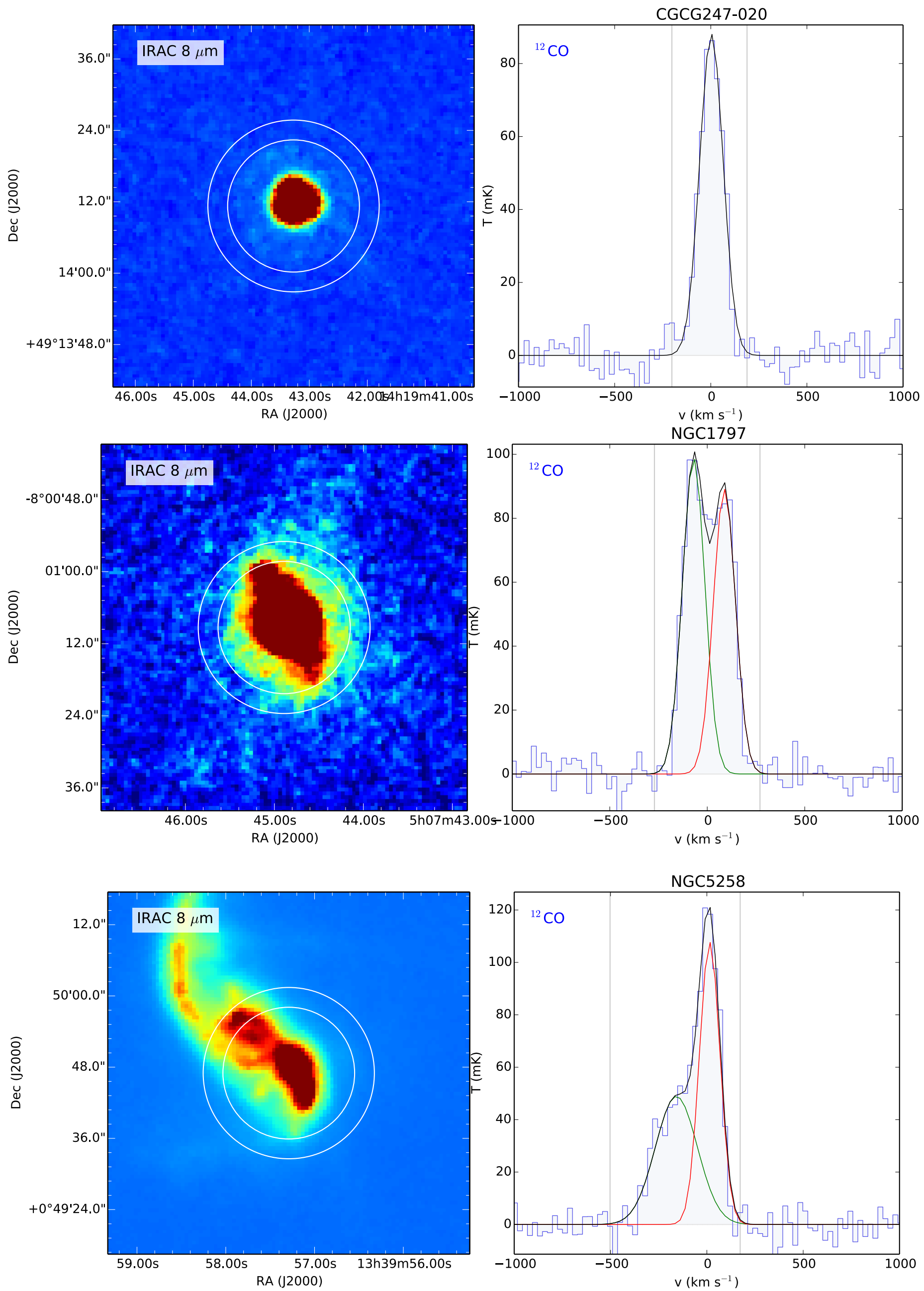

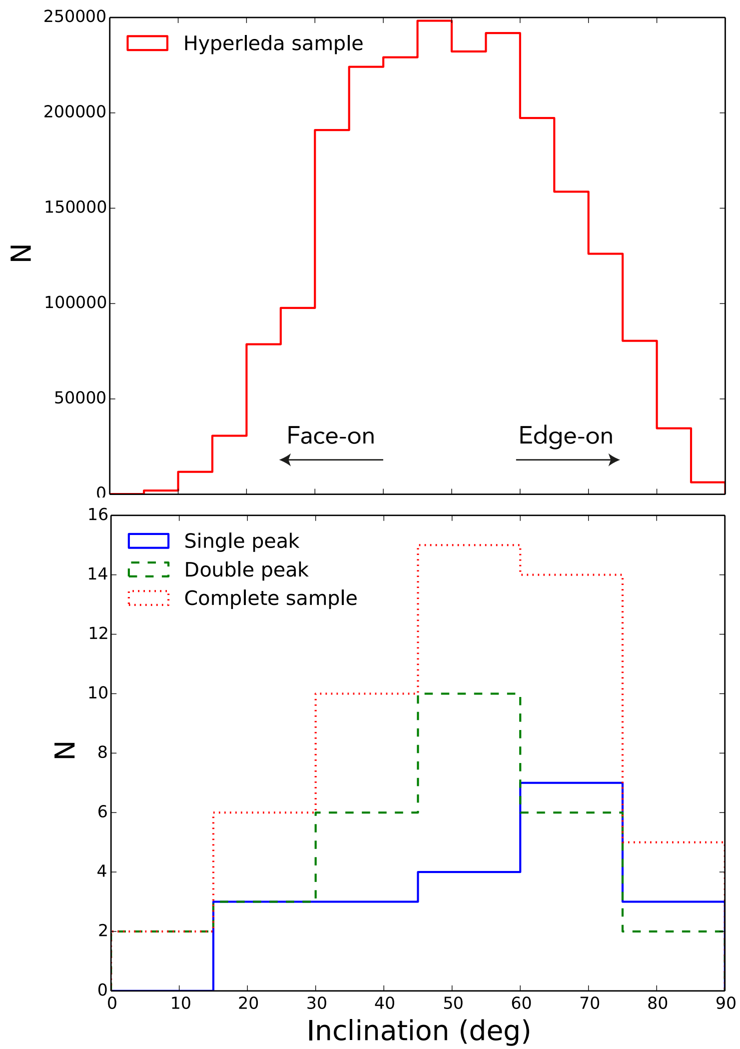

Intrinsic reason for spectral profiles

Molecular gas in (U)LIRGs

1. Characterization of the molecular gas properties of 56 (U)LIRGs
   - Most complete, uniformly observed sample so far

2. Constrains on SFE

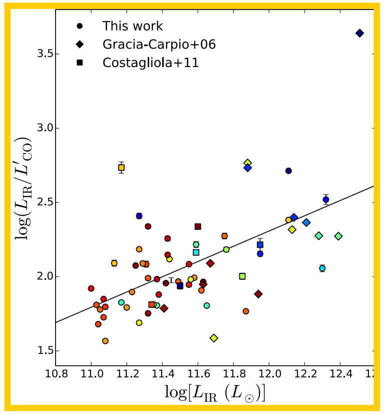

3. Dust temperature underestimation when using IRAS

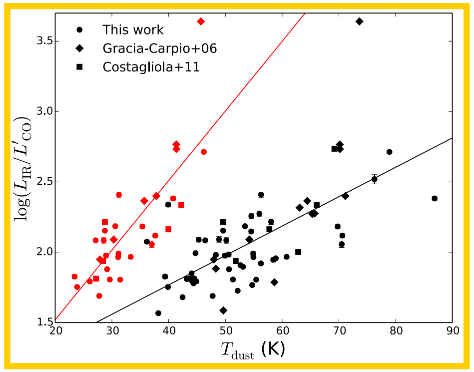

4. Spectral profiles
   - Inclination
   - Gas distribution

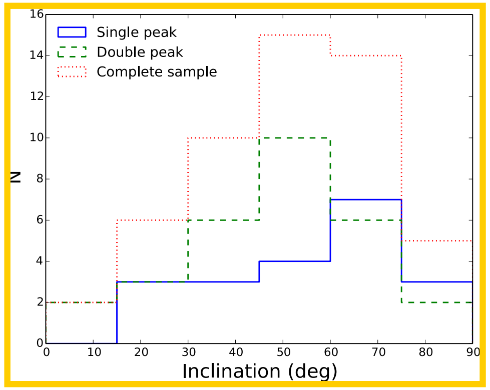

Outline

NGC1614: an exploratory study

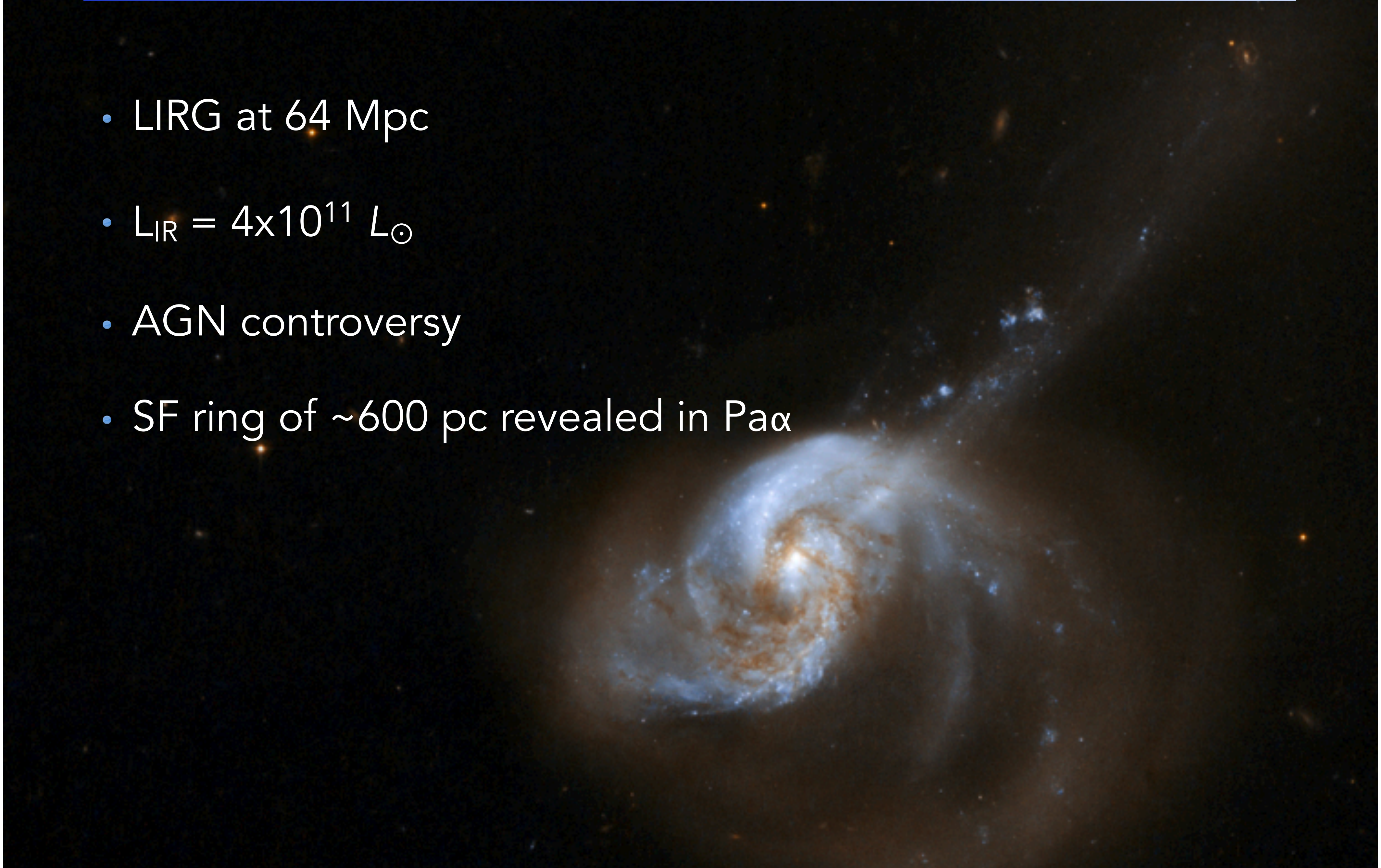

- LIRG at 64 Mpc
- L_{IR} = 4x10^{11} $L_{\odot}$
- AGN controversy
- SF ring of ~600 pc revealed in Paα

NGC1614: an exploratory study

- LIRG at 64 Mpc
- $L_{IR} = 4\text{x}10^{11}\ L_{\odot}$
- AGN controversy
- SF ring of ~600 pc revealed in Paα

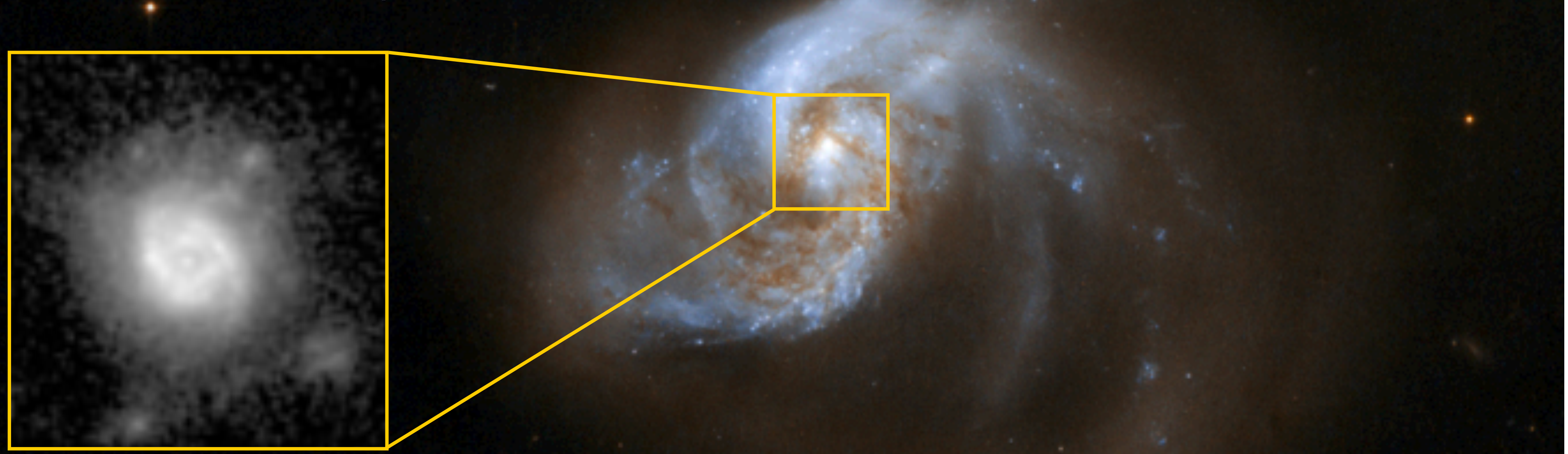

Alonso-Herrero *et al.*, 2001, ApJ

A multiwavelength study

- Morphological similarities
- Study of 7 regions within the ring

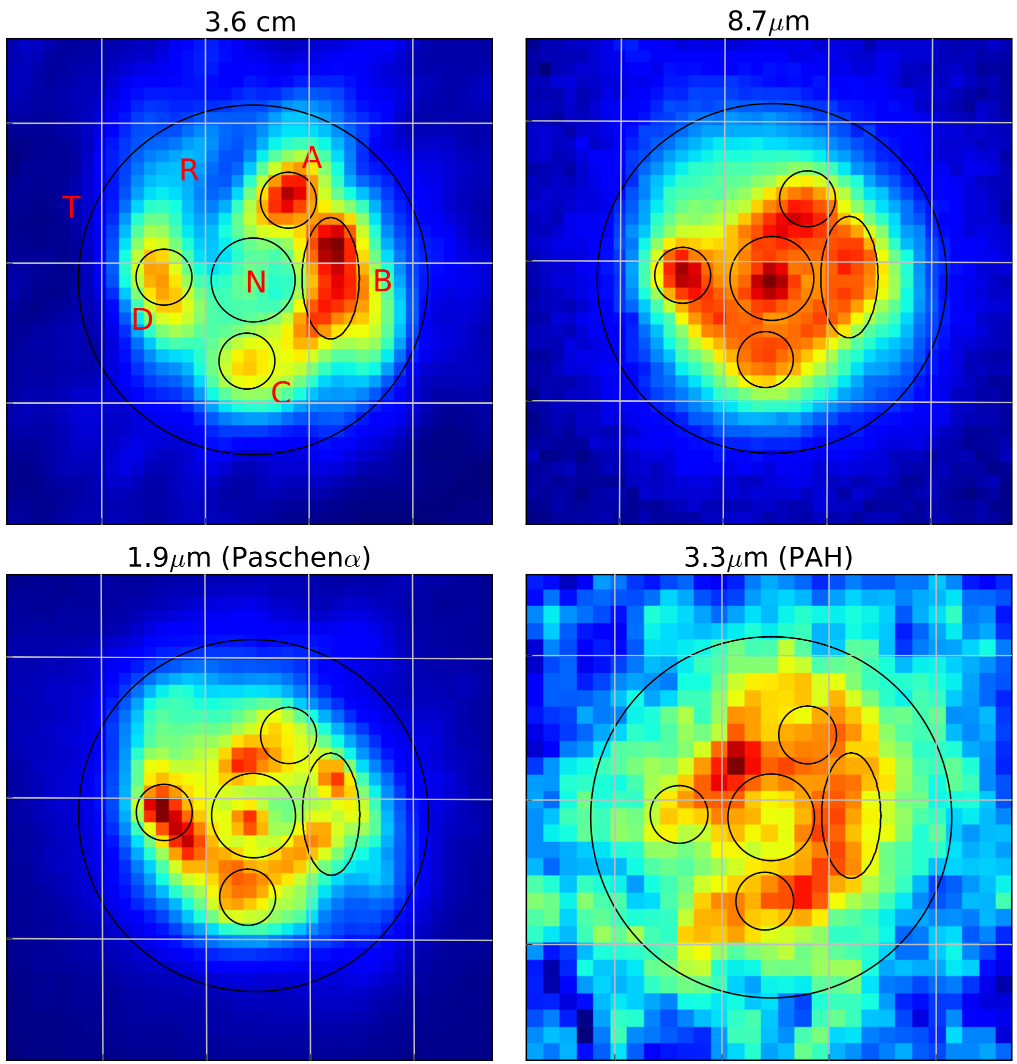

Herrero-Illana *et al.*, 2014, ApJ

Thermal and non-thermal radio emission

3.6 cm emission

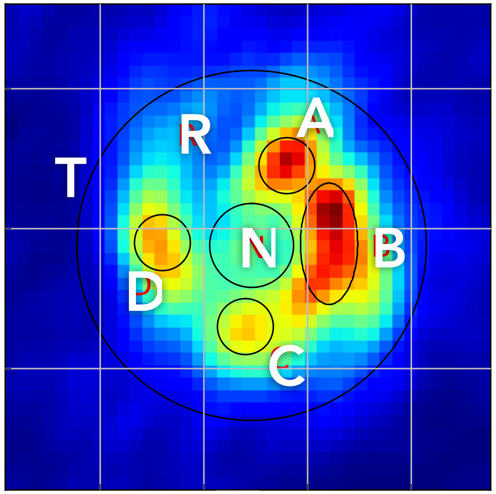

=

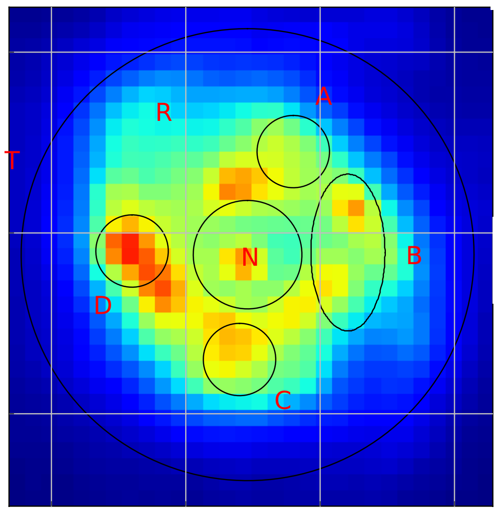

Thermal free-free

+

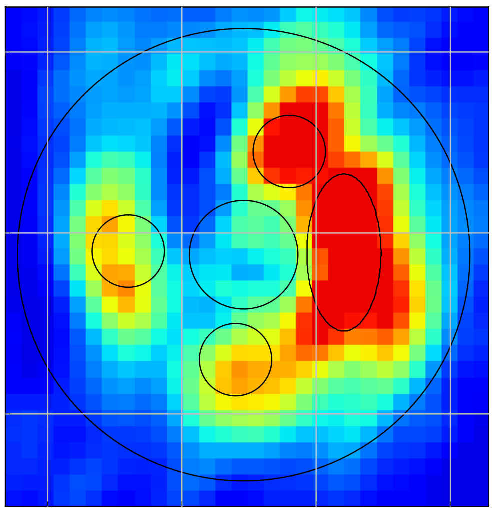

Non-thermal synchrotron

Assumed A_V = 4 mag

|

Unabsorbed Pa-α emission

|

$$S_{\rm thermal} = 1.076 \times 10^{13} \times F({\rm Pa}\alpha)\,\nu^{-0.1}$$

|

Thermal fraction

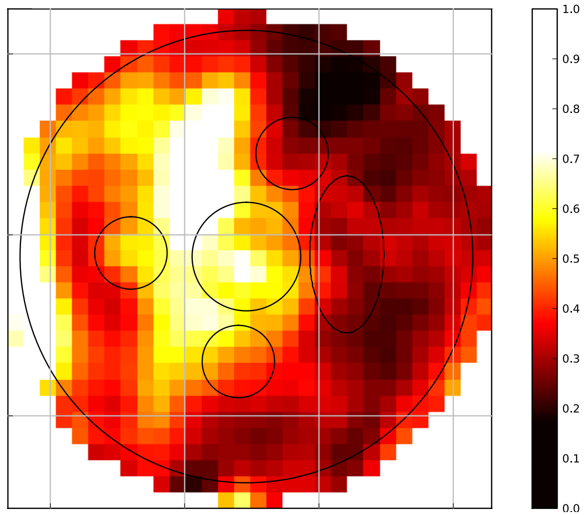

Herrero-Illana *et al.*, 2014, ApJ

Thermal and non-thermal radio emission

3.6 cm emission

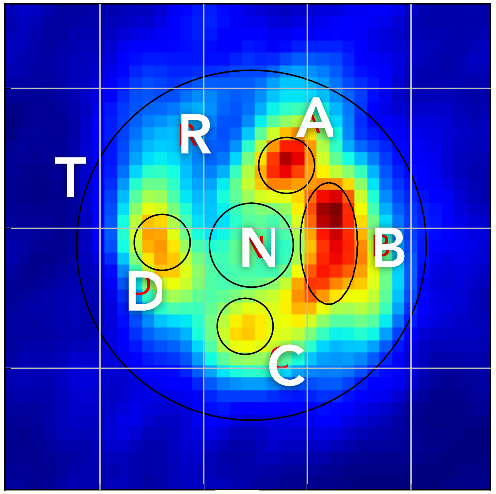

=

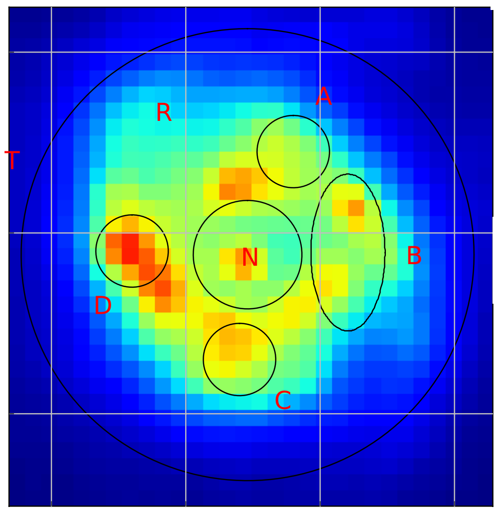

Thermal free-free

+

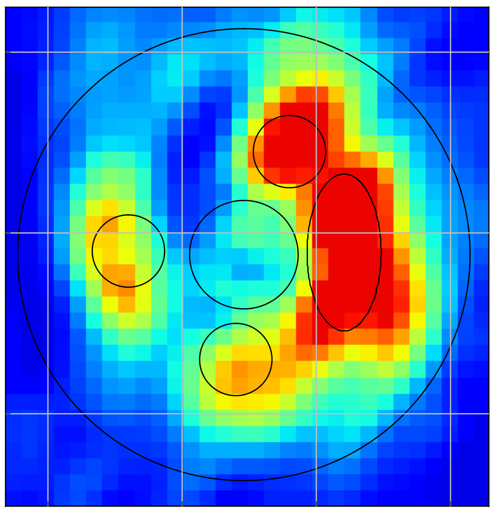

Non-thermal synchrotron

Assumed A_V = 4 mag

|

Unabsorbed Pa-α emission

|

$$S_{\rm thermal} = 1.076 \times 10^{13} \times F({\rm Pa}\alpha)\,\nu^{-0.1}$$

|

Thermal fraction

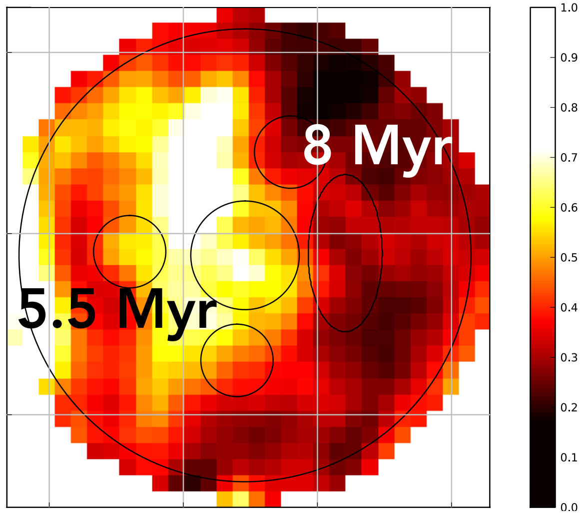

Herrero-Illana *et al.*, 2014, ApJ

Multi-epoch & multi-band observations

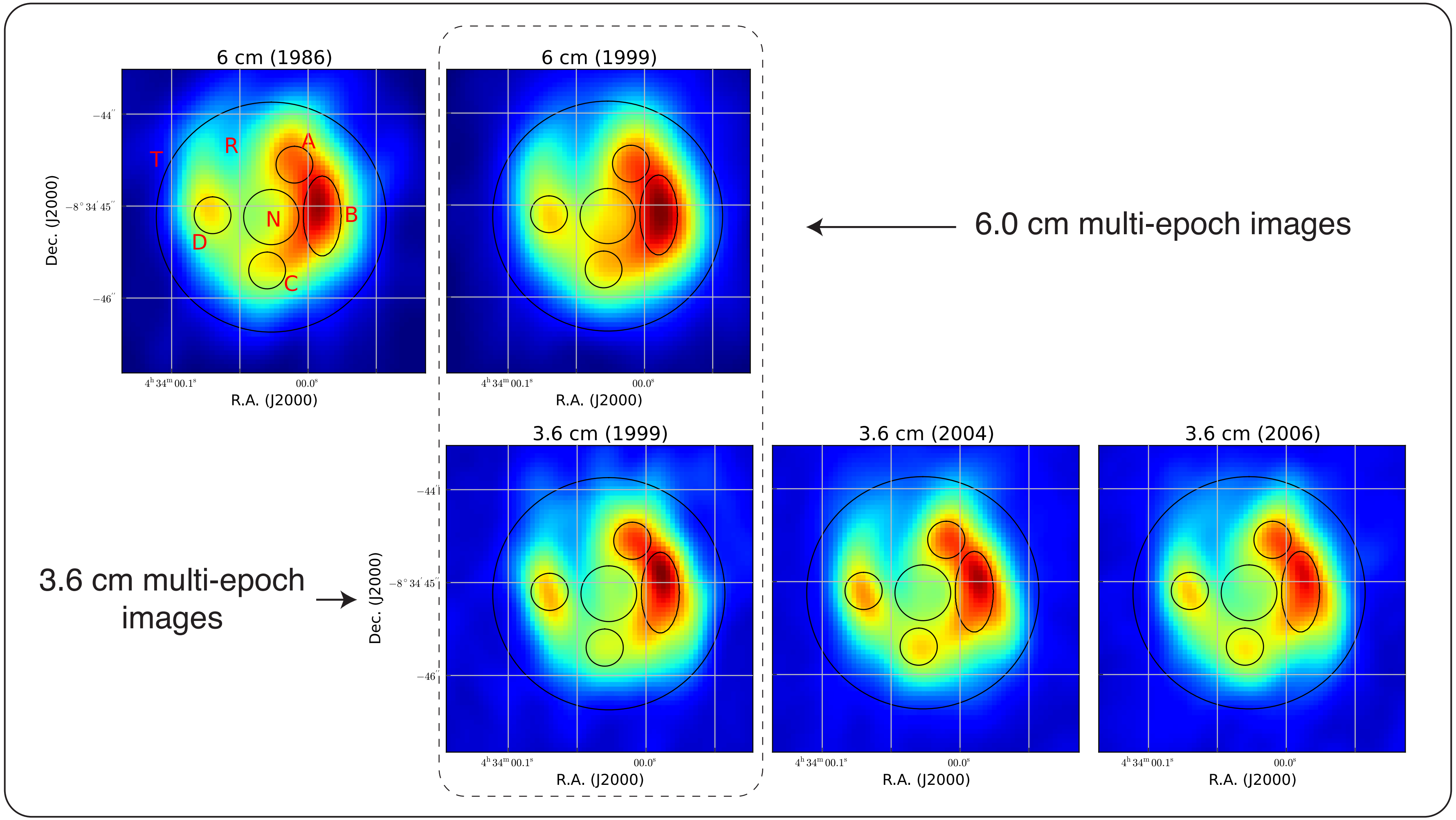

No significance variability

$$\alpha_{\mathrm{N}} \simeq -1.3$$

X-ray emission

- *Chandra* archive observations
- Models:
  - Thermal
    - MEKAL
    - VMEKAL
  - Non-thermal
    - PL
  - Mix
    - MEPL

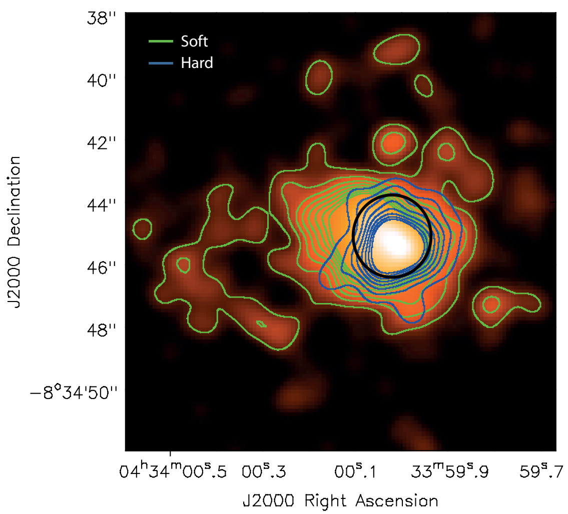

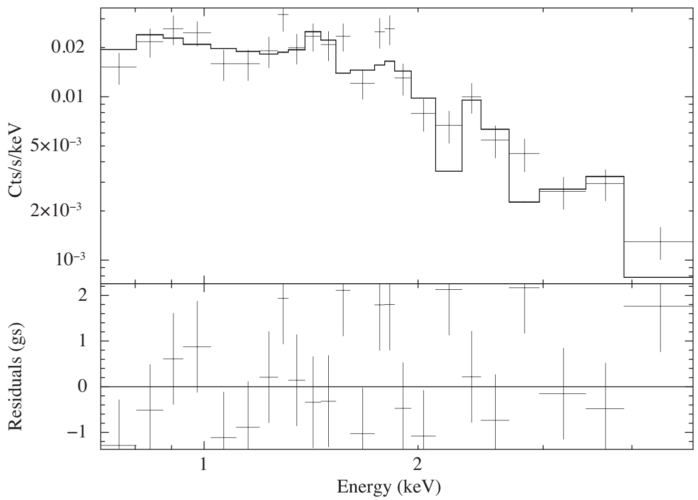

Herrero-Illana *et al.*, 2014, ApJ

X-ray emission

- *Chandra* archive observations
- Models:

Thermal		Non-thermal	Mix
MEKAL	VMEKAL	PL	MEPL

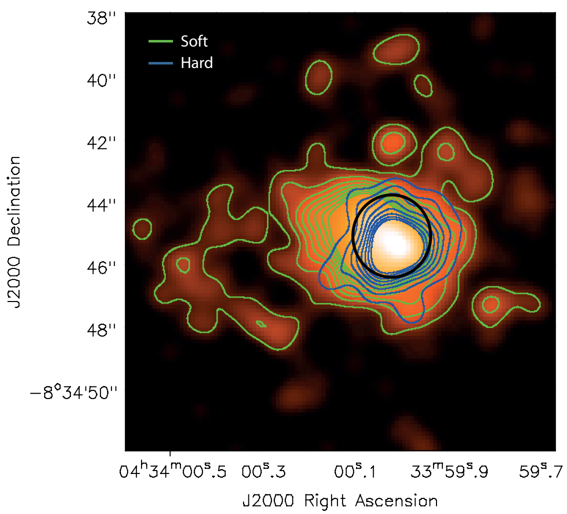

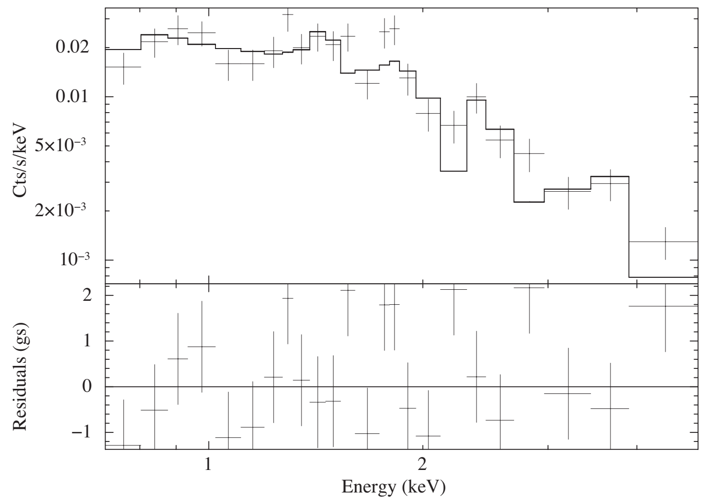

Herrero-Illana *et al.*, 2014, ApJ

Models the metal abundance pattern of type II SNe regions

Mg XI Si XIII S XV

$$\log L(0.5 - 2\,\mathrm{keV}) = 40.87^{+0.04}_{-0.05}\,\mathrm{erg/s}$$

$$kT = 1.7 \pm 0.7\,\mathrm{keV}$$

NGC1614 SED model fitting

- Exponentially decaying starburst
- Global fit
- SFR: 60 $M_{\odot}$/yr
- CCSN rate ~0.4 SN/yr

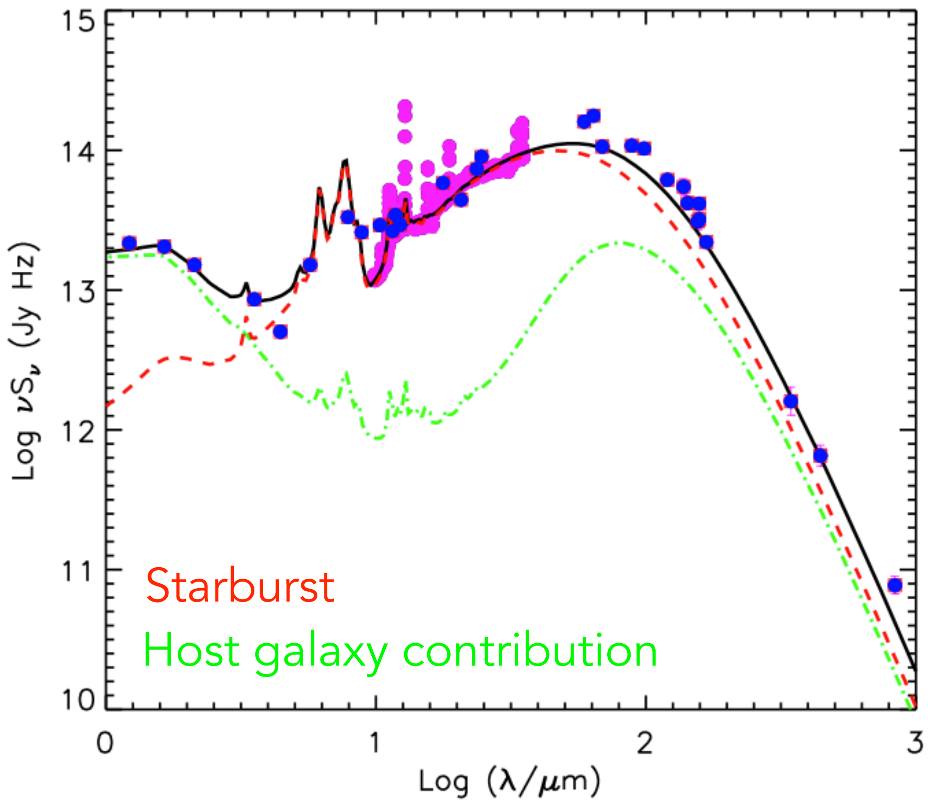

Herrero-Illana *et al.*, 2014, ApJ

NGC1614 as a case study

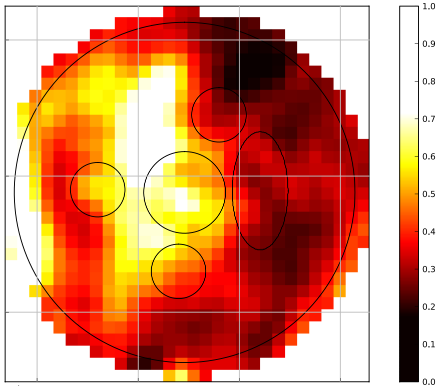

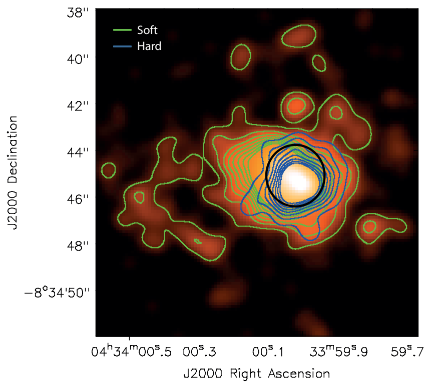

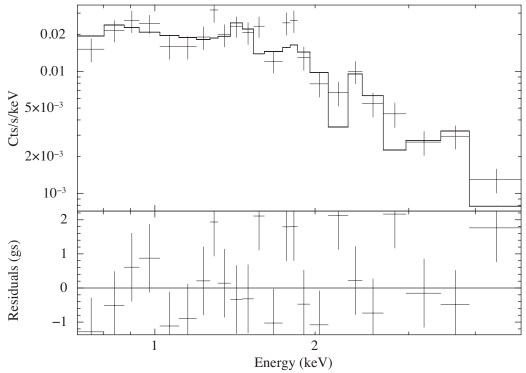

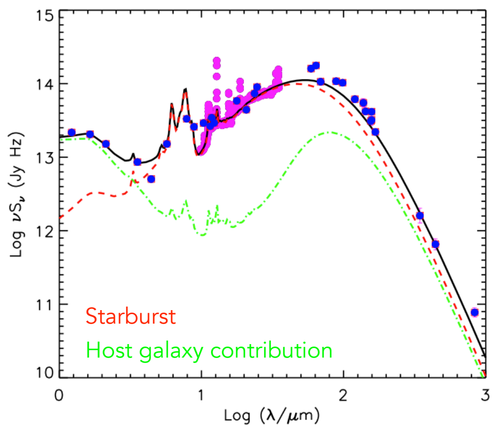

1. Central kpc characterization
2. SF ring age differentiation
3. SED modeling
4. All our analyzed observations suggest a pure starburst

Outline

A multiwavelength approach

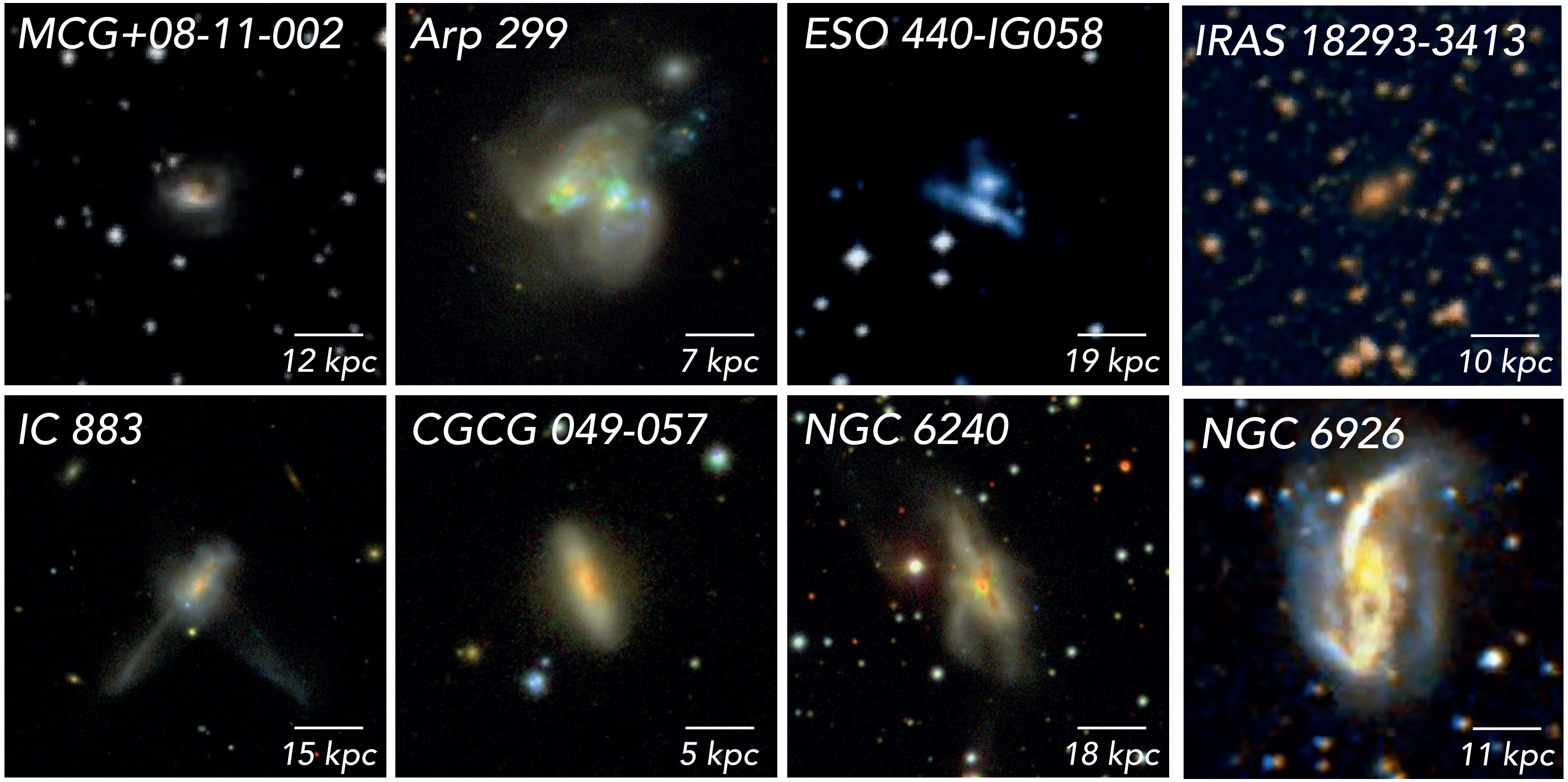

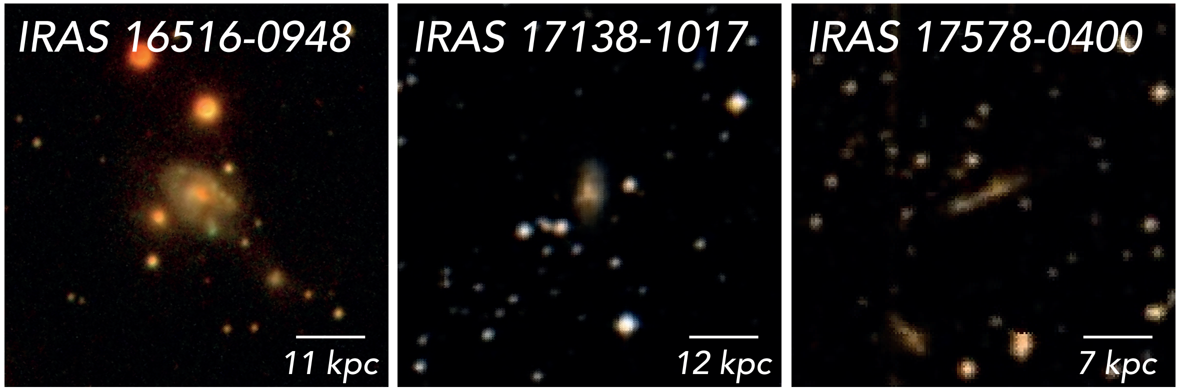

$48 < D_L$ / Mpc < 100

$11.24 < \log(L_{IR} / L_{\odot}) < 11.88$

Different stage mergers

Radio and Near-IR comparison

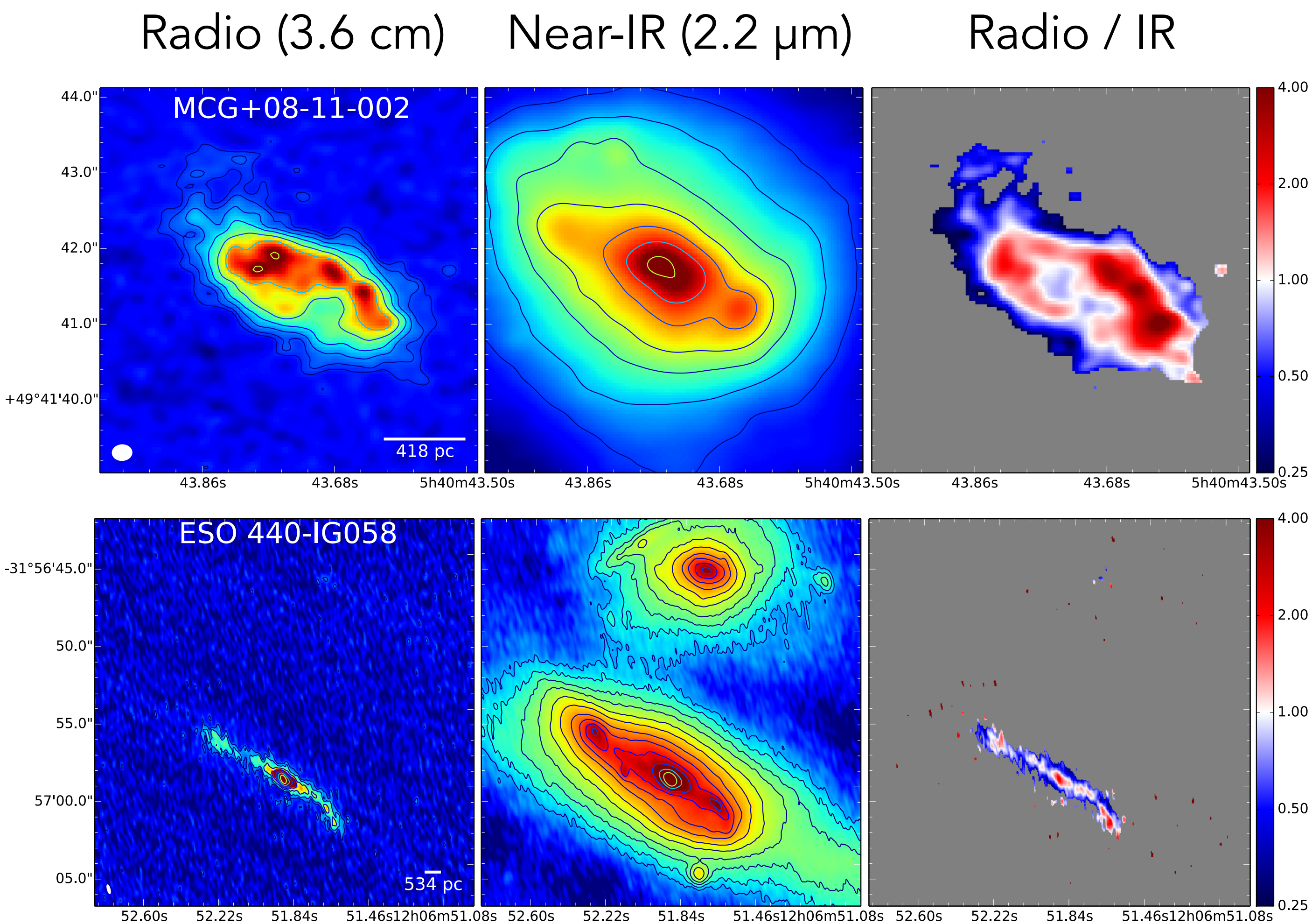

Radio and Near-IR comparison

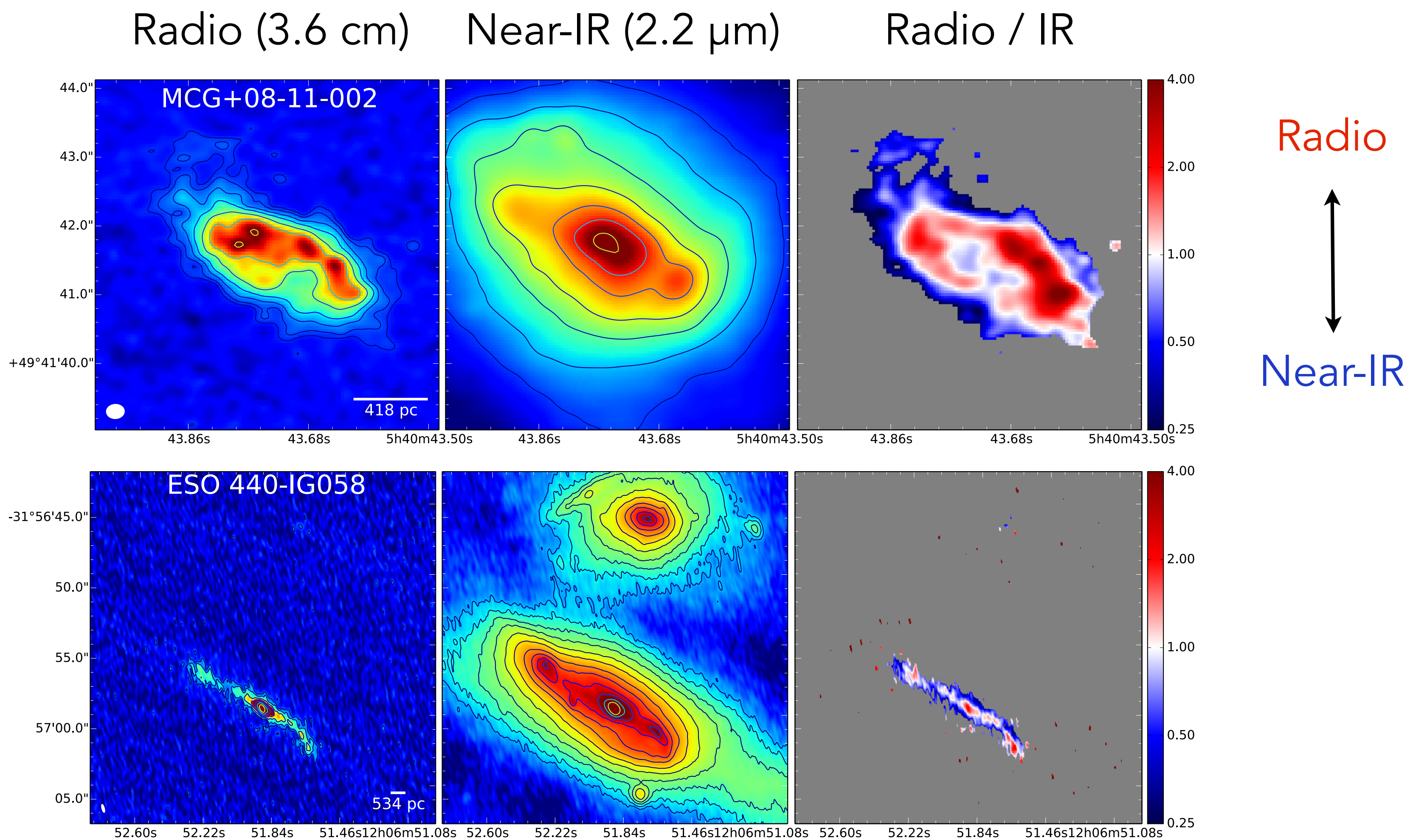

Radio and Near-IR comparison

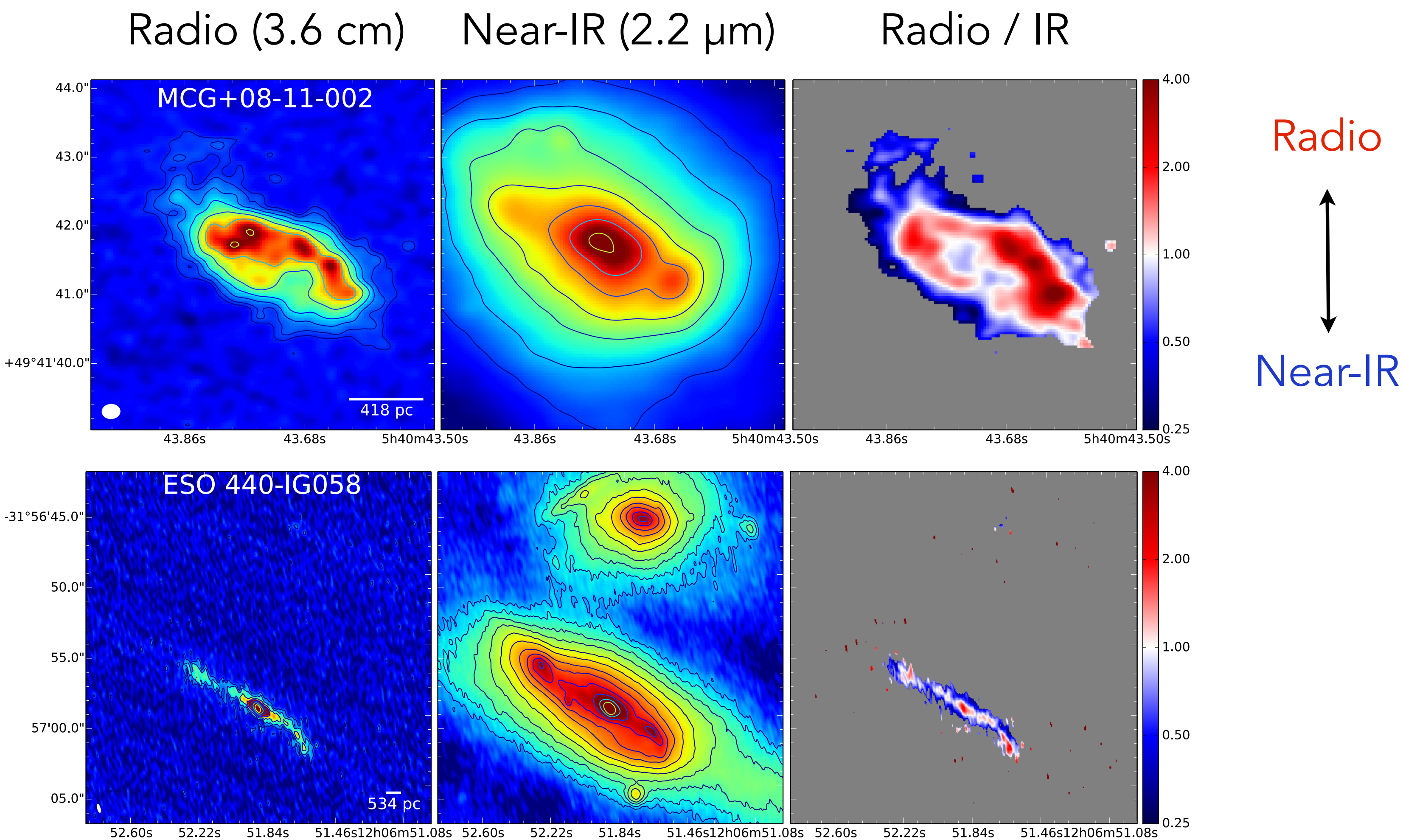

ESO440-IG058: nascent starburst?

Radio and Near-IR comparison

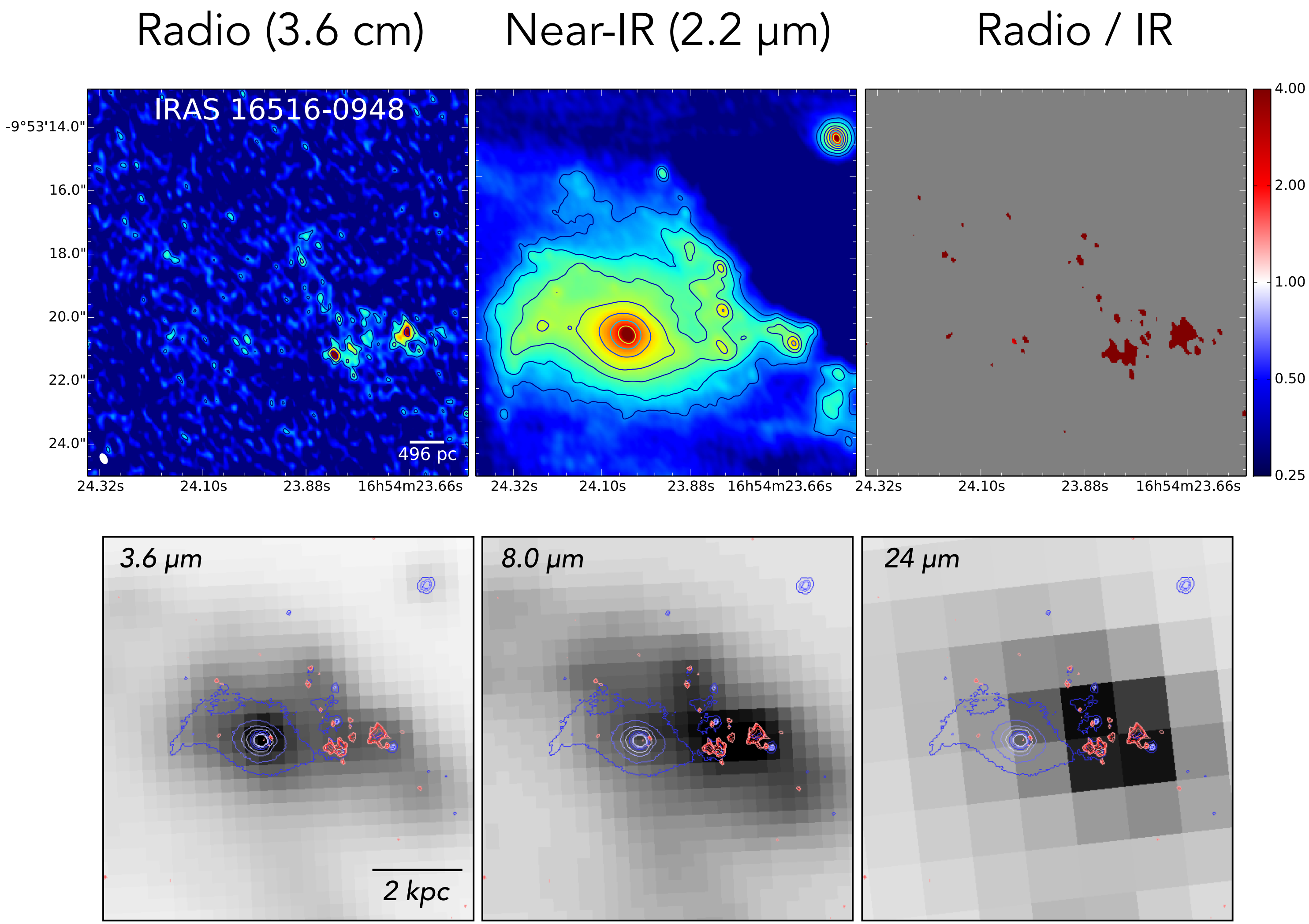

Off-nuclear starburst, possibly triggered by the merging process

Spectral index maps

$$I_\nu^{\text{sky}} = I_{\nu_0}^{\text{sky}} \left(\frac{\nu}{\nu_0} \right)^\alpha$$

Name	Average α
MCG+08-11-002	-1.09 ± 0.58
NGC 3690W	-1.01 ± 0.64
NGC 3690E	-0.65 ± 0.35
ESO 440-IG058	-0.60 ± 0.36
IC 883	-0.68 ± 0.90
CGCG 049-057	-0.78 ± 0.54
NGC 6240	-0.99 ± 0.76
IRAS 16516-0948	...
IRAS 17138-1017	-0.85 ± 0.80
IRAS 17578-0400	-0.64 ± 0.70
IRAS 18293-3413	-1.73 ± 0.70
NGC 6926	-0.76 ± 1.00

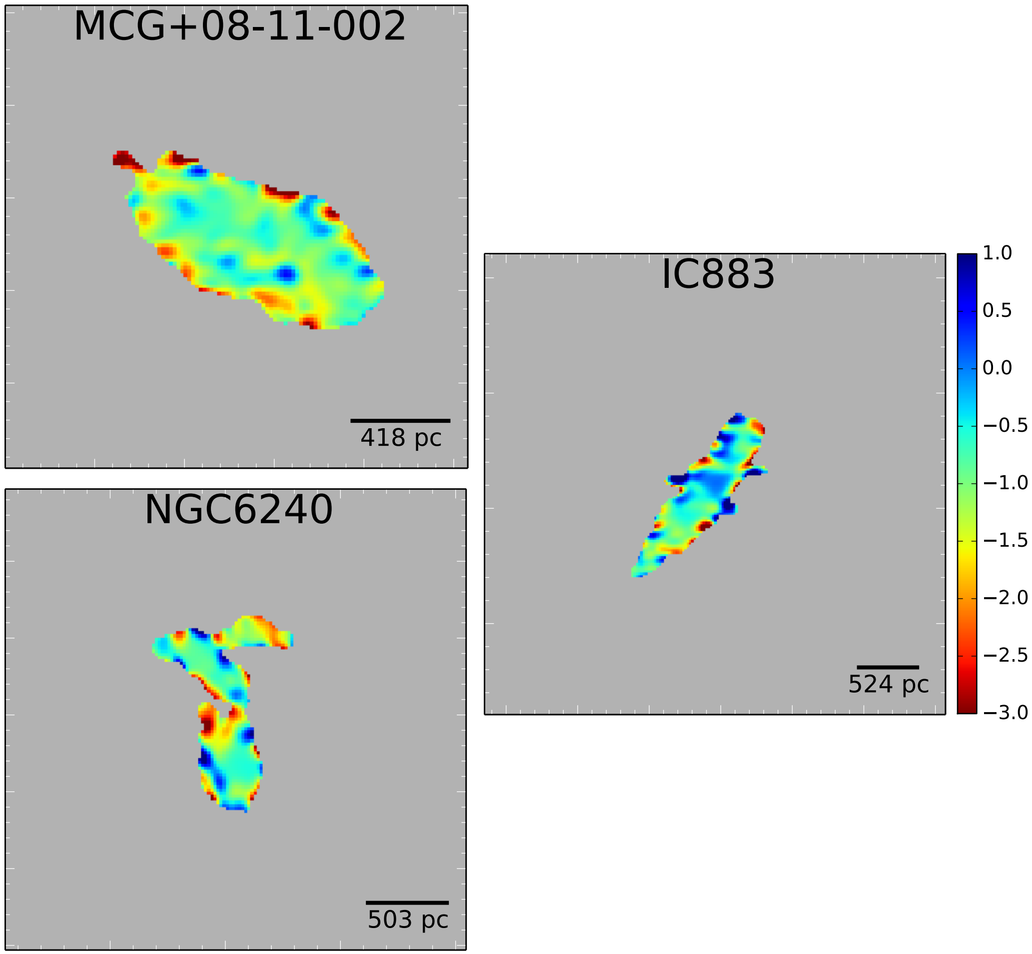

Our sources show typical starburst spectral indices

SED modeling

Source	Age SB (Myr)	CCSN rate (SN/yr)	AGN/SB
MCG+08-11-002	47.9	0.14	0.0
IC883	34.3	0.64	0.32
IRAS16516	27.1	0.16	0.0
IRAS17138	9.1	0.10	0.19
IRAS18293	22.4	0.81	0.0
NGC6926	7.7	0.02	7.76

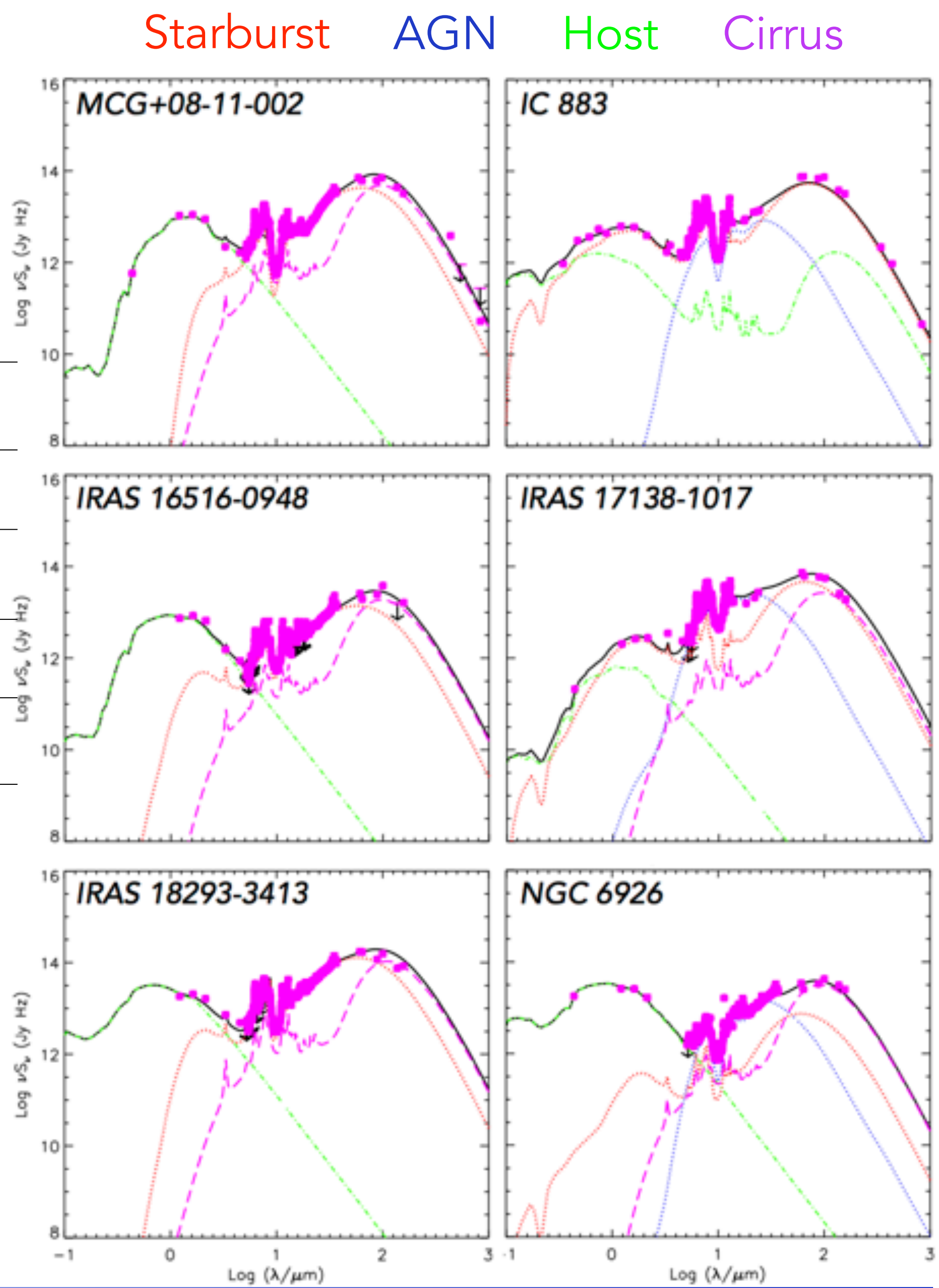

SED modeling

Source	Age SB (Myr)	CCSN rate (SN/yr)	AGN/SB
MCG+08-11-002	47.9	0.14	0.0
IC883	34.3	0.64	0.32
IRAS16516	27.1	0.16	0.0
IRAS17138	9.1	0.10	0.19
IRAS18293	22.4	0.81	0.0
NGC6926	7.7	0.02	7.76

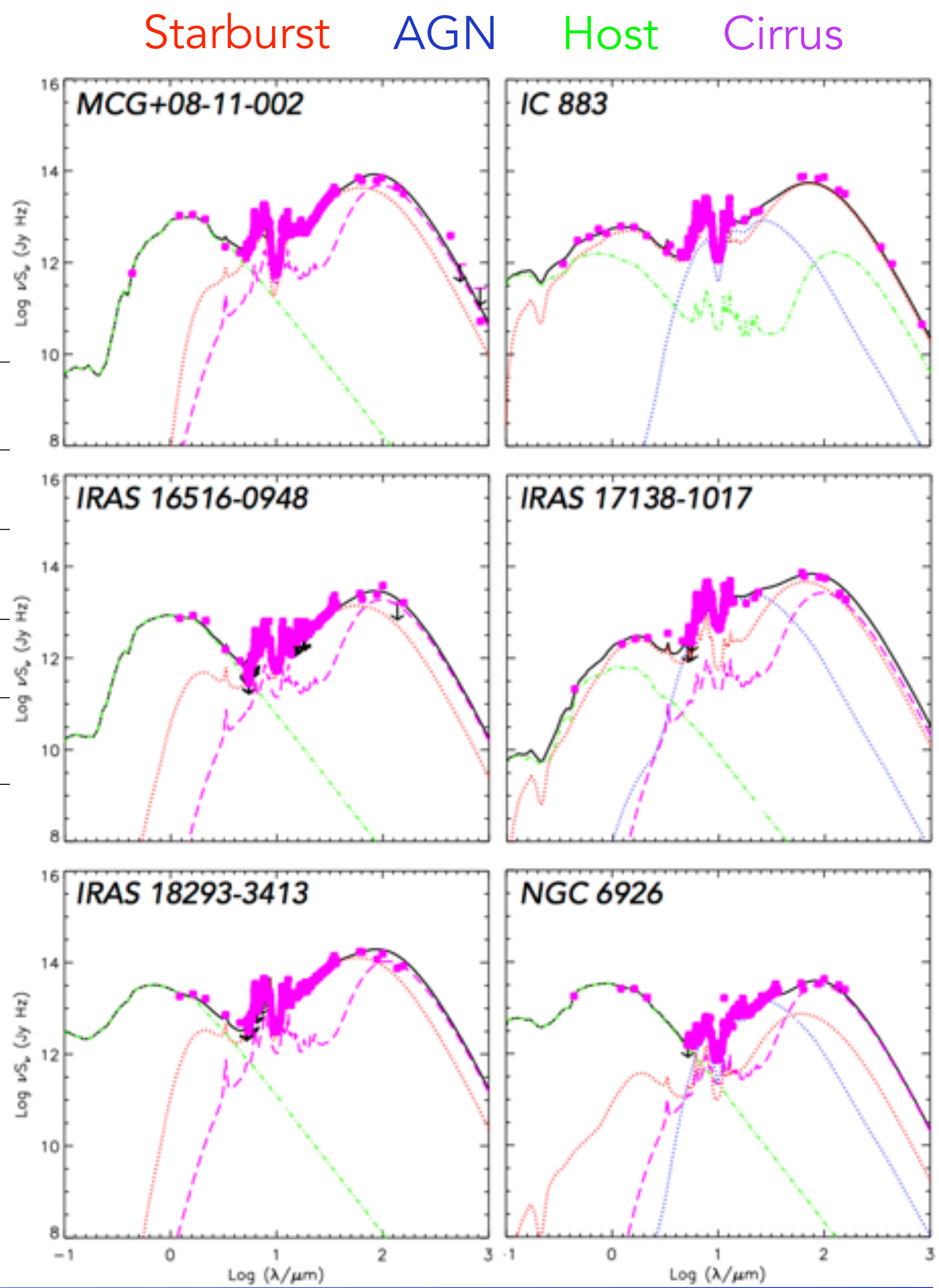

SED modeling

Source	Age SB (Myr)	CCSN rate (SN/yr)	AGN/SB
MCG+08-11-002	47.9	0.14	0.0
IC883	34.3	0.64	0.32
IRAS16516	27.1	0.16	0.0
IRAS17138	9.1	0.10	0.19
IRAS18293	22.4	0.81	0.0
NGC6926	7.7	0.02	7.76

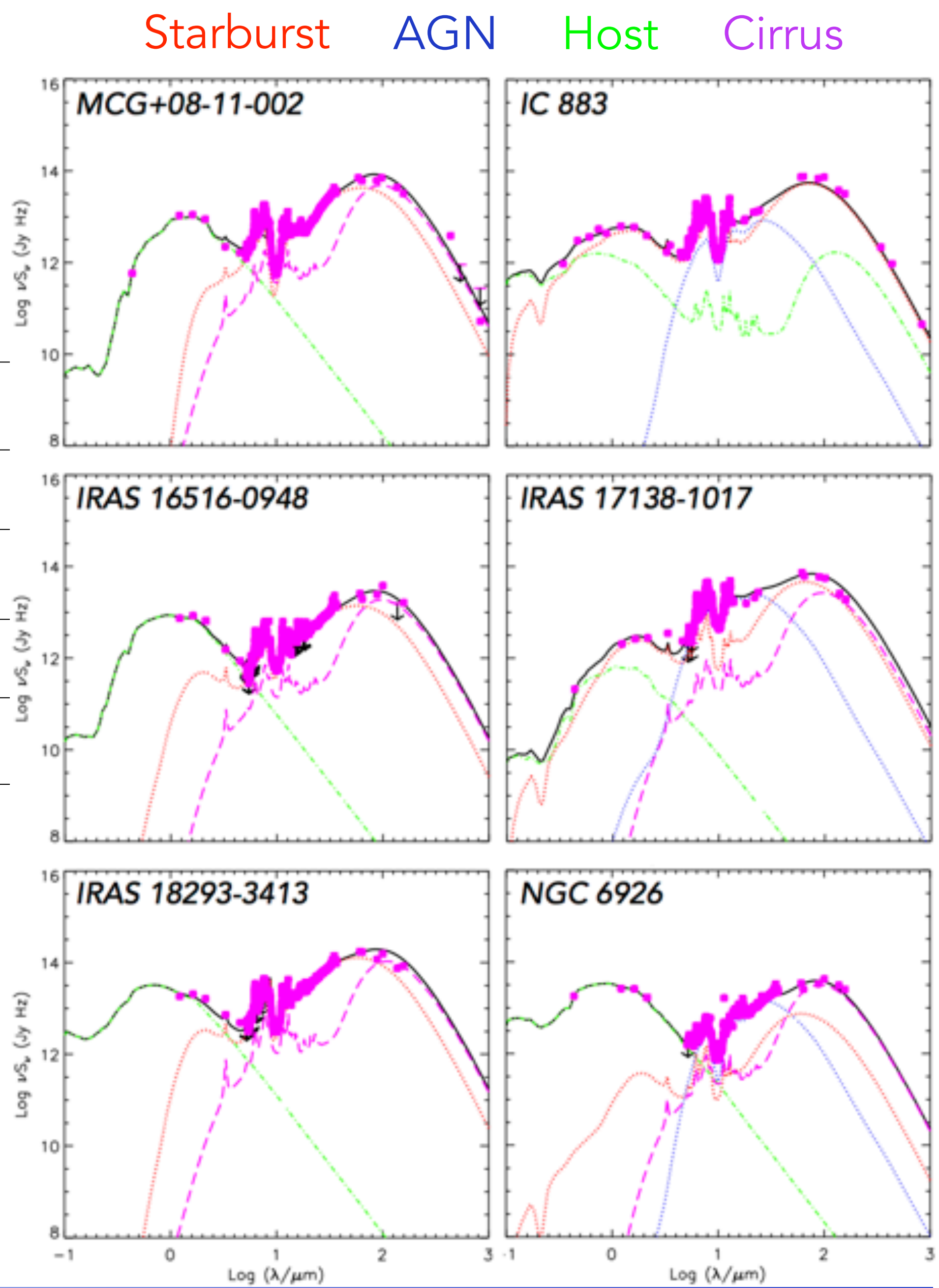

SED modeling

Source	Age SB (Myr)	CCSN rate (SN/yr)	AGN/SB
MCG+08-11-002	47.9	0.14	0.0
IC883	34.3	0.64	0.32
IRAS16516	27.1	0.16	0.0
IRAS17138	9.1	0.10	0.19
IRAS18293	22.4	0.81	0.0
NGC6926	7.7	0.02	7.76

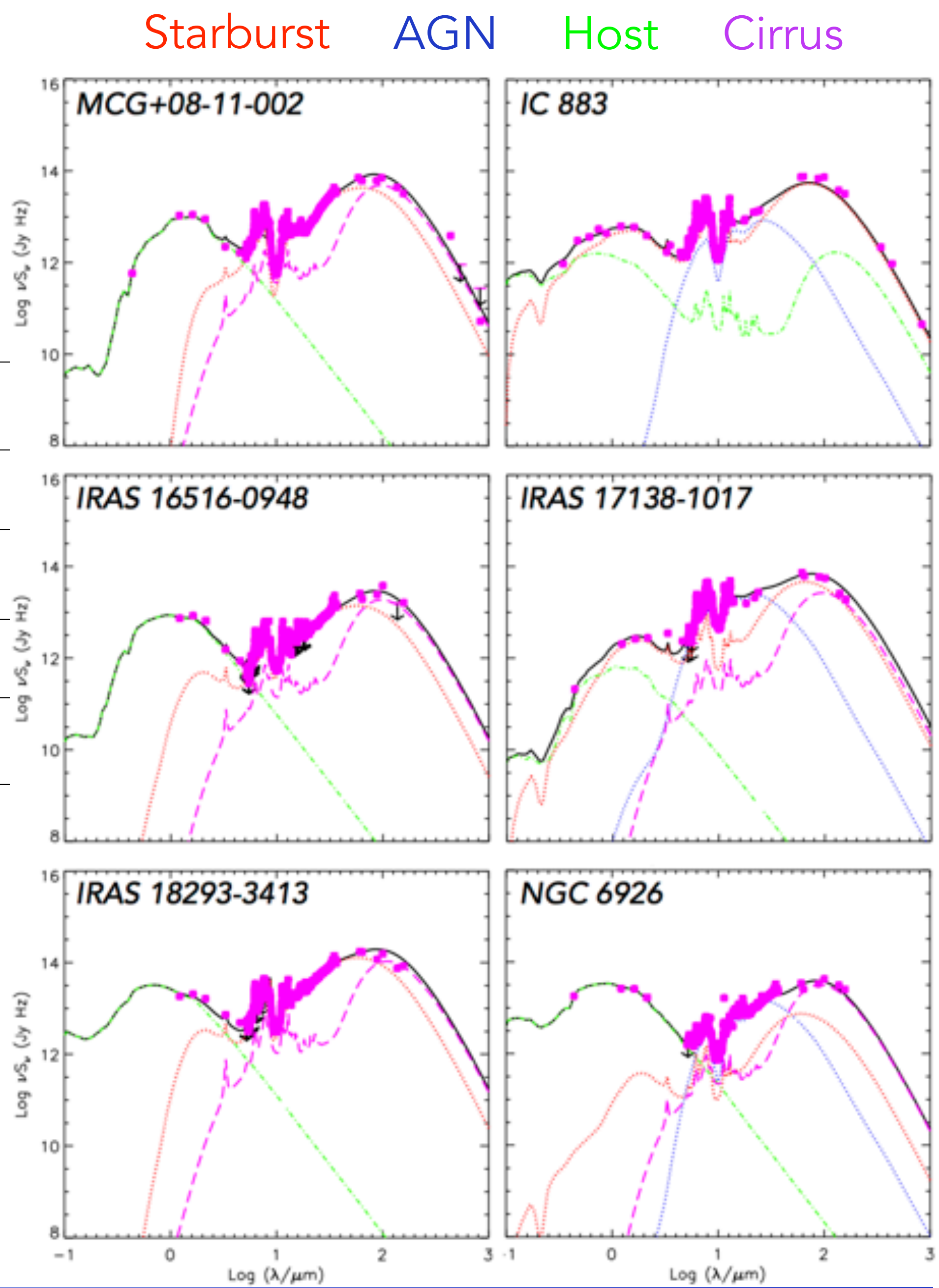

SED modeling

Source	Age SB (Myr)	CCSN rate (SN/yr)	AGN/SB
MCG+08-11-002	47.9	0.14	0.0
IC883	34.3	0.64	0.32
IRAS16516	27.1	0.16	0.0
IRAS17138	9.1	0.10	0.19
IRAS18293	22.4	0.81	0.0
NGC6926	7.7	0.02	7.76

AGN diagnostics

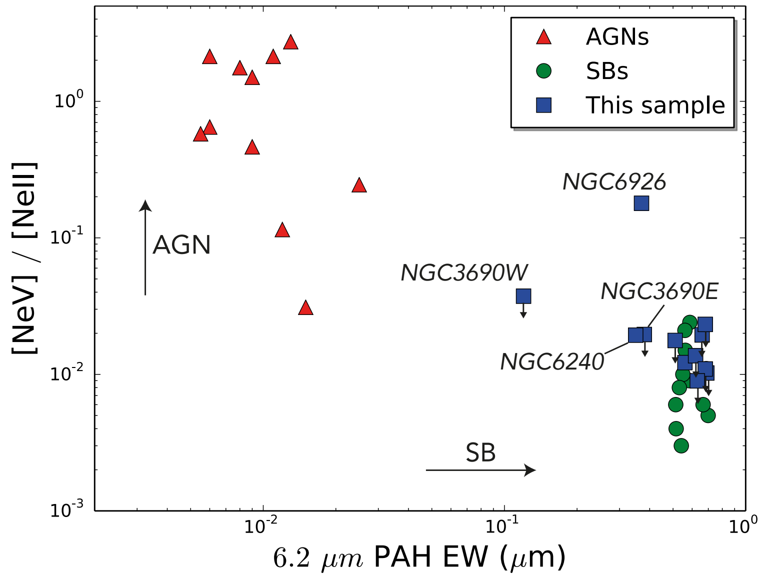

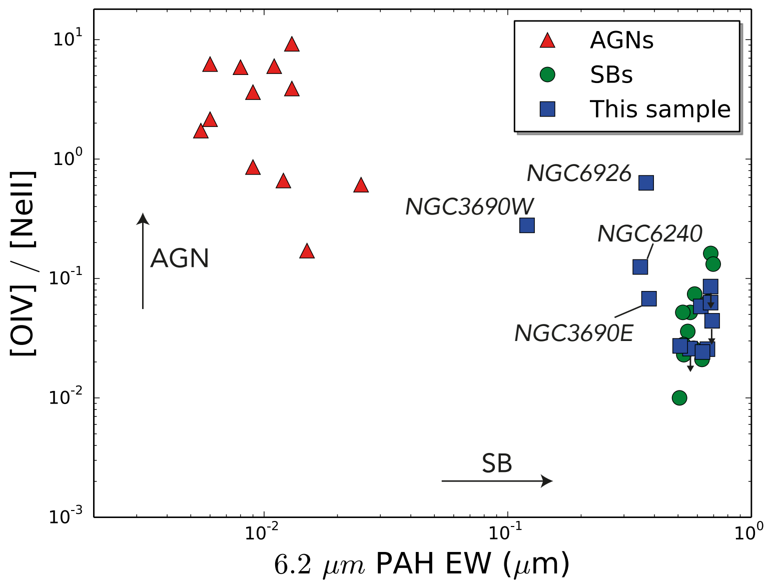

SED modeling

Source	Age SB (Myr)	CCSN rate (SN/yr)	AGN/SB
MCG+08-11-002	47.9	0.14	0.0
IC883	34.3	0.64	0.32
IRAS16516	27.1	0.16	0.0
IRAS17138	9.1	0.10	0.19
IRAS18293	22.4	0.81	0.0
NGC6926	7.7	0.02	7.76

General agreement between SED modeling and AGN diagnostics (handle it with care!)

AGN diagnostics

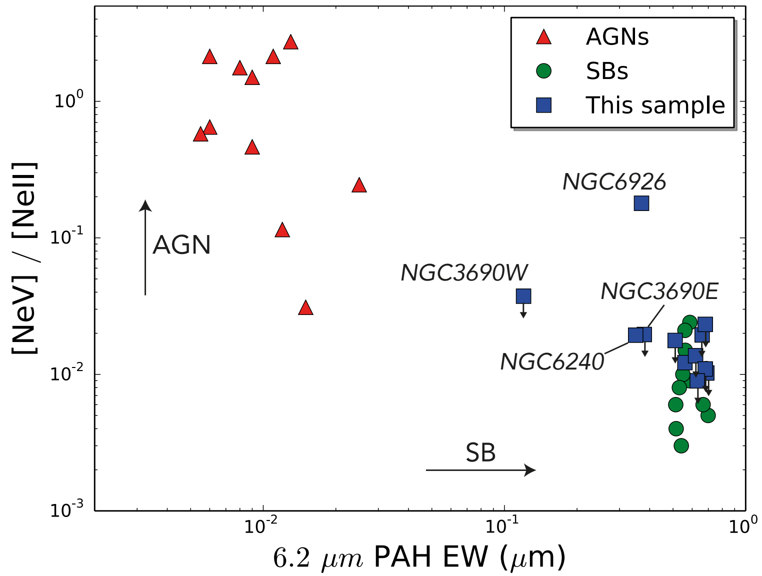

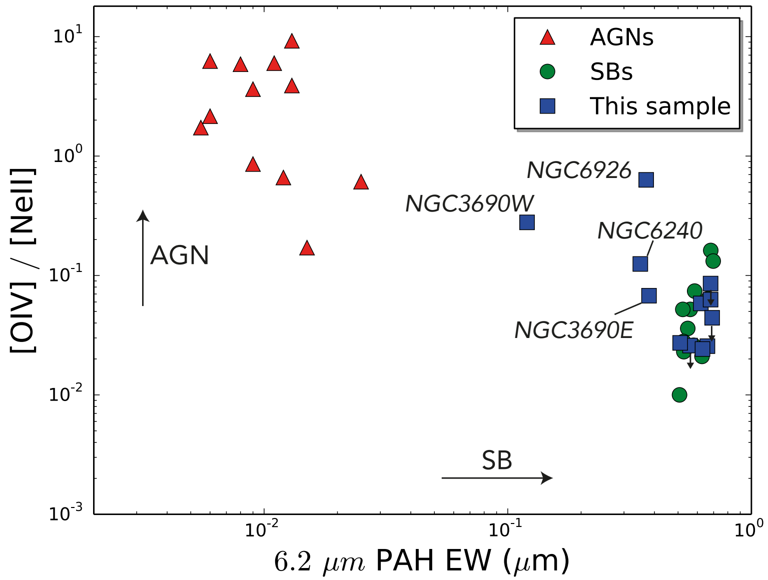

Multiwavelength study of LIRGs

1

No common pattern on Radio / near-IR maps

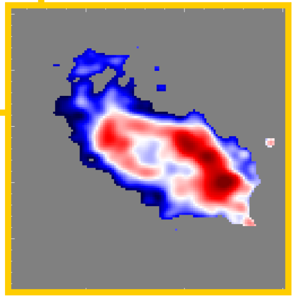

2

Off-nuclear SB on IRAS16156-0948

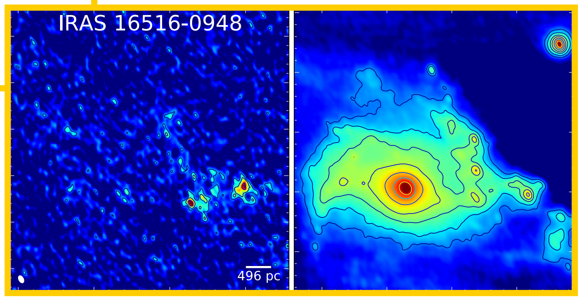

3

Typical starburst spectral indices

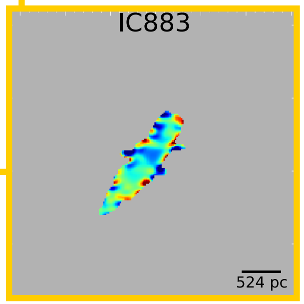

4

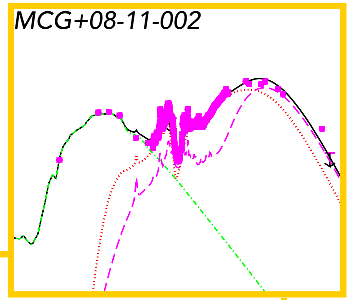

SED modeling

AGN diagnostics

Outline

LIRGI

J. Conway *M. Á. Pérez-Torres*

- Luminous Infra-Red Galaxy Inventory http://lirgi.iaa.es
- 42 of the most luminous northern LIRGs. Similar properties to SF galaxies at high-z
- $\log(L_{IR}) > 11.4$ - $D < 250$ Mpc
- 6 and 18 cm observations - 353 hours
- Complementary EVN observations

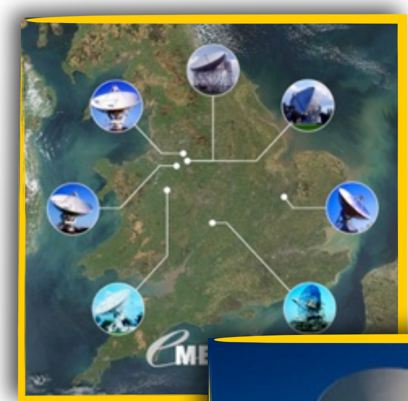

Lovell Telescope - 76 m

LIRGI

J. Conway *M. Á. Pérez-Torres*

eMERLIN

- Luminous Infra-Red Galaxy Inventory http://lirgi.iaa.es
- 42 of the most luminous northern LIRGs.
  Similar properties to SF galaxies at high-z
- log(L_{IR}) > 11.4 - D < 250 Mpc
- 6 and 18 cm observations - 353 hours
- Complementary EVN observations

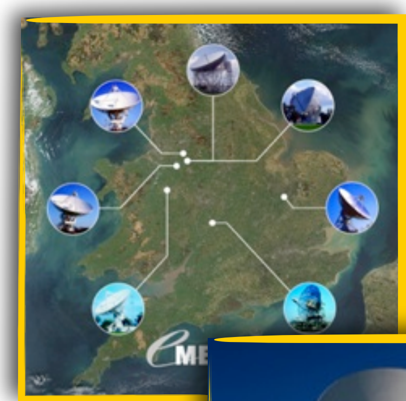

Lovell Telescope - 76 m

Naím Ramírez-Olivencia PhD Thesis!

Arp 299 overview

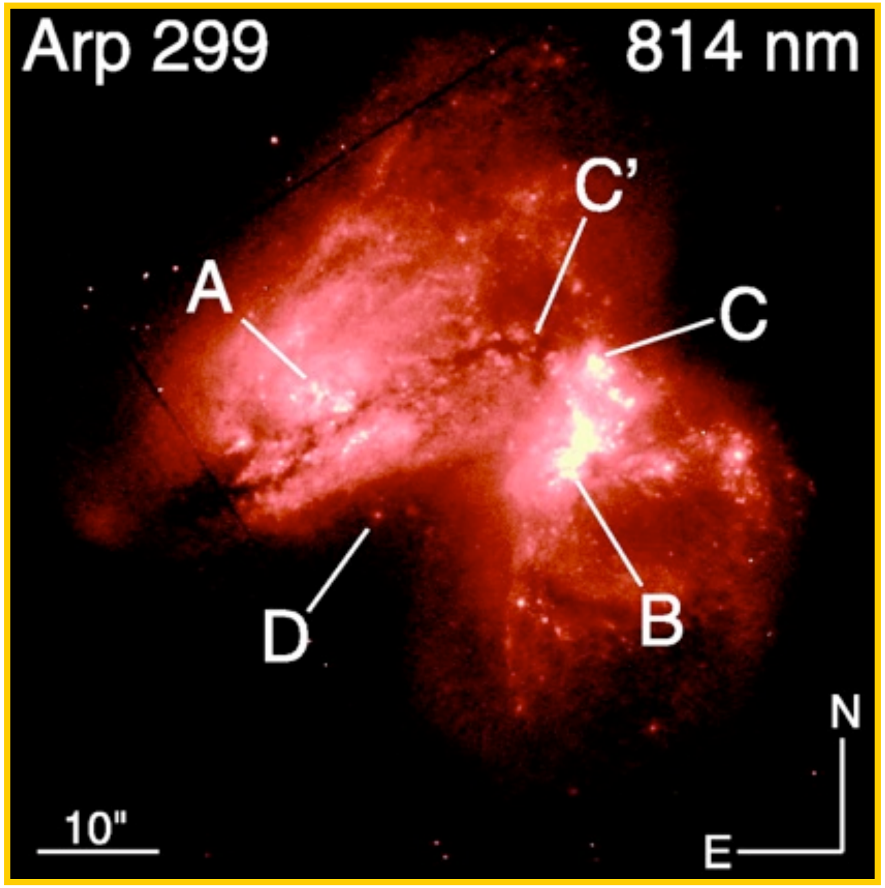

Neff *et al.*, 2004, ApJ

- Most luminous local LIRG
- L_{IR} ~7.6x10^{11} $L_{\odot}$
- D ~ 45 Mpc
- Mid-stage merger

Arp 299: e-MERLIN @ 5GHz

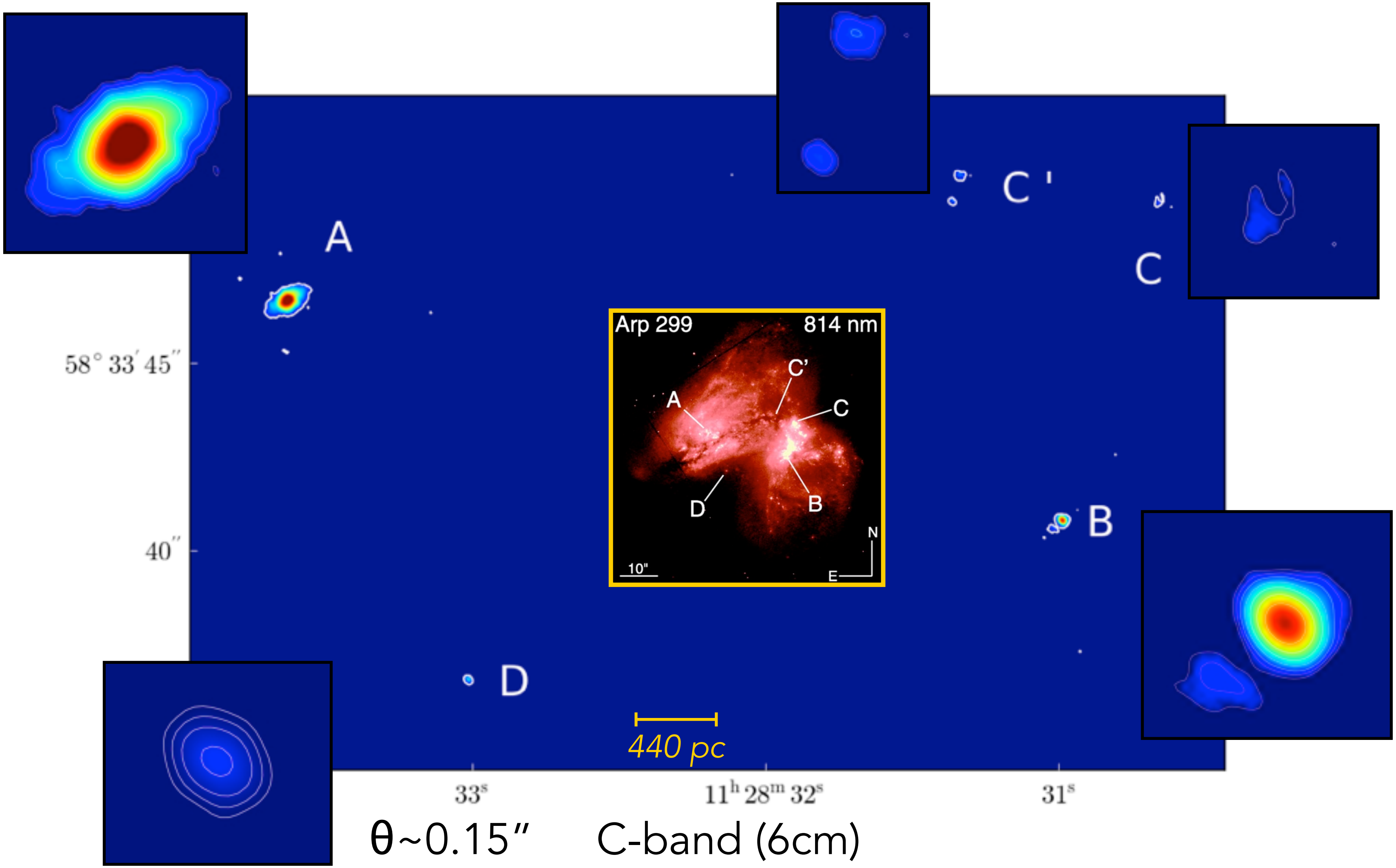

θ~0.15″ C-band (6cm)

Arp 299: e-MERLIN @ 5GHz

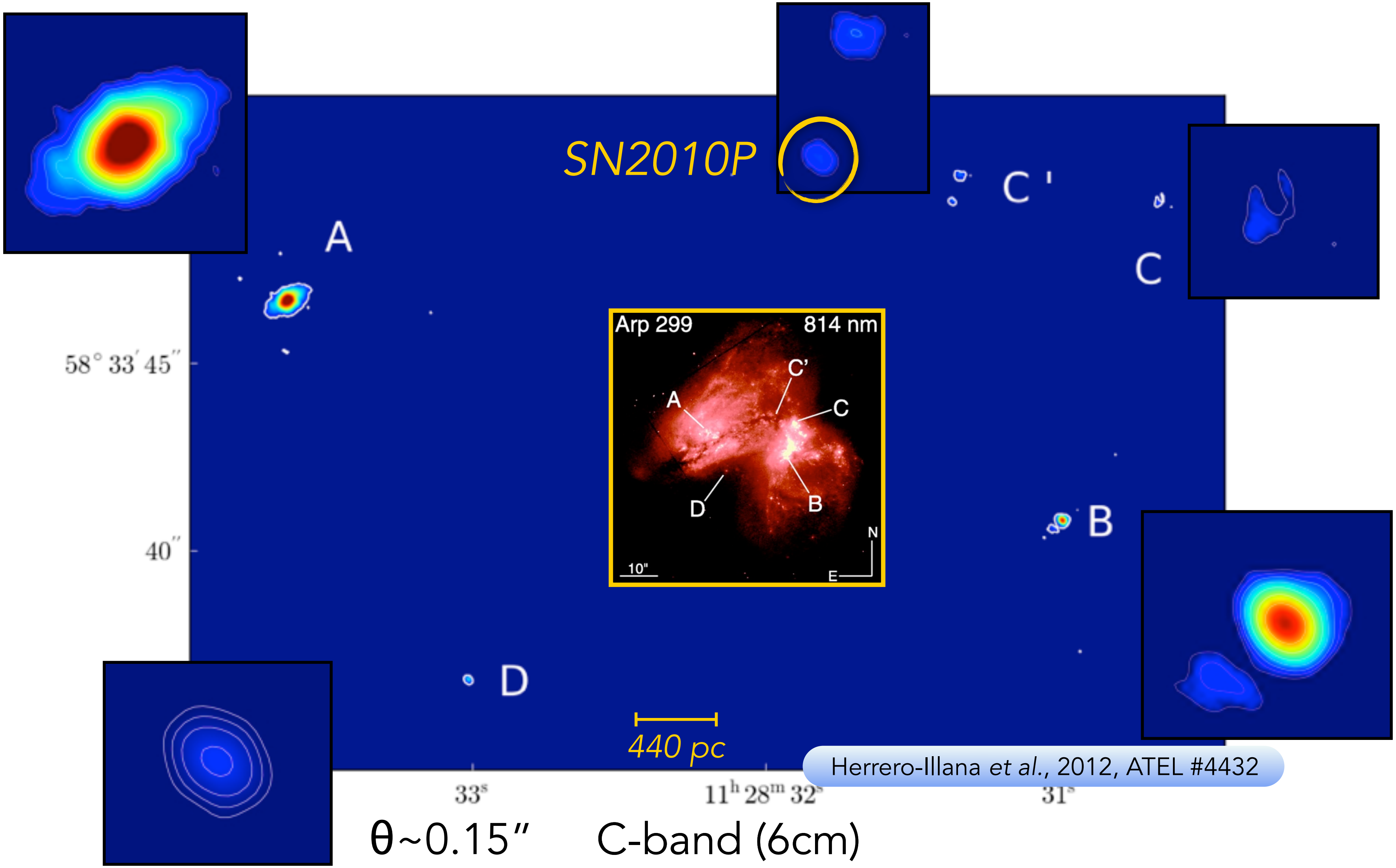

Herrero-Illana *et al.*, 2012, ATEL #4432

θ~0.15″ C-band (6cm)

Arp 299: e-MERLIN @ 5GHz

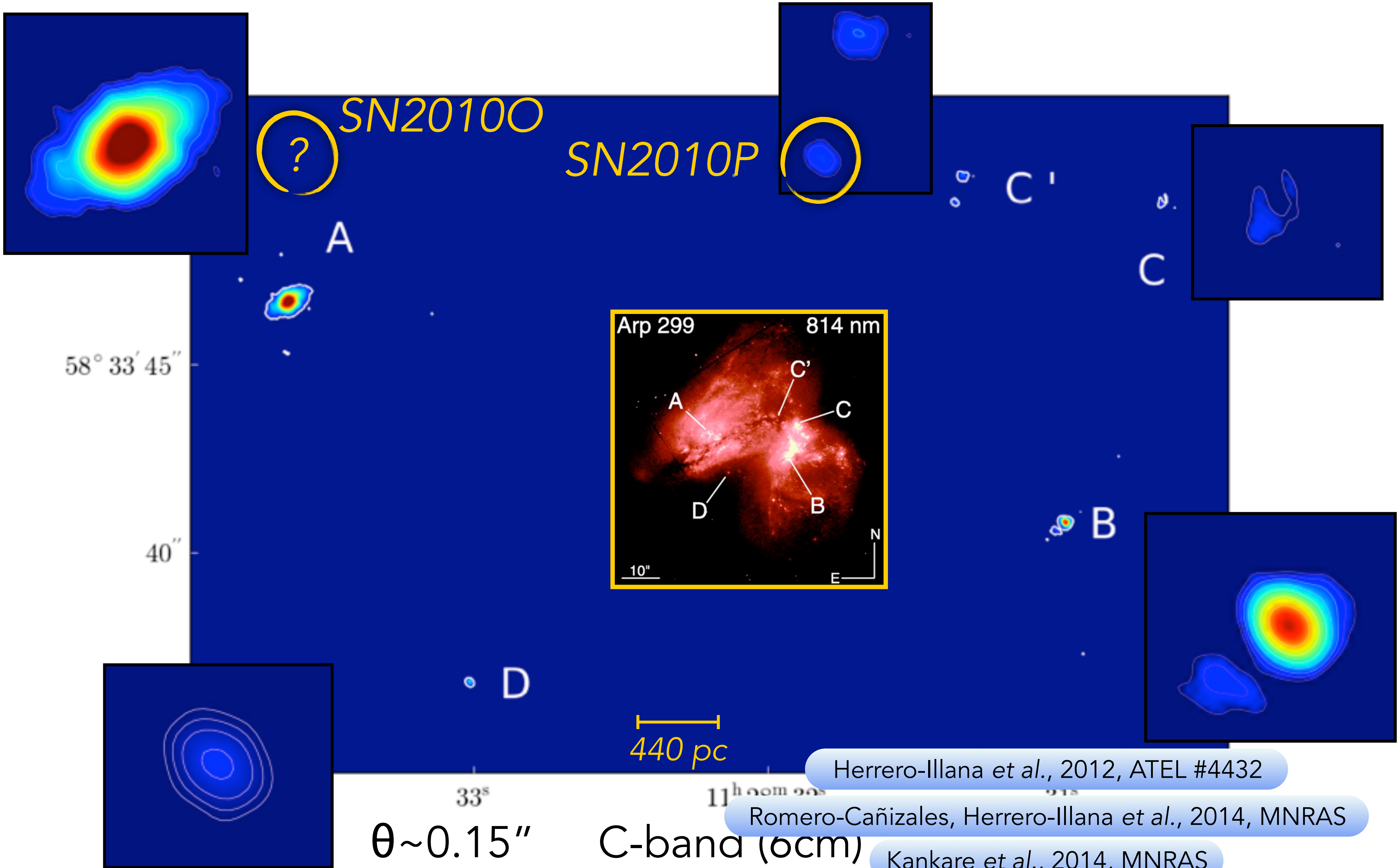

θ~0.15″ C-band (6cm)

Herrero-Illana *et al.*, 2012, ATEL #4432

Romero-Cañizales, Herrero-Illana *et al.*, 2014, MNRAS

Kankare *et al.*, 2014, MNRAS

SN2010P & SN2010O characterization

13 epochs, 4 radio bands

SN2010P & SN2010O characterization

13 epochs, 4 radio bands

SN2010P

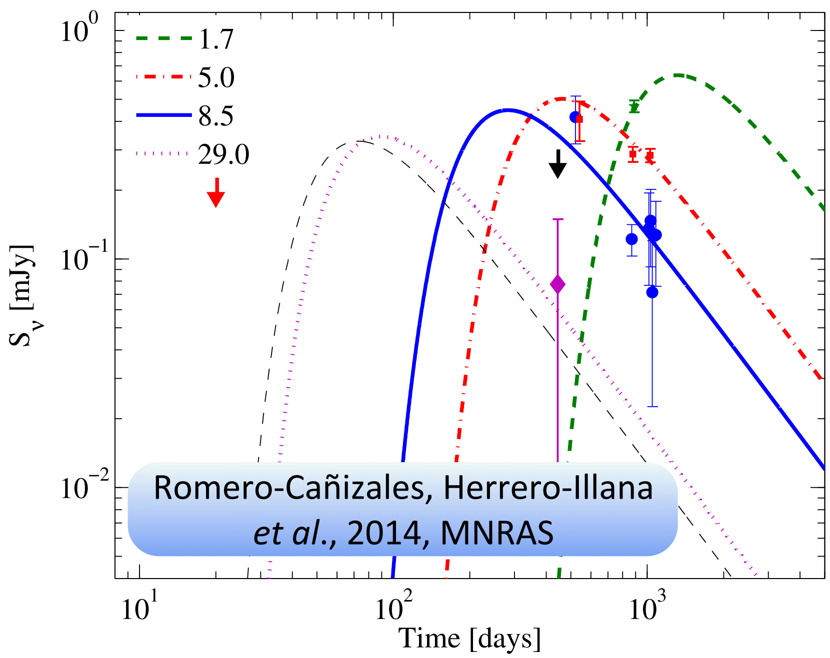

Type IIb

Most distant

Largest t_{peak}

SN2010P & SN2010O characterization

13 epochs, 4 radio bands

SN2010P

SN2010O

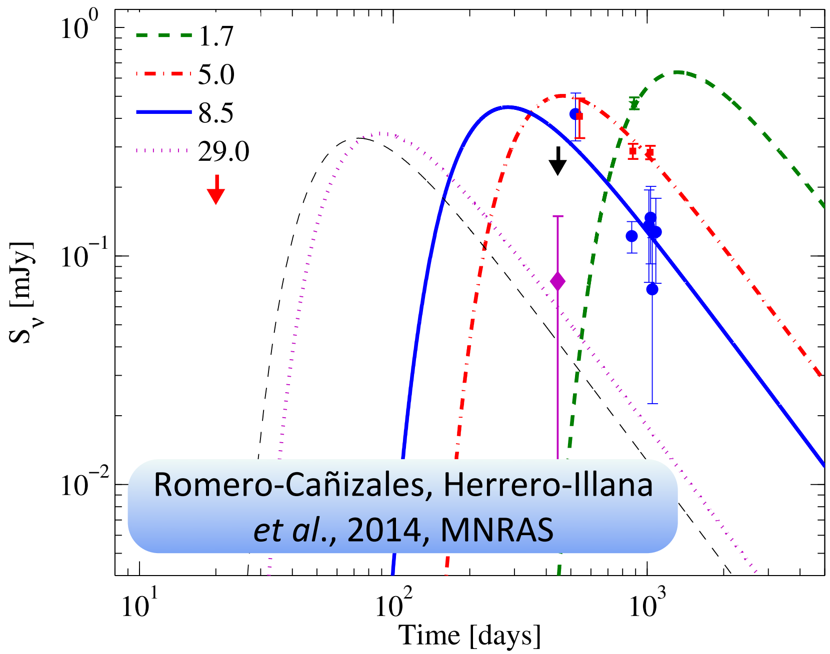

Type IIb

Most distant

Largest t_{peak}

Type Ib

Faint

Short radio life

Arp299-A EVN observations

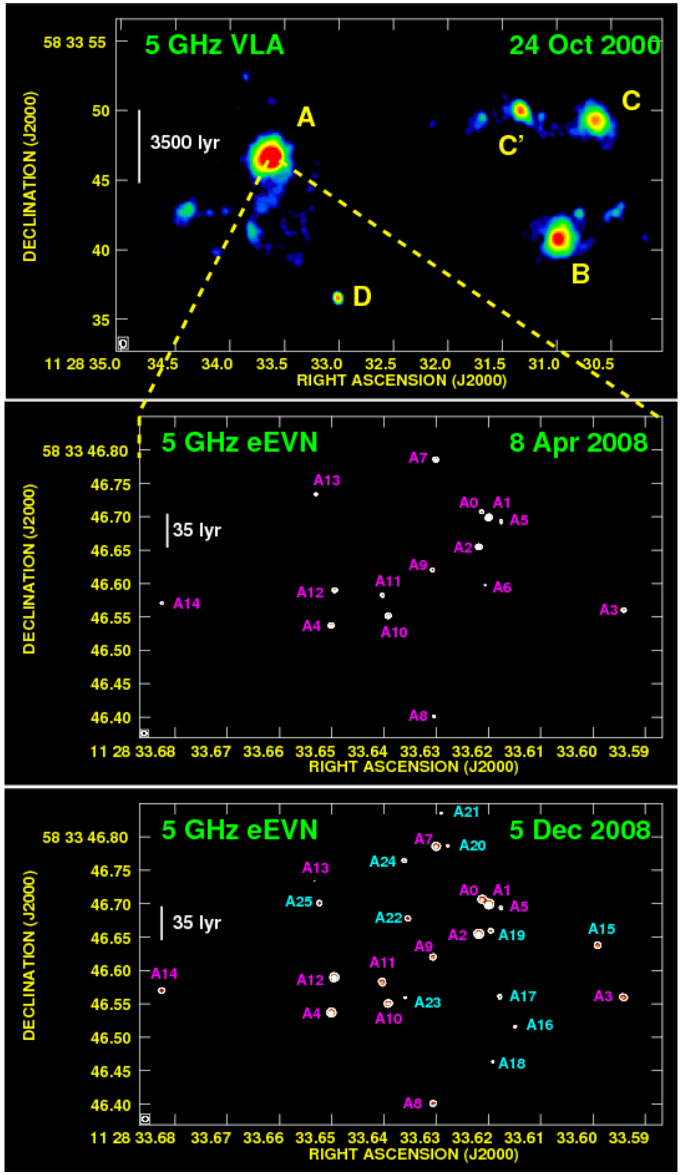

Pérez-Torres *et al.*, 2009, A&A

Bondi *et al.*, 2012, A&A

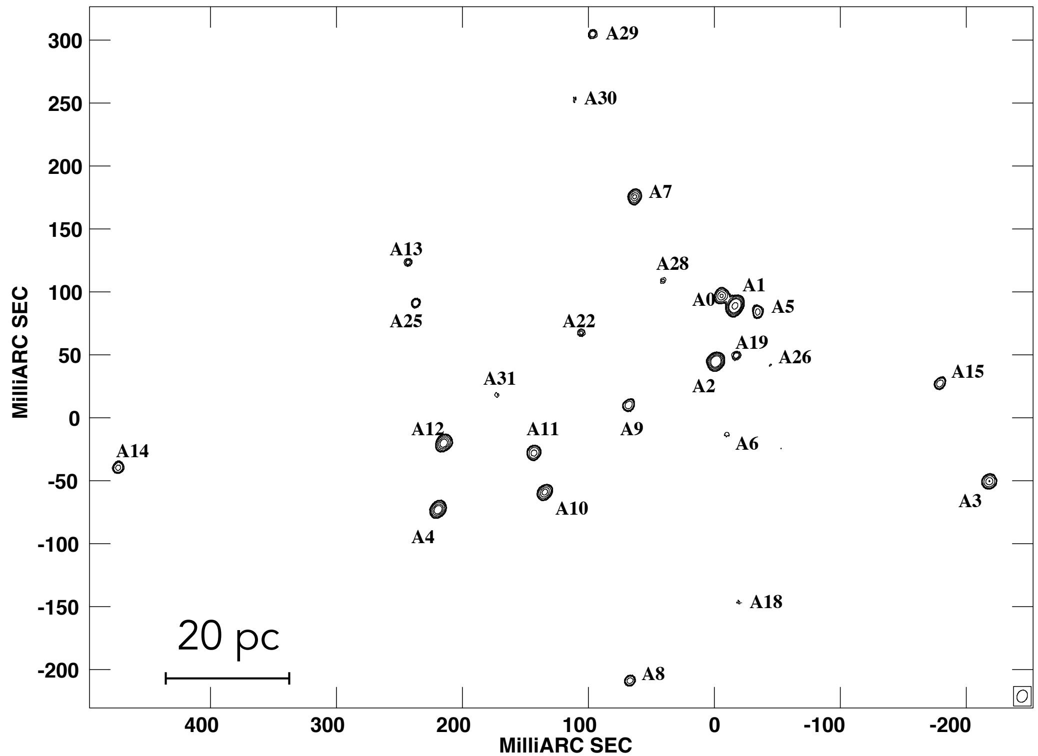

- 6 epochs in 2.5 years - Stacking @ 6cm
- 25 sources detected above 5σ
- 2 new SNe
- CCSN rate > 0.8 SN/yr

Outline

Circumnuclear disks

- Loss of angular momentum
- Inflows
- Reservoir of gas
- Circumnuclear disks around AGN

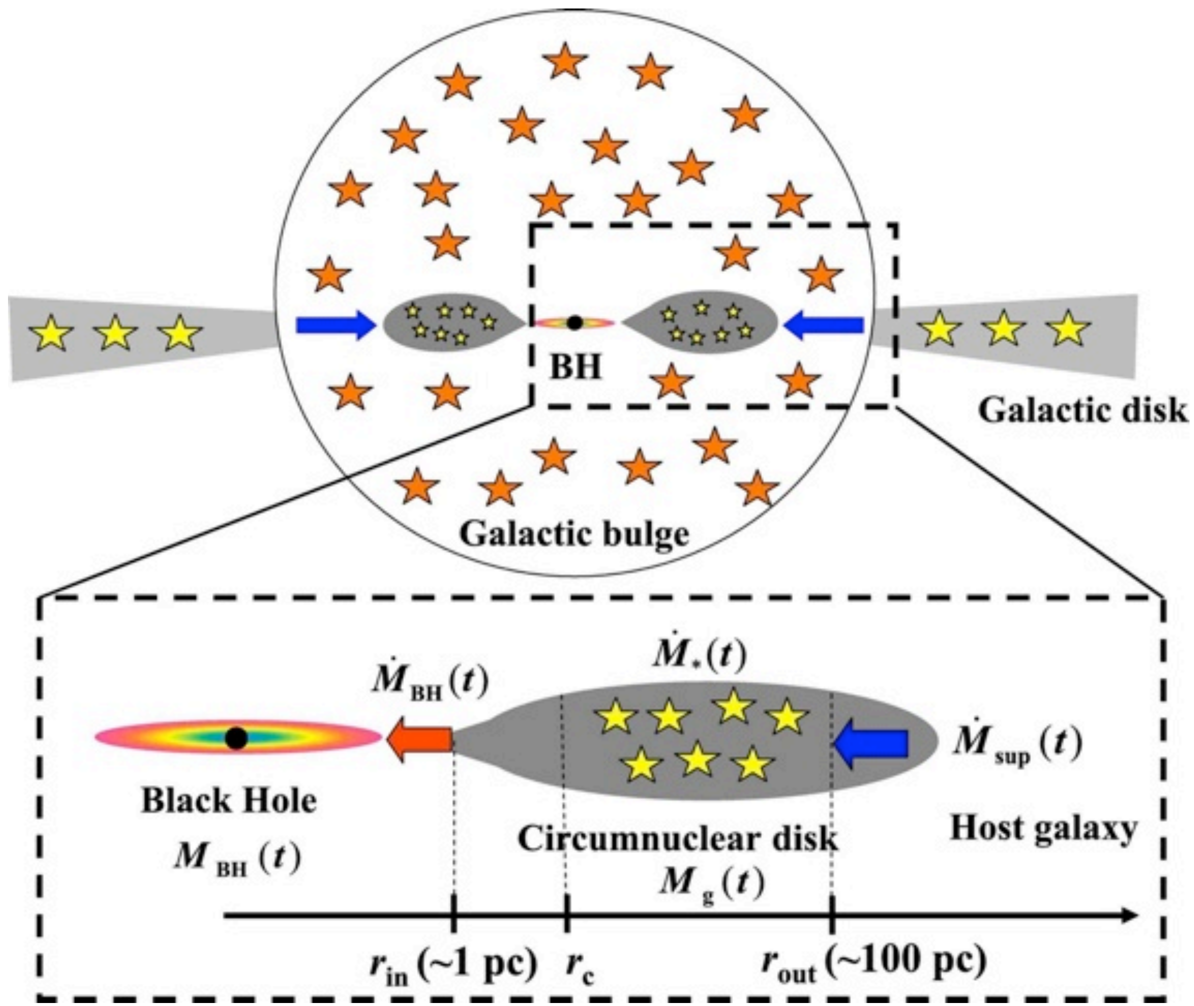

Kawakatu & Wada, 2008, ApJ

Method and previous studies

- Exponential disk: $\Sigma^{SN} = \Sigma_0^{SN} \exp(-r/h_{SN})$ — Scale length
- Surface density in concentric rings: $\frac{n_{SN}}{\pi(r_{i+1}^2 - r_i^2)}$
- Previous optical studies → Dust extinction; Angular resolution; Limited to galactic scales

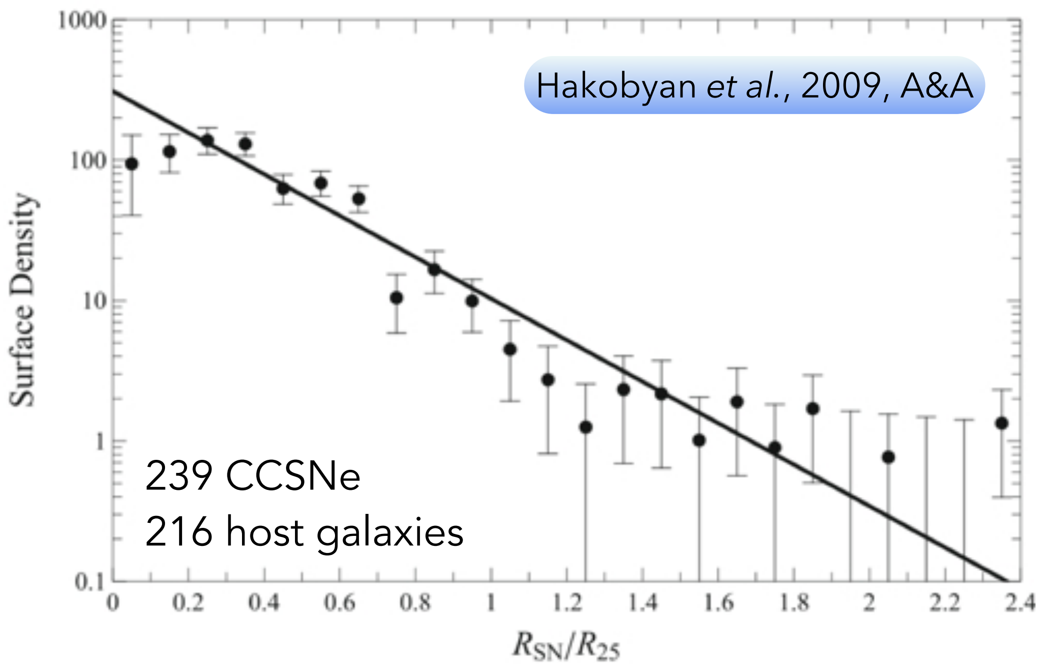

The sample

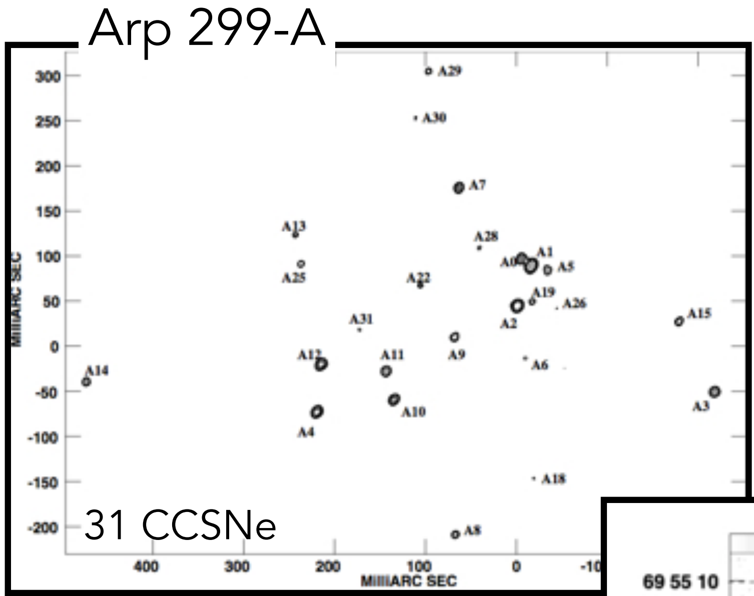

Bondi et *al.*, 2012, A&A

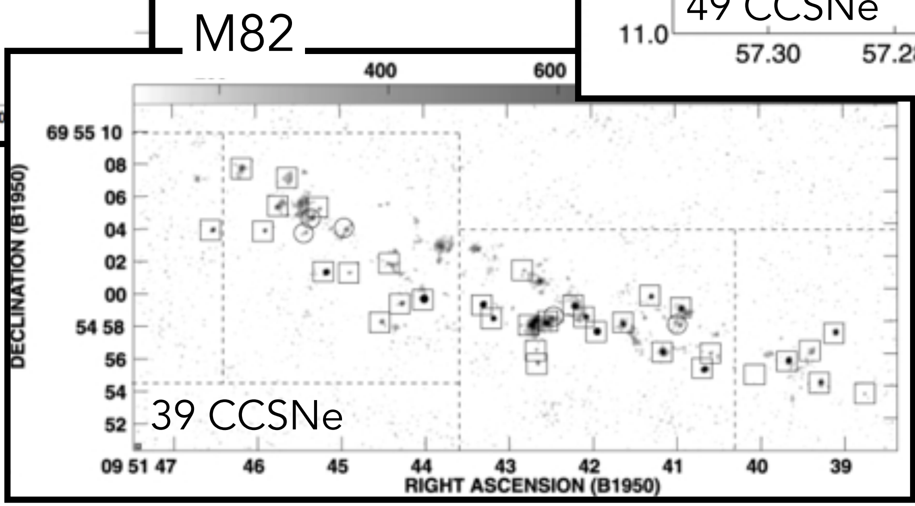

McDonald *et al.*, 2012, MNRAS

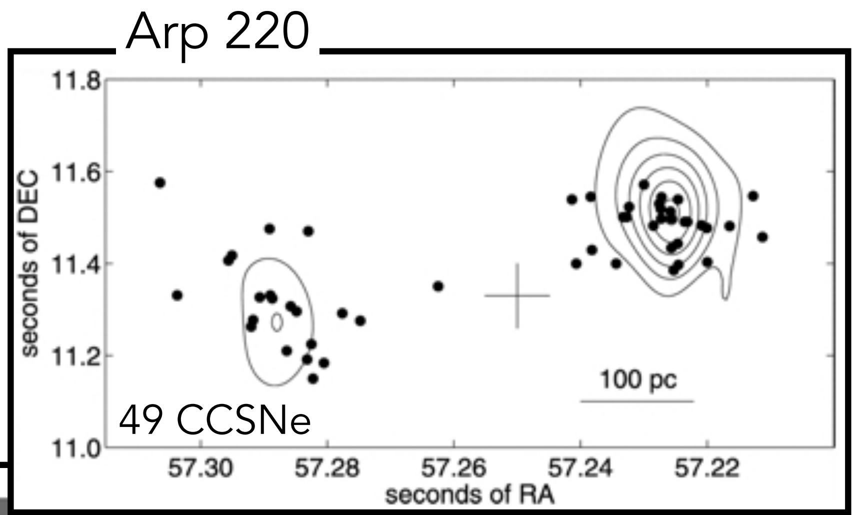

Parra et *al.*, 2007, ApJ

Scale length obtention

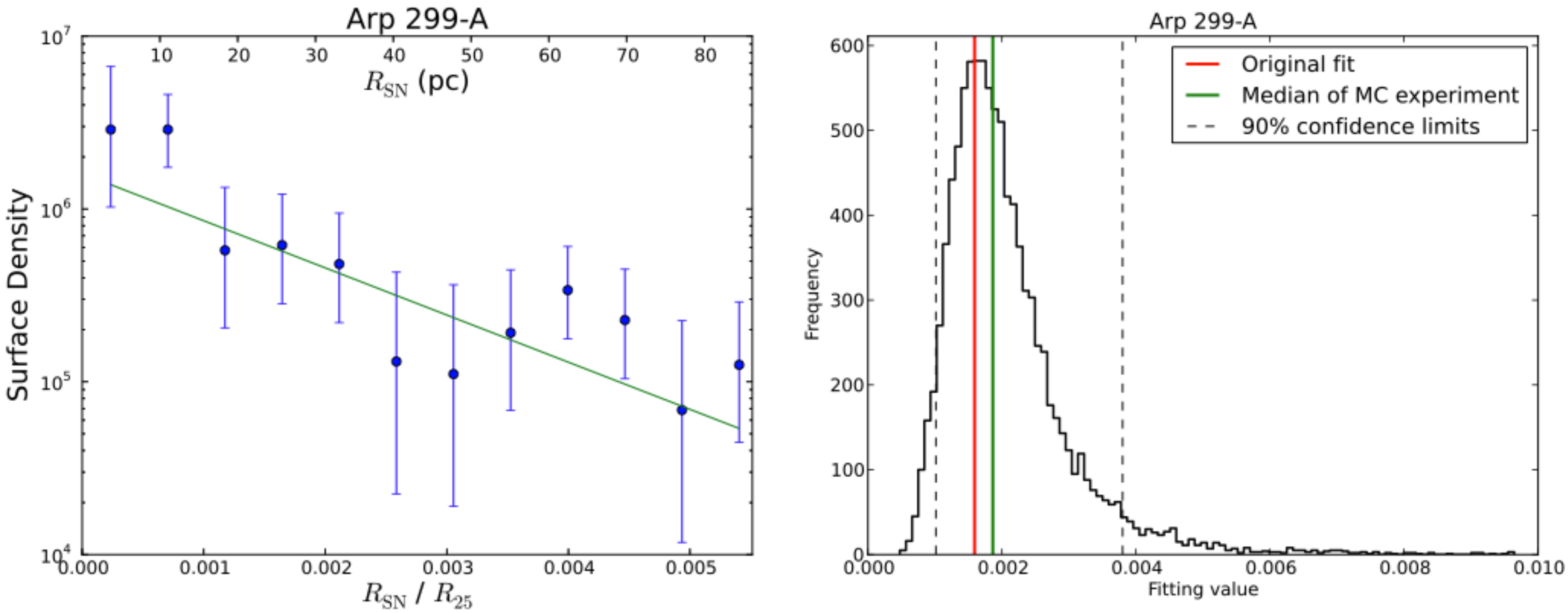

$$\Sigma^{SN} = \Sigma_0^{SN} \exp(-r/h_{SN})$$

Power-law profile

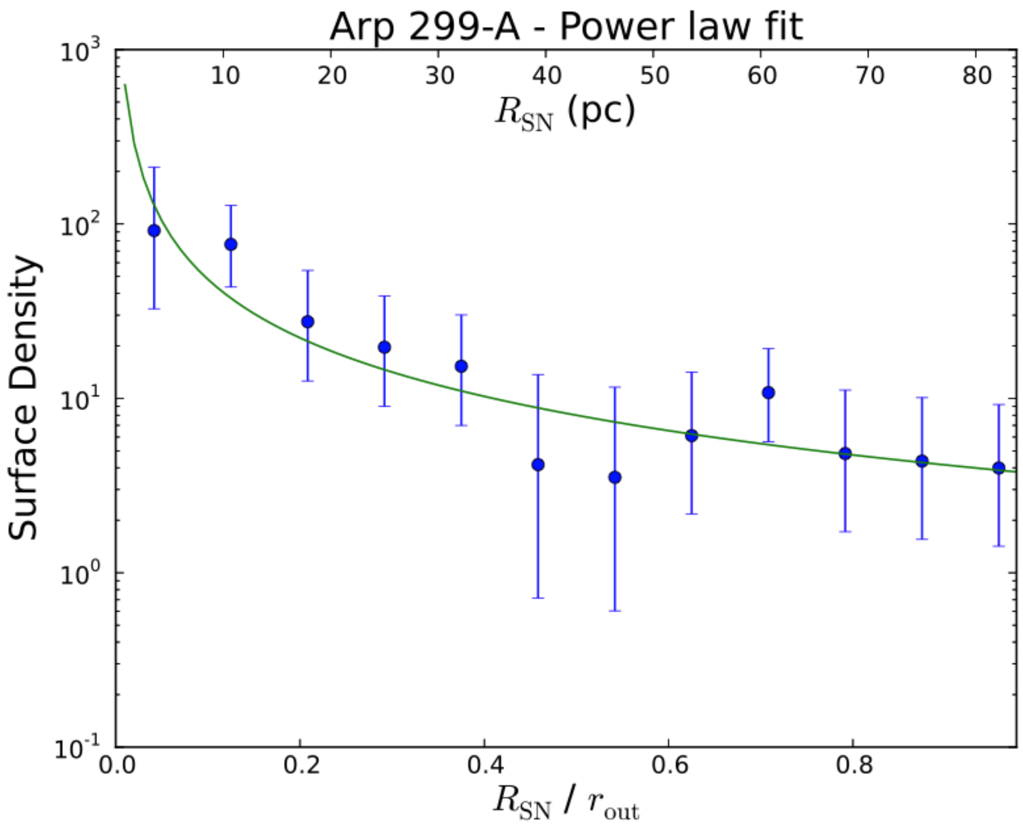

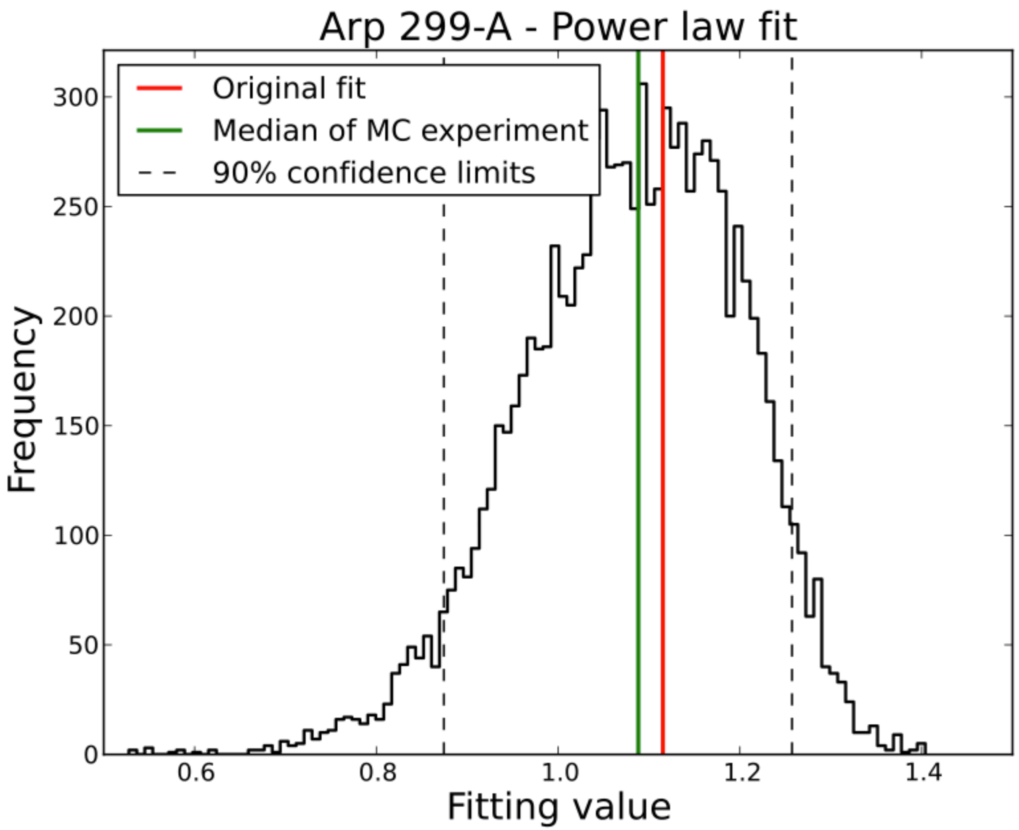

$$\Sigma^{\rm SN} = \Sigma_0^{\rm SN} \left(\frac{r}{r_{\rm out}} \right)^{-\gamma}$$

The radial distribution of SNe

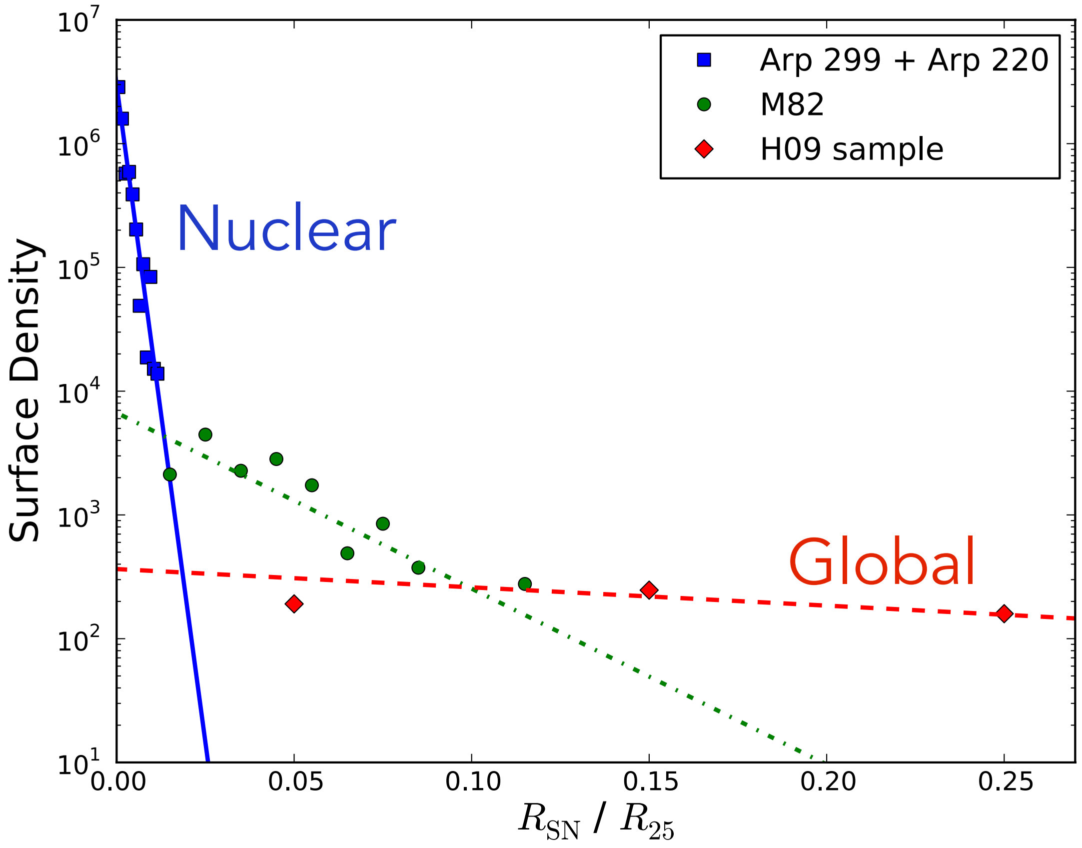

Herrero-Illana, Pérez-Torres & Alberdi, 2012, A&A

- Global VS nuclear distribution
- Circumnuclear disks:
  - Arp 299-A & Arp 220 ~20 pc
  - M82 ~160 pc
- Supports numerical models
  - $\gamma \sim 1$

Outline

1. Introduction
2. Observations
3. Results
   3.1. Molecular gas in (U)LIRGs
   3.2. NGC1614 as a case study
   3.3. Multiwavelength study of LIRGs
   3.4. Massive star formation in Arp299
   3.5. The radial distribution of supernovae
4. Conclusions

Bottom lines

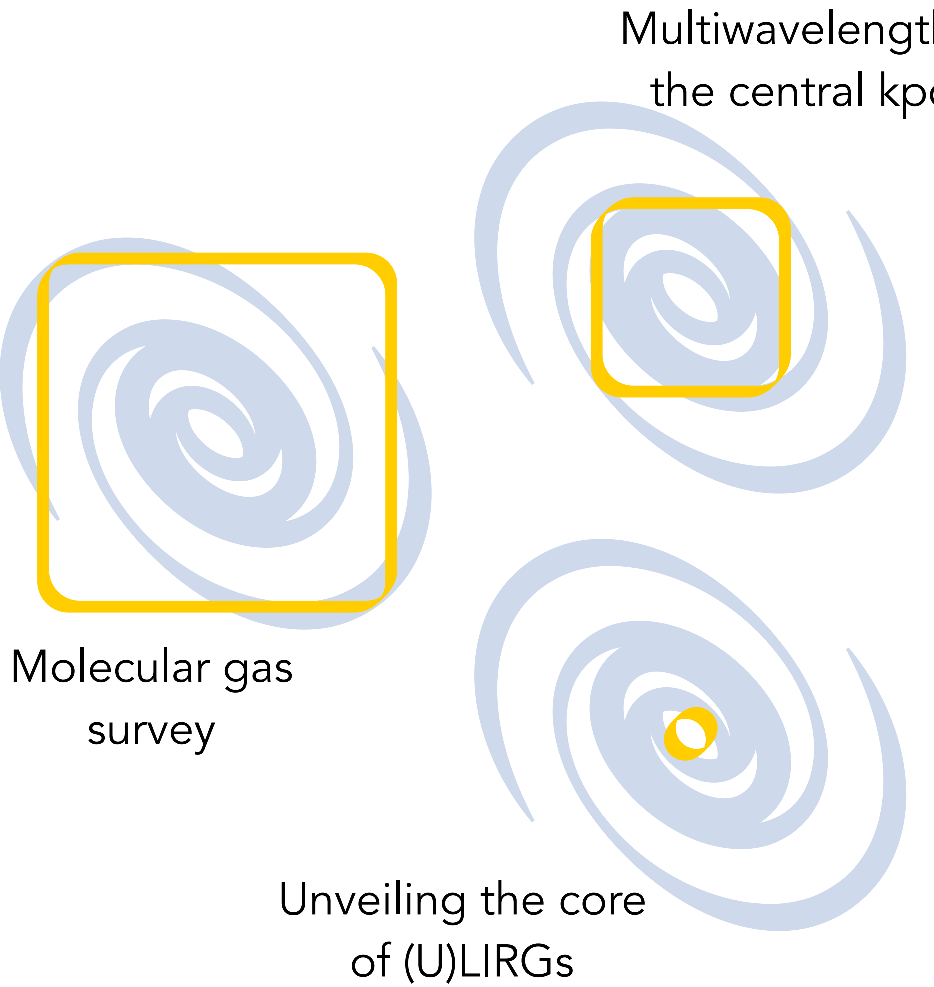

- Extreme SF & AGN in (U)LIRGs: perfect laboratory where to study these phenomena.
- A multiwavelength approach is crucial to understand these sources as global systems and understand its evolution.
- It is essential to study (U)LIRGs at different scales to characterize its different physical conditions.
- VLBI offers a unique tool to study nuclear processes.

Bottom lines

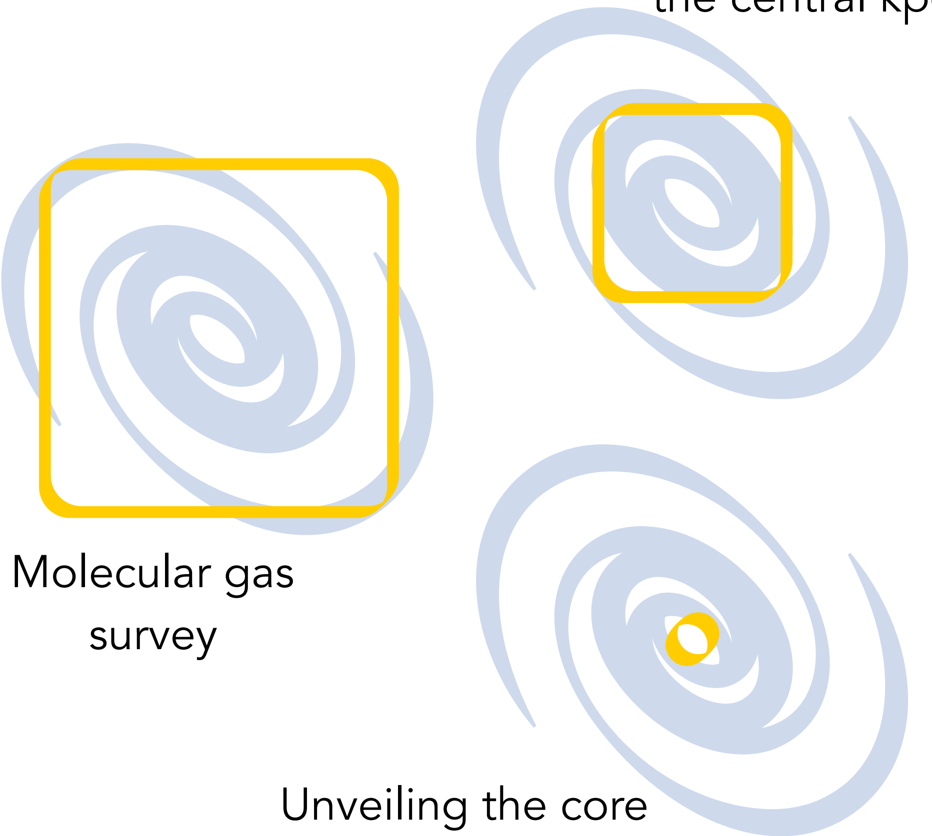

- Extreme SF & AGN in (U)LIRGs: perfect laboratory where to study these phenomena.
- A multiwavelength approach is crucial to understand these sources as global systems and understand its evolution.
- It is essential to study (U)LIRGs at different scales to characterize its different physical conditions.
- VLBI offers a unique tool to study nuclear processes.

Thanks!